

Self-consistent formulations for stochastic nonlinear neuronal dynamics

Jonas Stapmanns^{1,2,*}, Tobias Kühn^{1,2,*}, David Dahmen¹, Thomas Luu³, Carsten Honerkamp^{2,4}, and Moritz Helias^{1,2}

¹*Institute of Neuroscience and Medicine (INM-6) and Institute for Advanced Simulation (IAS-6) and JARA BRAIN Institute I, Jülich Research Centre, Jülich, Germany*

²*Institute for Theoretical Solid State Physics, RWTH Aachen University, 52074 Aachen, Germany*

³*Institut für Kernphysik (IKP-3), Institute for Advanced Simulation (IAS-4) and Jülich Center for Hadron Physics, Jülich Research Centre, Jülich, Germany and*

⁴*JARA-FIT, Jülich Aachen Research Alliance - Fundamentals of Future Information Technology, Germany*

(Dated: June 30, 2022)

Neural dynamics is often investigated with tools from bifurcation theory. However, many neuron models are stochastic, mimicking fluctuations in the input from unknown parts of the brain or the spiking nature of signals. Noise changes the dynamics with respect to the deterministic model; in particular classical bifurcation theory cannot be applied. We formulate the stochastic neuron dynamics in the Martin-Siggia-Rose de Dominicis-Janssen (MSRDJ) formalism and present the fluctuation expansion of the effective action and the functional renormalization group (fRG) as two systematic ways to incorporate corrections to the mean dynamics and time-dependent statistics due to fluctuations in the presence of nonlinear neuronal gain. To formulate self-consistency equations, we derive a fundamental link between the effective action in the Onsager-Machlup (OM) formalism, which allows the study of phase transitions, and the MSRDJ effective action, which is computationally advantageous. These results in particular allow the extension of the OM formalism to non-Gaussian noise. This approach naturally leads to effective deterministic equations for the first moment of the stochastic system; they explain how nonlinearities and noise cooperate to produce memory effects. Moreover, the MSRDJ formulation yields an effective linear system that has identical power spectra and linear response. Starting from the better known loopwise approximation, we then discuss the use of the fRG as a method to obtain self-consistency beyond the mean. We present a new efficient truncation scheme for the hierarchy of flow equations for the vertex functions by adapting the Blaizot, Méndez and Wschebor (BMW) approximation from the derivative expansion to the vertex expansion. The methods are presented by means of the simplest possible example of a stochastic differential equation that has generic features of neuronal dynamics.

* J. Stapmanns and T. Kühn contributed equally to this work

I. INTRODUCTION

Neuronal networks are interesting physical systems in various respects: they operate outside thermodynamic equilibrium [1], a consequence of directed synaptic connections that prohibit detailed balance [2]; they show relaxational dynamics and hence do not conserve but rather constantly dissipate energy; and they show collective behavior that self-organizes as a result of exposure to structured, correlated inputs and the interaction among their constituents. But their analysis is complicated by three fundamental properties: Neuronal activity is stochastic, the input-output transfer function of single neurons is non-linear, and networks show massive recurrence [3] that gives rise to strong interaction effects. They hence bear similarity with systems that are investigated in the field of (quantum) many particle systems. Here, as well, (quantum) fluctuations need to be taken into account and the challenge is to understand collective phenomena that arise from the non-linear interaction of their constituents. Not surprisingly, similar methods can in principle be used to study these two a priori distinct system classes [4–8].

But so far, the techniques employed within theoretical neuroscience just begin to harvest this potential. Here we will take essential steps towards this goal. Concretely, we adapt methods from statistical field theory and functional renormalization group techniques to the study of neuronal dynamics.

A central motivation for this work is a coherent presentation of the technical machinery, which is well-developed in other fields of physics [9], to study the statistics and in particular phase transitions in stochastic neuronal systems and to provide a bridge between the stochastic dynamics and effective descriptions with reduced complexity. The large number of synaptic inputs to each neuron in a network allows the application of mean-field theory [10–12] to explain many dynamical phenomena, among them first order phase transitions. The transition from a quiescent to a highly active state in a bistable neuronal network is a prime example of a first order phase transition in neuronal networks [12]. The activation of attractors embedded into the connectivity of a Hopfield network is a second [13]. Combined with linear response theory, network fluctuations can quantitatively be described in binary [14–16] and in spiking networks [17–22]. Also transitions into oscillatory states by Andronov-Hopf bifurcations are in the realm of linear response theory around a mean-field solution [23–26].

Second order phase transitions in neuronal networks are more challenging, because the behavior of the system is dominated by fluctuations on all length scales, so that mean-field theory and its systematic correction by loopwise expansion often break down [4]. But these transitions are highly interesting from a neuroscientific point of view, because networks then show large susceptibility to signals. Moreover, signatures of critical states are found ubiquitously in experiments: Parallel recordings in cell cultures [27] and in vivo [28] show power law distributions in the numbers of co-active neurons, suggestive of scale free dynamics. Critical states also have consequences for information processing: reservoir computing [29, 30] with random networks close to criticality indeed shows the highest computational performance [31], maximizing the wealth of transformations they perform.

Close to second order phase transitions, the method of choice is to compute the effective action by renormalization group techniques [32]. A particularly powerful implementation is the functional renormalization group (fRG) [33–35]. It has witnessed successes in condensed matter physics in problems ranging from classical and quantum critical phenomena over the explorations of the ground states of interacting many-body systems to the improved determination of effective model parameters from ab-initio theories. It systematically improves the physical description beyond mean-field theory by including fluctuations and by removing ambiguities.

To date, one of the most powerful and versatile sets of methods is available for neuronal networks of stochastic differential equations: The Martin-Siggia-Rose-de Dominicis-Janssen (MSRDJ) formalism [36–38] has been used to apply diagrammatic perturbation theory and systematic fluctuation expansions to neuronal networks [7, 8]. This formalism has in particular been applied to describe genuine non-equilibrium dynamics in physical systems [5], including disordered systems [39]. Combined with replica theory [40], it has recently been used to find an exact condition for the transition from regular to chaotic activity [41], to compute the memory capacity of driven random networks [42], and to study the effect of bi-directional connectivity [43, 44].

The aim of the current manuscript is to review a sequence of formulations for the statistics in neuronal-inspired stochastic dynamics, coherently presented in the order of increasing self-consistency: mean-field approximation, loop expansion, and functional renormalization group. To our knowledge, advanced methods such as the functional renormalization group, have so far not been applied to neuronal systems. We feel that a work explaining this method in the context of neuronal dynamics with help of minimal examples and in relation to the simpler approaches, the mean-field approximation and the loop expansion, may be helpful for many researchers in our field. The presentation together with these more widely used approaches also allows us to address some of the more subtle points that we could not find documented in the literature. In particular, we discuss issues of convexity of the cumulant-generating functional, the need for the Legendre-Fenchel transform in systems with dynamic symmetry breaking, the different definitions of the effective potential in equilibrium and non-equilibrium systems and its use to investigate phase transitions. We also point out particularities of the MSRDJ formalism compared to the field theories more commonly covered in text books.

The outline of the manuscript is as follows: In [Section II A](#), we recapitulate the mean-field solution of a stochastic differential equation and introduce its Onsager-Machlup (OM) field theory. We motivate this formulation by demonstrating that it allows the definition of an effective potential which locally acts like an energy and can be used to analyze phase transitions. Moving on to the MSRDJ-field theory, we review in [Section II B](#) the loop expansion, which enables practical calculations of probabilistic quantities, which, by construction, are self-consistent on the level of the first moments. We present an exact relation between the effective actions of these two formulations and therefore extend the definition of the OM effective action to case of non-Gaussian noise. The utility of the Onsager-Machlup effective action is illustrated in a neuronal dynamical equation close to the loss of balance; we show that this bifurcation point in the deterministic model corresponds to a continuous phase transition in the stochastic dynamics. [Section II C](#) contains a derivation of effective, deterministic, non-Markovian dynamics for the mean value of the stochastic process; it shows how fluctuations influence the relaxation back to baseline after a small perturbation and provides an intuition for the meaning of vertex functions. A stochastic linear convolution equation is presented that has the same second order statistics as the full non-linear system; it explains the meaning of self-energy corrections in the neuronal context. [Section II D](#) covers the functional renormalization group as a method that allows the self-consistent treatment up to arbitrary order of the vertex functions. In particular, in [Section II D 1](#) we present a new interpretation of the BMW approximation [45] within the vertex expansion. We show that all terms of the bare action flowing in this altered BMW-fRG-scheme leads to an improvement over the one-loop result. In [Section III](#) we discuss the presented concepts in comparison to other approaches and provide an outlook towards applications within theoretical neuroscience.

II. RESULTS

A. Effective action and effective potential

We here consider the following generic stochastic differential equation

$$dx(t) = f(x(t)) dt + dW(t), \quad (1)$$

where x could denote a magnetization, the firing rate or activity of a neuron or of a population of neurons, the concentration of some chemical substance, the number of animals that reproduce and die or the value of a stock [46–48]. We will focus on the neuroscientific interpretation, in which case we parameterize $f(x) = -x + Jg(x)$. We call J the synaptic weight of the self-feedback which is mediated by the nonlinearity $g(x)$, the gain function, which typically is a sigmoid. The explicit term $-x$ shall describe the leaky dynamics of neurons. We choose the stochastic increment $dW(t)$ as a centered Gaussian with first and second moments given by

$$\langle dW(t) \rangle = 0, \quad \langle dW(t)dW(s) \rangle = D\delta_{t,s}dt.$$

Throughout the text we use $\langle x^n \rangle$ to denote the n -th moment of x and $\langle\langle x^n \rangle\rangle$ to denote the n -th cumulant.

This article investigates a sequence of approximation techniques to compute the statistics of the system self-consistently. We present methods with increasing complexity and accuracy, starting with the simplest possible self-consistent approximation: the neglect of fluctuations altogether.

Mean-field approximation

The simplest self-consistent approximation of the statistics of the system consists of an ad hoc approach to the stochastic differential equation (1) that neglects the noise and instead solves the ordinary differential equation

$$\frac{d}{dt}x(t) = f(x(t)). \quad (2)$$

Finding the stationary solution to this differential equation amounts to a fixed point problem, that is $f(x_0) = 0$. Small fluctuations around that solution can, to first approximation, be accounted for by linearizing (1) around x_0 . By writing $x(t) = x_0 + \delta x(t)$, we obtain

$$\frac{d}{dt}\delta x(t) = f'(x_0)\delta x(t) + \xi(t) + \mathcal{O}(\delta^2 x(t)), \quad (3)$$

where ξ is a centered Gaussian white noise with variance D (formally the derivative of dW). Denoting the Fourier transform of x as X , we describe the first and second order statistics of these small fluctuations as

$$\begin{aligned} 0 &= \langle \delta X(\omega) \rangle = \frac{\langle \xi(\omega) \rangle}{i\omega - f'(x_0)}, \\ \langle \delta X(\omega) \delta X(\omega') \rangle &= \frac{2\pi D \delta(\omega + \omega')}{(i\omega - f'(x_0))(i\omega' - f'(x_0))}. \end{aligned} \quad (4)$$

This approach is, however, restricted to small noise amplitudes, and cannot be straight-forwardly generalized. From a conceptual point of view, this approximation is also not self-consistent, because we solve the deterministic equation (2) to determine the first moment x_0 and then study fluctuations around it to determine the second order statistics as (4). Such fluctuations would, in turn, affect the mean value, due to the non-linear parts of f . Continuing the Taylor expansion of f in (3) to second order, this ad hoc approach would then yield a correction to the mean given by $\langle x \rangle \simeq x_0 + \frac{1}{2} f''(x_0) \frac{D}{-2f'(x_0)}$, because the variance of the process, by (4), is $\langle \delta x^2 \rangle = \frac{D}{-2f'(x_0)}$. Thus we get an approximation for the mean that is inconsistent with the value x_0 that we assumed to perform the approximation in the first place. The common thrust of the methods surveyed in the remainder of this article is to strive for self-consistency of the statistics and to systematically compute such fluctuation corrections that are self-consistent also on the level of higher moments.

Path-integral formulation

To study the system more systematically, we introduce the path integral formalism, starting with its Onsager-Machlup (OM) formulation [49, 50]. We assign a probability $p[x] \mathcal{D}x$ to every path $x(t)$, where we define the integral measure $\mathcal{D}x$ as

$$\int \mathcal{D}x \dots := \lim_{N \rightarrow \infty} \int dx_{t_0} \dots \int dx_{t_{N-1}} \dots,$$

where t_0, \dots, t_{N-1} is a uniform discretization of the time axis. We here stick to the Ito convention, which means that we evaluate the integrand at the beginning t_i of every subinterval $[t_i, t_{i+1})$. For additive noise, as it appears in (1), all choices for a discretization converge to the same limit [51, chap. 4.3.6.]. Furthermore, we define $p[x] = \frac{1}{Z} \exp(S_{\text{OM}}[x])$ via

$$\begin{aligned} S_{\text{OM}}[x] &= -\frac{1}{2} \lim_{N \rightarrow \infty} \sum_{i=0}^{N-1} \left(\frac{x_{i+1} - x_i}{\Delta t} - f(x_i) \right)^T D^{-1} \left(\frac{x_{i+1} - x_i}{\Delta t} - f(x_i) \right) \Delta t \\ &= -\frac{1}{2} \int dt \left(\partial_t x - f(x(t)) \right)^T D^{-1} \left(\partial_t x - f(x(t)) \right) \end{aligned} \quad (5)$$

[49, 50, 52–54]¹ and

$$Z^{-1} := \int \mathcal{D}x \exp(S_{\text{OM}}[x])$$

is chosen such that the probability $p[x]$ is properly normalized. The probability of the occurrence of deviations from the solution fulfilling $\partial_t x = f(x)$ are suppressed exponentially. Allowing for arbitrary time-dependent solutions $x(t)$, for example by fixing the initial point $x(0) = x_0$ and the final point $x(T) = x_T$, $p[x]$ determines the probability for any path between these points; applied to the dynamics of the membrane potential of a neuron, it can be used to determine the probability to exceed the firing threshold. The rate of escape is, to leading exponential order, given by $p[x^*]$, where x^* minimizes S_{OM} (see e.g. Altland and Simons [see e.g. 55] section 10.5 or [56] section 5).

The moments of the ensemble of paths

$$\langle x(t_1) \dots x(t_n) \rangle := \int \mathcal{D}x p[x] x(t_1) \dots x(t_n) \quad (6)$$

can be expressed as functional derivatives with respect to $j(t)$ of the moment-generating functional

$$Z[j] := \int \mathcal{D}x p[x] \exp\left(\int dt j(t) x(t)\right), \quad (7)$$

¹ Note that the notation as an integral is meant symbolically: For concrete calculations of the path integral, one always has to use the discrete version with a finite sum, perform the integrations and draw the limit afterwards.

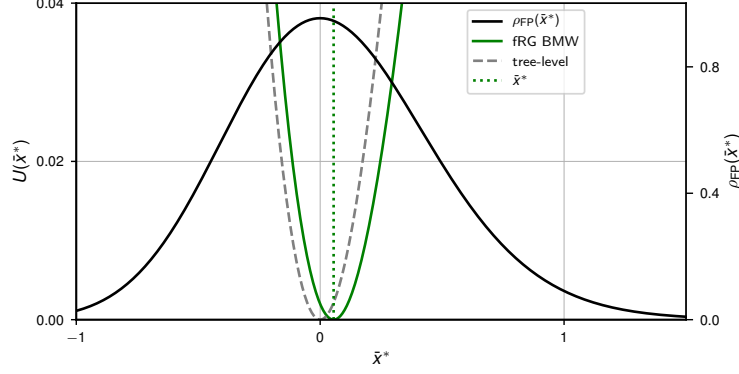


Figure 1. Effective potential $U(\bar{x})$, as defined in (13), in different approximations. Practically, we used (14) where we replaced the bare quantities by the corrected ones. The dashed line represents the tree-level approximation (14) and the solid line the fRG result with truncation after $\Gamma_{\bar{x}x\bar{x},\text{fl.}}^{(3)}$ including the BMW approximation, see Section IID 1. The probability density obtained as the solution of the Fokker-Planck equation [58] is shown in black for comparison. The dotted line indicates the position of the mean value \bar{x} computed via the fRG calculation. Parameters for specific choice of $f(x)$, see (28): $l = 0.5$, $\beta = 0.15$, $D = 0.17$.

²evaluated at $j(t) = 0$. The cumulant generating function (or Helmholtz free energy)

$$W = \ln Z \quad (8)$$

encodes the statistics in terms of cumulants, the derivatives of W . Cumulants encode the statistics more efficiently than moments, because higher order cumulants do not contain information already contained in lower orders.

In the following we review some central results that show the relation between the two commonly used path integral representations, the Onsager-Machlup formulation and the Martin-Siggia-Rose-de Dominicis Janssen formulation. Subsequently, we derive a novel relation between the corresponding effective actions.

MSRDJ Formulation

Practical computations in the Onsager-Machlup formalism are complicated by the action involving a second order differential operator. It has been realized by Martin et al. [36] that, computing response functions simultaneously together with correlation functions (6), simplifies practical computations. This is achieved by introducing a second field, the response field \tilde{x} by expressing the Onsager-Machlup action with Gaussian noise (5) as a Legendre transform

$$S_{\text{OM}}[x] = \sup_{\tilde{x}} S_{\text{MSRDJ}}[x, \tilde{x}], \quad (9)$$

where $x^T y = \int_{-\infty}^{\infty} x(t) y(t) dt$ denotes the inner product with respect to time. The argument of the supremum is the Martin-Siggia-Rose-de Dominicis-Janssen (MSRDJ) action [36–38, 57], defined on the $2N$ -dimensional phase space as

$$S_{\text{MSRDJ}}[x, \tilde{x}] := \tilde{x}^T (\partial_t x - f(x)) + \tilde{x}^T \frac{D}{2} \tilde{x}. \quad (10)$$

Alternatively, one may obtain this result by performing a Hubbard-Stratonovitch transform, that is by using the identity $e^{-\frac{x^2}{2}} = \frac{1}{i\sqrt{2\pi}} \int_{-\infty}^{\infty} e^{\frac{\tilde{x}^2}{2} + \tilde{x}x} d\tilde{x}$ with the response field as an additional auxiliary variable \tilde{x} . The MSRDJ formulation has the advantage that only a single first order differential operator in time appears.

² Note the sign convention of the action which is defined without a minus sign in front. We will stick to this convention throughout this text.

With the expressions for the actions S_{OM} and S_{MSRDJ} , one can calculate moments and cumulants of activity as derivatives of the respective functionals Z and W . For a self-consistent determination of the mean activity, it is, however, beneficial to consider the variational problem of some functional $\Phi[x^*; j]$ that assumes stationary points at the true mean value $\tilde{x}(t) \equiv \langle x(t) \rangle$. The defining equation $\Phi^{(1)}[\tilde{x}; j] = 0$ for that stationary point necessarily has the form of a self-consistency equation — its left hand side is a function of the mean, which will therefore necessarily appear on the right hand side, too.

Indeed such a functional is readily defined via the Legendre-Fenchel transform

$$\begin{aligned}\Gamma_{\text{OM}}[x^*] &:= \sup_j j^T x^* - W[j], \\ \Phi[x^*; j] &:= \Gamma_{\text{OM}}[x^*] - j^T x^*.\end{aligned}\tag{11}$$

The so-defined Γ_{OM} is the effective action (or Gibbs free energy) [4]. It is central to the study of phase transitions, which reduces to finding the stationary points or regions of Φ [59, i.p. Chapter 6]. The variational formulation naturally solves the problem that derivatives of W become multi-valued at first order phase transitions; when W has a cusp and thus the system has multiple states with different values for the mean $\langle x(t) \rangle$ at the same set of parameters. We study an example where spontaneous symmetry breaking causes such a cusp in [Section II A](#).

Since $W[j]$ is convex down in j , the Legendre-Fenchel transform in (11) is well-defined. Note that the Legendre-Fenchel transform is a generalization of the Legendre transform for cases where W is non-differentiable (see also [Section IV C](#) for a proof of convexity of W). At such points, Φ has a flat segment, but is continuously differentiable everywhere³ and is thus analytically simpler than the non-analytical W (for a more detailed discussion on convexity, spontaneous symmetry breaking, and the necessity of the Legendre-Fenchel transform, see [Section IV C](#)).

Another advantage is that symmetries of S_{OM} are also symmetries of Γ_{OM} , giving rise to Ward-Takahashi identities [60] and the study of Goldstone fluctuations in symmetry broken states of systems that admit a continuous symmetry.

The simplest approximation to the effective action is the tree-level approximation. In correspondence to (2) we replace the integral over all configurations x in the definition of Z in (7) by its supremum, which yields $W[j] \simeq \ln \sup_x \exp(S_{\text{OM}}[x] + j^T x) - \ln Z[0]$. The monotonicity of \exp and the involution property of the Legendre transform (11) then yield

$$\Gamma_{\text{OM}}[x^*] \simeq -S_{\text{OM}}[x^*] + \text{const.}\tag{12}$$

The name “tree-level” comes from the fact that if expanded in x^* , only diagrams of tree shape contribute (see e.g. Zinn-Justin [4, p. 128] or Helias and Dahmen [61, Appendix: Equivalence of loopwise expansion and infinite resummation]). In the evaluation of the integral, one therefore neglects all fluctuations. Still, taking derivatives of Γ or W , one can study the fluctuations to leading order – we show below that this approximation is identical to computing the linear response in (3).

Limiting the study to stationary solutions $\bar{x}^* := x^*(t) = \text{const.}$, such that $X(\omega) = 2\pi\delta(\omega)\bar{x}^*$, it is convenient to introduce the effective potential

$$U(\bar{x}^*) := \frac{1}{T}\Gamma_{\text{OM}}(\bar{x}^*),\tag{13}$$

with T being the total time during which we observe the system. The effective potential is the effective action evaluated at stationary points (compare Kopietz et al. [62, chap. 9]). Therefore it is stationary at the point that corresponds to the mean value of the system, giving rise to its name. Its curvature at this point is the inverse of the zero Fourier mode of the correlation (see remark at the end of [Section IV E](#)). The effective potential further plays the role of a rate function that describes departures of the temporal average from the ensemble average in the limit of long observation times [63, Section III].

In tree level approximation (12) and with (5) we have

$$U_0(\bar{x}^*) = -\frac{1}{T}S_{\text{OM}}(\bar{x}^*) = \frac{1}{2TD} \int_0^T dt (-f(\bar{x}^*))^2 = \frac{1}{2D} (f(\bar{x}^*))^2.\tag{14}$$

³ At least in physically reasonable settings: A discontinuity in the derivative in Φ means that the derivative of Γ has a discontinuity, too, and therefore W , in turn, would have a flat segment. In such systems, changing the source field would not affect the mean.

For $D > 0$, its curvature at the minimum $\bar{x}^* = \bar{x}$ equals the inverse of the zero-frequency fluctuations $\langle X(0)^2 \rangle - \langle X(0) \rangle^2$ around the mean, which we deduce by using $f(\bar{x}) = 0$ from

$$U_0''(\bar{x}) = \frac{\partial^2}{\partial \bar{x}^{*2}} U_0(\bar{x}^*) \Big|_{\bar{x}} = \frac{(f'(\bar{x}))^2}{D}, \quad (15)$$

compared to the covariance (4) in linear response. The effective potential for the example (1) is shown in Figure 1. Next we investigate how to compute the effective action in the MSRDJ formalism.

MSRDJ effective action

As for the Onsager-Machlup form, we define the cumulant generating functional in the MSRDJ formalism as

$$W[j, \tilde{j}] = \ln \int \mathcal{D}x \int \mathcal{D}\tilde{x} \exp(S[x, \tilde{x}] + j^T x + \tilde{j}^T \tilde{x}). \quad (16)$$

Compared to its OM-form, $W[j, \tilde{j}]$ in addition incorporates the response properties of the system as differentiating once with respect to \tilde{j} and j each, respectively, yields the response function, the deviation of the mean of the process caused by a δ -shaped inhomogeneity. The effective action in the MSRDJ formalism $\Gamma[x, \tilde{x}]$ is defined in analogy to (11) as

$$\Gamma[x^*, \tilde{x}^*] = \tilde{j}^T \tilde{x}^* + \sup_j j^T x^* - W[j, \tilde{j}], \quad (17)$$

where \tilde{j} is chosen such that the right hand side is stationary. Since W is convex down in j , taking the Legendre-Fenchel transform with regard to j is involutive; this even holds for $W[j, \tilde{j}]$ that are non-differentiable in j . We show in Section IV D that the transform from j to x^* renders the resulting functional differentiable in \tilde{j} , given the system is in thermodynamic equilibrium.

Like Z and W , Γ contains the full information of the system, including effects from noise-driven fluctuations. The definition of Γ as the Legendre transform of W implies the identities

$$\begin{aligned} \Gamma_x^{(1)}[x^*, \tilde{x}^*] &:= \frac{\delta}{\delta x} \Gamma[x^*, \tilde{x}^*] = j, \\ \Gamma_{\tilde{x}}^{(1)}[x^*, \tilde{x}^*] &:= \frac{\delta}{\delta \tilde{x}} \Gamma[x^*, \tilde{x}^*] = \tilde{j}, \end{aligned} \quad (18)$$

that are implicit equations for x^* and \tilde{x}^* , the equations of state. For the physically relevant value $j = 0$ of the source field, normalization in systems with conserved probability implies that the first equation (18) always admits a solution $\tilde{x}^* \equiv 0$ (Section IV A). We further show in Section IV D that the second equation is then equivalent to the requirement that the average fluctuations around the true mean value average to zero within the Onsager-Machlup formalism; the additional Legendre transform from \tilde{j} to \tilde{x} can therefore be regarded a formal step only that does not require convexity of $W[j, \tilde{j}]$ in \tilde{j} . Approximating $\Gamma \simeq -S$ up to the tree level, reduces (18) to the naive mean-field approximation (2) showing their tight relation. The resulting path maximizes the probability, thus minimizes U_0 . Because it ignores fluctuations, we also refer to it as the saddle point approximation, or the mean-field approximation.

The implicit equations are a self-consistent way to determine the sources required for given averages x^* and \tilde{x}^* . To see this, we note that an analogous definition to (17) with $y = (x, \tilde{x})$ and $k = (j, \tilde{j})$ reads

$$\begin{aligned} \Gamma[y^*] &= -\ln \int_y \exp(S[y] + k^T(y - y^*)) \\ \text{with } \frac{\delta \Gamma}{\delta k} &\stackrel{!}{=} 0. \end{aligned} \quad (19)$$

⁴The latter condition enforces that we integrate over ensembles of configurations that obey the constraint $\langle y \rangle = y^*$; in other words, the mean values for both fields x and \tilde{x} take the values given by the argument of Γ . The right hand

⁴ Here the symbol “ $\stackrel{!}{=}$ ” denotes “is supposed to equal”; that is, the argument of the function is to be determined such that equality holds.

side of (19) will hence depend via y^* on the approximation performed for Γ ; it takes on self-consistently determined values.

The information about the second cumulant of x is captured in the relation

$$\Gamma^{(2)}[x^*, \tilde{x}^*] = \begin{pmatrix} \frac{\delta^2 \Gamma[x^*, \tilde{x}^*]}{\delta \tilde{x} \delta x} & \frac{\delta^2 \Gamma[x^*, \tilde{x}^*]}{\delta \tilde{x}^2} \\ \frac{\delta^2 \Gamma[x^*, \tilde{x}^*]}{\delta x \delta \tilde{x}} & \frac{\delta^2 \Gamma[x^*, \tilde{x}^*]}{\delta x^2} \end{pmatrix} = \begin{pmatrix} \frac{\delta^2 W[j, \tilde{j}]}{\delta \tilde{j}^2} & \frac{\delta^2 W[j, \tilde{j}]}{\delta \tilde{j} \delta j} \\ \frac{\delta^2 W[j, \tilde{j}]}{\delta j \delta \tilde{j}} & \frac{\delta^2 W[j, \tilde{j}]}{\delta j^2} \end{pmatrix}^{-1} = [W^{(2)}]^{-1}, \quad (20)$$

that follows by differentiating (18). Differentiating the latter relation $n-1$ -times with respect to j , using $\frac{\partial}{\partial j} = \frac{\partial x^*}{\partial j} \frac{\partial}{\partial x^*} = (\Gamma^{(2)})^{-1} \frac{\partial}{\partial x^*}$, and repeated application of (20) yields expressions for the n -th cumulant, expressed in terms of derivatives of Γ [64, p. 115ff].

The use of the MSRDJ formalism simplifies the calculations of the effective action with respect to the Onsager-Machlup formalism. As a consequence of the response fields being only auxiliary variables, their expectation values vanish, i.e. $\langle \tilde{x}^n \rangle = 0 \forall n$ for solutions with stationary statistics (for a proof see Coolen [65] or appendix Section IV E).

Computing the effective potential in the MSRDJ formalism

For systems in thermodynamic equilibrium, the deterministic force appearing in (1) can be written as $f(x) = -V'(x)$. As a consequence, the stationary distribution obeys

$$p(x) \propto \exp\left(-\frac{2}{D}V(x)\right). \quad (21)$$

For such systems, de Dominicis has defined an effective potential

$$U_{\text{DD}}[\bar{x}^*] = V(\bar{x}^*) + \dots \quad (22)$$

(see Section IV G i.p. Eq. (80)); here “...” are fluctuation corrections. For a typical network dynamics in multiple dimensions, the deterministic force can usually not be written in such a form. For example, if one considers a coupling term $\sum_j J_{ij}x_j$ between neurons [66]; only for a symmetric matrix $J_{ij} = J_{ji}$ it is the derivative of the potential $V(x) = \frac{1}{2} \sum_{ij} x_i J_{ij} x_j$.

The Onsager-Machlup effective action, however, is fully valid in the non-equilibrium setting. We show in Section IV E that if the effective actions in both formalisms exist they are related by

$$\Gamma_{\text{OM}}[x^*] = \underset{\tilde{x}^*}{\text{extremize}} \Gamma_{\text{MSRDJ}}[x^*, \tilde{x}^*]. \quad (23)$$

Choosing \tilde{x}^* in (23) so that it extremizes Γ_{MSRDJ} , conserves the full information on the fluctuations. The more convenient MSRDJ formalism can therefore be used to perform the actual computation and only subsequently one obtains the physically and probabilistically interpretable Onsager-Machlup form.

Note, however, that the information on the response is not contained in the definition of the corresponding effective potential (13) because the supremum operation in (23) introduces a dependence between \tilde{x} and x which, dually, fixes $\tilde{j} = 0$. Therefore, we cannot choose the perturbation \tilde{j} freely anymore. Eq. (23) holds for arbitrary statistics of the noise, while the analogous relation for the respective actions (9) is in general not true if the noise is not Gaussian, as demonstrated by example in the appendix Section IV F, i.p. Eq. (74).

The definition (23) hence makes the physically interpretable Onsager-Machlup effective action available even if an Onsager Machlup action S_{OM} cannot be formulated in the non-Gaussian case. Therefore, relating approximations of the respective effective actions can be nontrivial: Cooper et al. derived that Γ and Γ_{OM} of the KPZ-model yield the same effective equations if one performs a saddle-point approximation in the auxiliary fields of the Hubbard-Stratonovitch transform of the non-Gaussian parts of the respective actions [67]. We here provide a general relation between the two effective actions, that is valid in full generality beyond specific approximations. It may therefore be used to check whether a pair of approximations, each formulated for one of the two effective actions, is equivalent. The finding by Cooper et al. [67] is one such pair of equivalent approximations.

A simple special case arises if the noise, including all fluctuation corrections, remains Gaussian. The field \tilde{x} then still appears quadratically in the effective action. Taking the supremum over \tilde{x} in (23) is then identical to performing the integral over \tilde{x} . A corollary is that under these conditions, the Onsager-Machlup effective action has the same form as its tree level approximation (5), only with vertices $S^{(n)}$ replaced by effective vertices $-\Gamma^{(n)}$. For example the noise matrix $D = S_{\tilde{x}\tilde{x}}^{(2)}$ is replaced by $-\Gamma_{\tilde{x}\tilde{x}}^{(2)}$; an approximation that is valid if corrections of order $\mathcal{O}(\tilde{x}^3)$ are small. We assume this special case in Figure 1 to determine the effective action including fluctuation corrections.

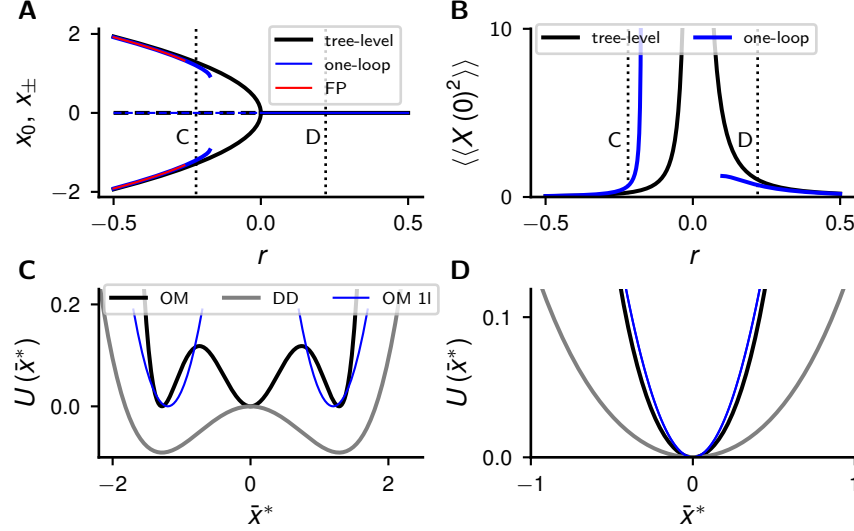


Figure 2. **Critical point at the loss of balance.** Dynamical equation (24) as a model of the population activity. **A** Stationary points of the deterministic system (tree level, black) and the stochastic system (one-loop, blue) as a function of $r = 1 - J$. For $r < 0$, the fixed point $x_0 = 0$ is unstable (dashed lines). Exact solution from Fokker-Planck equation (FP) in red. The dotted vertical lines denote the values of r that are used in panel C and D. **B** Zero-frequency variance $\langle X(0)^2 \rangle - \langle X(0) \rangle^2 = U''_{OM}(\bar{x}^*)^{-1}$ of the stochastic system as a function of r at the stable stationary points determined from the curvature of the tree-level approximation (black) and one loop approximation (blue) of U_{OM} . The one-loop result for $r > 0$ is shown only for $r > r_c$, where r_c is the value of the leak term below which the one-loop corrections are greater than the tree-level contributions (Ginzburg criterion [60, chap. 6.4]), i.e. $|\Gamma_{\bar{x}\bar{x},\text{fl}}^{(2)}| > |r|$. **C** Effective potentials U_{OM} (26) and U_{DD} (27) in the broken symmetry phase ($r = -0.31$, black dotted vertical lines in A and B). Tree level approximation (U_{OM} : black, U_{DD} : gray) and one-loop approximation of U_{OM} (81) (blue); one-loop approximation is expanded up to second order in $\delta x = x^* - x_{\pm}^1$, where $x_{\pm}^1 \neq 0$ is the one-loop stationary point of U_{OM} shown in A (blue curve). **D** Same as C, but in the symmetric phase ($r = 0.22$, black dotted vertical lines in A and B); one-loop result expanded in δx around $x_0 = 0$. For all panels $u = 0.2$ and $D = 0.05$.

Example: De Dominicis and Onsager-Machlup effective actions of a bistable system

To illustrate these two approaches, the de Dominicis equilibrium effective potential (22) and the Onsager-Machlup form (13), we chose a stereotypical setting of a bistable system for which both approaches are possible; the dynamics of a population activity of the form

$$dx(t) + x(t) dt = J(x(t) - \frac{1}{3}x^3(t)) dt + dW(t), \quad (24)$$

shown in Figure 2. We may think of $x - x^3/3$ as the lowest order approximation of the commonly used neuronal non-linearity of the form $\tanh(x)$ and dW is a Wiener increment with variance D . The parameter J plays the role of a synaptic coupling. The deterministic part can be written as the gradient of the potential $V(x) = \frac{r}{2}x^2 + \frac{u}{12}x^4$; the system is hence identical to fluctuations around the equilibrium state of a Ginzburg-Landau model [5, model A]. In this analogy, the parameter $r = 1 - J$ plays the role of the reduced temperature – when it vanishes, the system is at a critical point – and $u = J$ is the strength of the interaction. The fix points in the noiseless case ($D = 0$) are

$$x_0 := 0, \quad x_{\pm} := \pm \sqrt{-\frac{3r}{u}}, \quad \text{for } r < 0; u > 0, \quad (25)$$

The trivial fix point $x_0 = 0$ is stable as long as $r > 0$. As r becomes negative, the two stable fixed points x_{\pm} come into existence. They move out of zero in a continuous manner; the hallmark of a continuous phase transition, shown in Figure 2A. So the system becomes bistable if the level of recurrent positive feedback is high enough; namely at $J > 1$; the deterministic system shows a pitchfork bifurcation. This is what happens in a network if excitation becomes dominant, so that the balanced state [10] is destabilized and a pair of stable states, one at high and another at low activity appear [12]. Furthermore, one notices that the time-scale of fluctuations diverges if $J \rightarrow 1$, $r \rightarrow 0$, because the leak term in (24) vanishes.

In the stochastic system, the effective potential can be used to investigate this continuous phase transition. The corresponding effective potential (13) takes the form

$$\begin{aligned} U_{\text{OM}}(\bar{x}^*) &= \frac{1}{2D} (V'(\bar{x}^*))^2 \\ &= \frac{1}{2D} (\bar{x}^*)^2 \left(r + \frac{u}{3} (\bar{x}^*)^2 \right)^2, \end{aligned} \quad (26)$$

shown in Figure 2B. This effective potential differs from the one constructed by de Dominicis. The latter with (79) yields

$$\begin{aligned} U_{\text{DD}}(\bar{x}^*) &= V(\bar{x}^*) \\ &= \frac{1}{2} (\bar{x}^*)^2 \left(r + \frac{u}{6} (\bar{x}^*)^2 \right), \end{aligned} \quad (27)$$

shown in Figure 2C and D for $r < 0$ and $r > 0$, respectively. However, the fixed points (25) are the stationary points of V and thus of U_{DD} . These are also stationary points of U_{OM} . In addition, U_{OM} has the stationary solutions that are roots of $0 = V''(\bar{x}^*) = r + u(\bar{x}^*)^2$, namely $\bar{x}_{\pm}^* = \sqrt{-\frac{r}{u}}$ (as minima). These are the inflection points of V , which denote the points at which the static theory (21) has a diverging propagator [see also 60, discussion at the end of section 6.4].

The vicinity of the joint stationary points of U_{DD} and U_{OM} can also be seen in the light of equal-time versus frequency-zero fluctuations. The curvature of U_{DD} and hence, to leading order, of V — by (21) — is the inverse of the equal-time covariance $(\frac{2}{D} U_{\text{DD}}''(\bar{x}^*))^{-1} = \langle x(t)x(t) \rangle - \langle x(t) \rangle \langle x(t) \rangle$. The curvature of U_{OM} at a stationary point yields — by (15) and (4) — the covariance of the zero frequency fluctuations $(U_{\text{OM}}''(\bar{x}^*))^{-1} = \langle X(0)^2 \rangle - \langle X(0) \rangle^2$. These two relations show that points of vanishing curvature in both cases (26) and (27) signify the divergence of fluctuations; hence a critical point. In the current example, both effective potentials show that such a fluctuation infinity at the fixed point $\bar{x}^* = 0$ appears if $r = 0$; at the point where the network dynamics changes from inhibition dominance ($r > 0$) to excitation dominance ($r < 0$), shown in Figure 2B. Including the one-loop corrections, the divergence of the fluctuations appears at smaller $r < 0$, whereas for positive r fluctuations are reduced compared to the tree-level approximation. Thus, the transition temperature r_c seems to be shifted towards smaller r which is similar to the Ginzburg-Landau model where fluctuation corrections reduce r_c . The one-loop corrections to the effective potential diverge as $r \rightarrow 0$, as expected at a continuous phase transition. The solution to the equation of state disappears already way above $r = 0$, as shown in Figure 2A. This shows that the behavior of the system close to $r \simeq 0$ is indeed strongly fluctuation-driven and qualitatively different from the simple bifurcation in its deterministic counterpart, the tree-level approximation. This simple example illustrates that deterministic and stochastic models of neuronal activity may show qualitatively quite different behavior in particular at such critical points. The details of the calculations for this model are presented in Section IV H.

For $r < 0$ the system thus possesses two degenerate solutions. If the external drive \tilde{j} to the system is varied, we observe a first order phase transition — as \tilde{j} crosses zero, the mean jumps over from one local minimum of U to the other. As Γ_{OM} , U is convex if we knew it exactly; we would hence have a flat segment between the two local minima in Figure 2C. The non-convexity of the approximations (26) and (27) is an artifact of the simple approximation used here; in particular whether there is a local minimum in U_{DD} or a local maximum in U_{OM} as $\bar{x}^* = 0$ is inconsequential; both would be replaced by a straight line in the convex envelope of U ; the latter is obtained because W , computed as the Legendre transform of the (non-convex) approximation of $\Gamma_{\text{OM/DD}}$, has different left and right-sided derivatives. Transforming back one obtains a convex approximation of Γ and hence U (see Section IV C for a detailed discussion of convexity and differentiability of W).

Note also that on a global scale, the identification of U_{OM} with an energy landscape is not possible, because it assumes stationarity and is therefore only valid near a stable fixed point. As a consequence, the maxima of U_{OM} do not indicate borders of the basin of attraction of this stable fixpoint, contrary to what would be expected for an energy. Moreover, unstable fixed points of the system will show up as minima of U_{OM} , as is obvious from the tree level approximation (12) that is positive semidefinite and vanishes whenever $f(x^*) = 0$.

B. Loop expansion

The effective action characterizes the state of a stochastic system. Fluctuations provide corrections to the effective action that are commonly defined as $\Gamma =: -S + \Gamma_{\text{fl}}$. A standard approach in statistical physics and quantum field theory to obtain these corrections is the loop expansion. For an introduction, consult for example the books by Kleinert [48,

chap. 3.23.] or Zinn-Justin [4, chap. 7.7.ff]. This technique has first been applied in the context of neuronal networks by Buice and Chow [68]; see e.g. [8, 61] for recent reviews.

We here briefly outline the loop expansion on the concrete example for four reasons. First, all terms in the action are at least of linear order in the response field \tilde{x} ; its equation of state therefore always admits a trivial solution $\tilde{x} \equiv 0$ and the $\tilde{x}\tilde{x}$ -propagator vanishes. These are features specific to the MSRDJ formalism that deserve some comments. Second, to illustrate that the Feynman diagrams (sometimes referred to as Mayer graphs [59, 69]) in the one-loop approximation are essentially the same as those that appear in the less standard functional renormalization group method. Third, the loop expansion gives us the leading order fluctuation corrections beyond tree level, $\Gamma = -S$. It will allow us in subsequent sections to derive an effective deterministic equation for the mean and a linear convolution equation for the variance of the process. One-loop corrections also show which new vertices are generated along the renormalization group flow. And fourth, the loop expansion provides a systematic way to derive self-consistency equations for the mean of a process, an idea that is conceptually continued in the functional renormalization group approach to arbitrary orders of the statistics.

In contrast to mean field theory, the loopwise expansion can be improved systematically because it is an expansion in a parameter that measures the fluctuation strength, often related to the system size. Here, we consider a one-dimensional system, but it also depends on a small parameter that organizes the loop expansion, as we will demonstrate below [Section IV I](#).

Because the solvable part of our theory is Gaussian, we express cumulants of higher order by cumulants of order two in x and \tilde{x} . We call

$$\Delta(t-s) = \begin{pmatrix} \langle x(t)x(s) \rangle & \langle x(t)\tilde{x}(s) \rangle \\ \langle \tilde{x}(t)x(s) \rangle & \langle \tilde{x}(t)\tilde{x}(s) \rangle \end{pmatrix} = \begin{pmatrix} \begin{array}{c} x(t) \xleftarrow{\quad} x(s) \xrightarrow{\quad} x(t) \xleftarrow{\quad} \tilde{x}(s) \\ \tilde{x}(t) \xrightarrow{\quad} x(s) \qquad \qquad \qquad 0 \end{array} \end{pmatrix}$$

the propagators of the theory, where we have chosen a representation in time, but we will often switch to frequency space (and back). Further ingredients are the bare interaction vertices which, in general, are given by the non-quadratic components of the action, in our case the Taylor coefficients of the term $\tilde{x}f(x)$.

Henceforth, we consider the corrections to the mean value, the variance and one of the three-point vertices in the neuroscientific case, where $f(x) = -x + Jg(x)$. For small activities we can expand the gain function and keep only its linear and quadratic terms. This is in line with the observation that activation functions are typically convex in the vicinity of the working point [70]. We define

$$g(x) = x + \alpha x^2.$$

Therefore, the only bare vertex is $S_{\tilde{x}xx}^{(3)}$. We choose this quadratic nonlinearity also for pedagogical reasons, as it constitutes the simplest nontrivial example which is suitable to demonstrate the methods. For practical calculations it is convenient to switch the parameterization to

$$f(x) = -lx + \beta x^2, \tag{28}$$

where $l = 1 - J > 0$ and $\beta = \alpha J > 0$. Then in frequency domain the bare propagator reads

$$\begin{aligned} \Delta^0(\omega, \omega') &= (-S^{(2)})^{-1} = \left(\begin{pmatrix} 0 & -i\omega + m \\ i\omega + m & -D \end{pmatrix} \frac{\delta(\omega + \omega')}{2\pi} \right)^{-1} \\ &= \left(\begin{array}{cc} \frac{D}{\omega^2 + m^2} & \frac{1}{-i\omega + m} \\ \frac{1}{i\omega + m} & 0 \end{array} \right) 2\pi \delta(\omega + \omega'), \end{aligned} \tag{29}$$

where $m = -l + 2\beta x^*$ plays the role of a mass-like term in the theory. For the definition of the Fourier transform, as we use it throughout this text, see [Section IV M](#). Similarly, for the interaction vertex we obtain

$$= \frac{1}{2} S_{\tilde{x}XX}^{(3)} = -\frac{\beta}{(2\pi)^2} \delta(\omega_1 + \omega_2 + \omega_3).$$

The frequencies are conserved at each vertex and each propagator. Since in the action $S[x, \tilde{x}]$ the function $f(x)$ is multiplied with one \tilde{x} , see (10), we conclude that the n -th Taylor coefficient of $f(x)$ leads to an interaction vertex with n incoming x -legs and one outgoing \tilde{x} -leg.

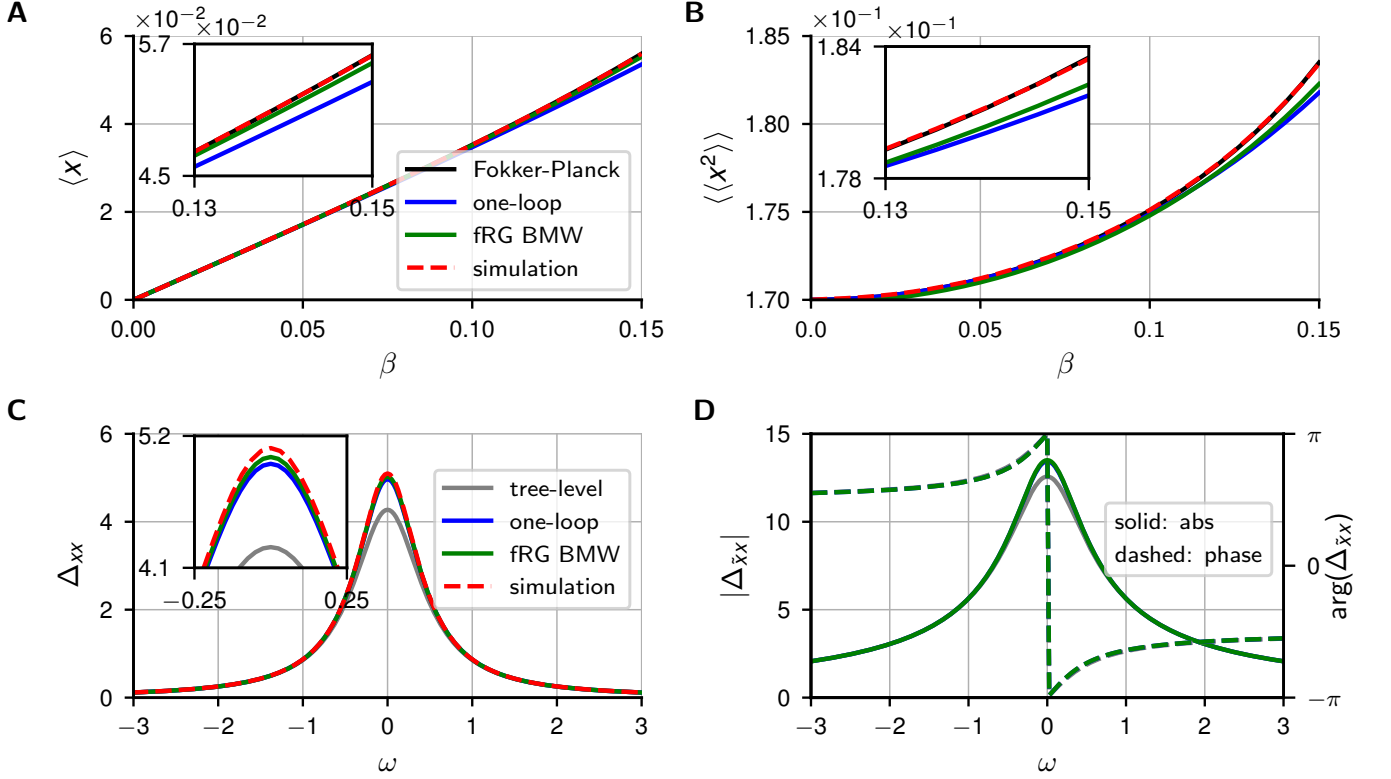


Figure 3. Mean (A) and variance (B) as functions of the strength β of the nonlinearity for different methods. Parameters: $l = 0.5$, $D = 0.17$. C Power spectrum of the system from simulations compared to different approximations. D Absolute value (solid lines) and phase (dashed lines) of the response function. Its zero-mode corresponds to the integrated response of a neural network to a delta-shaped perturbation - for other frequencies the response is weighted according to the respective mode. The results of the one-loop and the fRG BMW approximation coincide at this resolution. For comparison between simulations and theory results of the response of the system was subject to small (but not infinitesimally small) perturbations, see Section II C, Figure 4. Parameters for (C) and (D): $l = 0.5$, $D = 0.17$ and $\beta = 0.15$.

a function of time. Thus it is more complicated than determining the stationary statistics considered here (see e.g. [75] for more details on rare events in meta-stable systems).

We will demonstrate in the next chapter by comparing to simulations that neglecting the possibility of escaping is justified in the presence of a leak term for sufficiently low noise and nonlinearity.

C. Time dependence of statistics

The effective potential contains information about the stationary time-averaged statistics of the system; in particular the mean value and the variance at vanishing frequency. But applications often also require us to study the time-dependent response of the system. In the context of neuronal networks, for example, we would like to quantify the response of the system to an applied stimulus. The simplest approximation (3) that neglects the effect of the noise also provides us with the lowest order approximation of such a response. A special “input” is the noise-mediated influence of the past of the mean value of x on itself. To study this phenomenon, we have to keep \tilde{x} as an independent variable, even if we do not consider an explicit input $-\tilde{j}$ here. In the following we will see how the effective action (17) allows us to systematically describe this effect by deriving an effective integro-differential equation for the mean value. This view will also provide direct interpretations for the derivatives of the effective action, also known as vertex functions: they appear as convolution kernels in the effective equation of motion for the moments of the system. We call derivatives of the action “bare vertices” and those of the effective action “full vertices”.

Effective equations of motion

It turns out that it is convenient to expand Γ around a reference point $(\bar{x}, \bar{\tilde{x}})$

$$\begin{aligned}\Gamma[x^*, \tilde{x}^*] &= \sum_{n=0}^{\infty} \sum_{m=0}^{\infty} \frac{1}{n!m!} \frac{\delta^{n+m}\Gamma}{(\delta x^*)^n (\delta \tilde{x}^*)^m} [\bar{x}, \bar{\tilde{x}}] \delta x^n \delta \tilde{x}^m \\ &= \text{const.} + \Gamma^{(1)}[\bar{x}, \bar{\tilde{x}}] \begin{pmatrix} \delta x \\ \delta \tilde{x} \end{pmatrix} + \frac{1}{2} \begin{pmatrix} \delta x \\ \delta \tilde{x} \end{pmatrix}^T \Gamma^{(2)}[\bar{x}, \bar{\tilde{x}}] \begin{pmatrix} \delta x \\ \delta \tilde{x} \end{pmatrix} + \dots,\end{aligned}\quad (32)$$

where we introduced the derivatives $\frac{\delta^{n+m}\Gamma}{(\delta x^*)^n (\delta \tilde{x}^*)^m}$, the vertex functions, as covectors and the deflections $\delta x(t) := x^*(t) - \bar{x}$ and $\delta \tilde{x}(t) := \tilde{x}^*(t) - \bar{\tilde{x}}$ together with the notation

$$\begin{aligned}& \frac{\delta^{n+m}\Gamma}{(\delta x^*)^n (\delta \tilde{x}^*)^m} [\bar{x}, \bar{\tilde{x}}] \delta x^n \delta \tilde{x}^m \\ &:= \Pi_{i=1}^n \int dt_i \Pi_{j=1}^m \int ds_j \frac{\delta^{n+m}\Gamma[x^*, \tilde{x}^*]}{\delta x^*(t_1) \dots \delta x^*(t_n) \delta \tilde{x}^*(s_1) \dots \delta \tilde{x}^*(s_m)} \Big|_{x^*=\bar{x}, \tilde{x}^*=\bar{\tilde{x}}} \delta x(t_1) \dots \delta x(t_n) \delta \tilde{x}(s_1) \dots \delta \tilde{x}(s_m) \\ &=: \Gamma \left(\underbrace{x \dots x}_{n\text{-times}} \underbrace{\tilde{x} \dots \tilde{x}}_{m\text{-times}} \right) \delta x^n \delta \tilde{x}^m.\end{aligned}\quad (33)$$

We determine the true mean values \bar{x} and $\bar{\tilde{x}}$ of the two fields by solving the two implicit equations $\Gamma^{(1)}[x^*, \tilde{x}^*] \stackrel{!}{=} 0$ (compare (18)). All further Taylor coefficients (or Volterra kernels) in (32) have physical meanings. $\Gamma_{\tilde{x}\tilde{x}}^{(2)}$ includes all corrections to the Gaussian component of the noise and the mixed second order derivatives are the inverse of the response functions. Consequently, $\Gamma^{(2)}$ contains the corrections to the second cumulant since it is the inverse of $W^{(2)}$. The Taylor coefficients of order n describe the interdependence of measurements at n points in time. We make this more explicit by considering $\Gamma_{\tilde{x}\tilde{x}\tilde{x}}^{(3)}$ in the equation of state $\frac{\delta}{\delta \tilde{x}^*(t)} \Gamma[x^*, \tilde{x}^*] = \tilde{j}(t)$, which, using the decomposition $\Gamma = -S + \Gamma_{\text{fl}}$, takes the form

$$\begin{aligned}\tilde{j}(t) &= -\left(\frac{\partial}{\partial t} - f'(\bar{x})\right) \delta x(t) - D \delta \tilde{x}(t) + \frac{1}{2} f''(\bar{x}) \delta x(t) \delta x(t) + \dots \\ &\quad + \int ds \Gamma_{\tilde{x}\tilde{x}, \text{fl}}^{(2)}(t, s) \delta x(s) \\ &\quad + \frac{1}{2} \int ds \int du \Gamma_{\tilde{x}\tilde{x}\tilde{x}, \text{fl}}^{(3)}(t, s, u) \delta x(s) \delta x(u) + \dots\end{aligned}\quad (34)$$

The second equation of state (18) $\Gamma_x^{(1)} = j \equiv 0$ admits the solution $\tilde{x}^* = 0$ if probability is conserved (see e.g. Section IV A). Thus, Γ_{fl} accounts for the corrections due to the noise. Additionally, we neglect all higher order terms as well as the remaining components of $\Gamma^{(3)}$, which are subleading, as we discuss in Section II D after (46). Looking at the fluctuation corrections in (34), we notice that in general the noisy system exhibits interactions that are non-local in time (cf. (33)) even if the deterministic system does not contain such terms. As a consequence, it is not possible to define a potential for which $\partial_t x(t) = -\partial_x V(x)$ even if we set $\tilde{x} = 0$, in contrast to the tree-level approximation of a one-dimensional system. The first occurrence of an effective equation of motion as (34) in the context of neuronal networks has been presented in [76, eqs. (42) and (43)] using the Doi-Peliti formalism [77, 78] applied to Markovian systems with discrete state spaces.

Relaxation of a small departure from the mean

As an example, we consider the response of the system to a stimulus, represented by the deflection of the system from its mean value at time $t_0 = 0$ by setting $\tilde{j}(t) = -\delta x(0) \delta(t)$ in (34) and examine the equation of motion that describes its relaxation back to the baseline. We ensure that we consider only non-escaping trajectories by setting $\tilde{x} \equiv 0$ (see Section IV A). By inserting the tree-level approximation $\Gamma_{\text{fl}} = 0$ into (34), we obtain

$$\partial_t \delta x(t) = -l \delta x(t) + \beta \delta x(t)^2,$$

which we can integrate analytically

$$\delta x(t) = \frac{l}{\beta} \frac{1}{1 + e^{lt} \left(\frac{l}{\beta c} - 1 \right)} = c e^{-(l-c\beta)t + \mathcal{O}((lt)^2)} + \mathcal{O}\left(\left(\frac{\beta c}{l}\right)^2\right), \text{ where } c = \delta x(0).$$

We notice that the second term in the denominator is due to the nonlinearity and leads to a slower relaxation of the system back to its mean value compared to the time constant l^{-1} of the linear part of the dynamics. In one-loop approximation, the equation of motion reads

$$\begin{aligned} \partial_t \delta x(t) = & m \delta x(t) + \beta \delta x(t)^2 \\ & - \frac{2\beta^2 D}{m} \int_{t_0}^t dt' \underbrace{e^{2m(t-t')}}_{\propto \Gamma_{\bar{x}, \text{fl.}}^{(2)}(t, t')} \delta x(t') \\ & - \frac{8\beta^3 D}{m} \int_{t_0}^t dt' \int_{t_0}^t dt'' \underbrace{H(t' - t'') e^{2m(t-t'')}}_{\propto \Gamma_{\bar{x}xx, \text{fl.}}^{(3)}(t, t', t'')}, \end{aligned} \quad (35)$$

where $H(t)$ denotes the Heaviside step function. Let us inspect the single terms in (35) in more detail: The first line is the tree-level contribution. $\Gamma_{\text{fl.}}^{(2)}$ mediates a linear self-feedback for the departure δx of the process from its stationary value. One of the interpretations of $\Gamma_{\bar{x}xx}^{(3)}$, writing it as $\Gamma_{\bar{x}xx}^{(3)}(t, t', t'') = \frac{\delta}{\delta x(t'')} \Gamma_{\bar{x}x}^{(2)}(t, t')$, is that it quantifies the change of the linear response kernel of the self-energy at times t, t' due to a change of the activity at time t'' . This shows that only the interplay between an interaction and noise, as apparent by the prefactors composed of both β and D , creates a self-interaction of the mean that is non-local in time. This phenomenon is also generally observed if certain degrees of freedom are implicitly taken into account to describe the quantity of interest [79, e.g. chap. 1.6].

An alternative way to arrive at (35) is to derive ODEs for the first two moments from the Fokker-Planck equation [58] and to use a Gaussian closure. The loop expansion then amounts to a Taylor expansion of the Fokker-Planck solution in δx and assuming that $\langle x^3 \rangle \ll \langle x^2 \rangle$, $\langle x \rangle$ (known as Gaussian closure), as we show in detail in Section IV J.. In Figure 4 we compare the full Fokker-Planck solution with Gaussian closure to the one-loop result. Indeed, the semi-logarithmic plot of the relaxation as a function of time shows an elevated time constant due to fluctuations compared to the tree-level approximation. Analyzing the origin of the elevated time constant, Figure 4C compares the different contributions to the right hand side of (35). The linear part of the tree-level approximation yields the largest contribution. For sufficiently long times, we find that the linear part of the one-loop correction comes next with opposite sign compared to the term stemming from the bare interaction: This shows that only the cooperation of the non-linearity with the fluctuations in the system causes this correction and is more important than the non-linearity itself, the quadratic tree level contribution. Furthermore, the three-point interaction gets enhanced by the fluctuation corrections, so that in total, the relaxation is slower than in the deterministic system.

In the context of neuronal dynamics this example shows how the response of a system to a stimulus is shaped by the presence of non-linearities and noise. An increase of the time scale of the response may be employed by such systems to implement increased memory for past stimuli. In heterogeneous networks, where the linear part of the dynamics is given by a matrix that couples different neurons as $dx(t) = -x(t) + Jx(t)dt + \dots$, the effective leak term $m = J - 1$ correspondingly becomes a matrix. The i -th eigendirection of the matrix then evolves with time-scale $(\lambda_i - 1)^{-1}$. For random connectivity, the eigenvalues are typically circularly distributed in the complex plane [80]; thus a quasi-continuum of time-scales appears already in tree-level approximation [1, Fig 6]. The one loop corrections to the self-energy generate additional time-scales, as shown in eq. (35) and also (83) and (84) for the one-dimensional case. The emergence of multiple time-scales has been discussed previously in the literature. Some works proposed multiple adaptation mechanisms as the origin [81]. Others have shown that time scales of responses to stimuli may change systematically within the hierarchy of a complex neuronal network, from fast time-scales in early areas, to long ones in higher levels of the hierarchy [82]. Loop corrections obtain an important meaning when considering the influence of non-recorded neurons on the correlation structure of the observed ones [83]: A one-loop correction to the self-energy in this context contains the reverberation of activity within the network, thus including the indirect effect due to the presence of non-recorded neurons. Such reverberations generate additional time-scales in the mutual coupling kernel between individual neurons, mediated via the non-recorded intermediate cells.

Power spectrum So far we have discussed an effective equation of motion for the mean value of the process that also allowed us to obtain an interpretation for the various vertex functions. We can ask a corresponding question for the second order statistics, namely whether there is a linear system that possesses the same second order statistics as the full non-linear system. Such a reduction may be useful to obtain insights into the structure of network fluctuations and also to reduce the complexity of stochastic non-linear systems to simpler, linear ones.

Indeed, we can use the expressions for the derivatives of the effective action to write down the action of a linear system that, up to second order, reproduces the stationary statistics of the full system. To this end we define

$$S_{\text{lin}} := - \left(\delta \tilde{x}^T \Gamma_{\bar{x}x}^{(2)} \delta x + \frac{1}{2} \delta \tilde{x}^T \Gamma_{\bar{x}\bar{x}}^{(2)} \delta \tilde{x} \right). \quad (36)$$

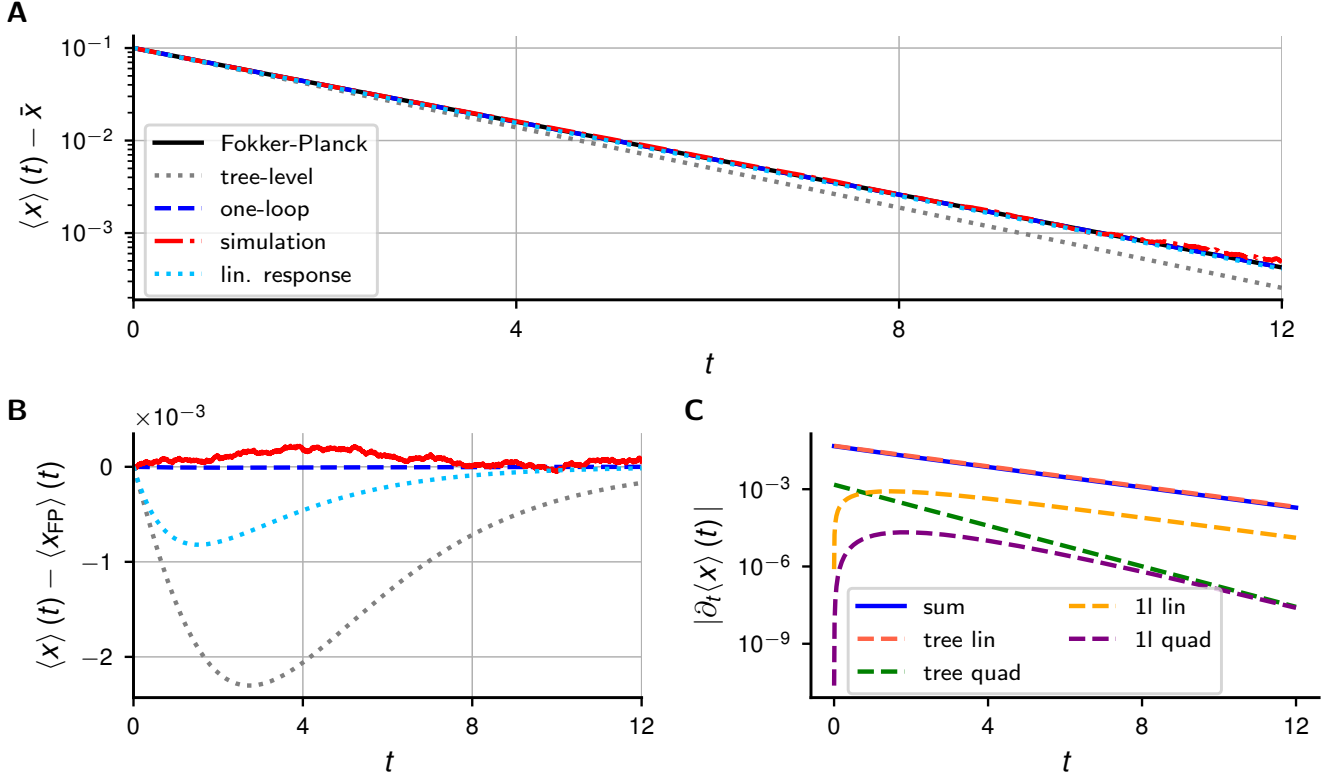


Figure 4. Relaxation after deflection described by effective equation of motion. The one-loop result is given by (35) and the Fokker-Planck result by the coupled differential equations (86) and (87). For the simulations, we let the activity of the system decay to its baseline and then stimulate it by a small perturbation δx_0 applied to the current value of x . Subsequently, the activity relaxes back to its stationary state. **A** Mean activity averaged over $2.9 \cdot 10^9$ trials of the relaxation process. **B** Difference between the various approximations and the simulation to the Fokker-Planck result. The linear response (dotted light blue) contains solely the terms in (35) that are linear in δx . **C** Different contributions to the right hand side of (35). Sum shows the full right hand side (blue); linear part in δx of the tree level term (dashed salmon pink); quadratic part in δx of the tree level terms (dashed green); linear term of one-loop correction (dashed yellow); quadratic term of one-loop corrections (dashed violet).

The corresponding equation of motion reads

$$\frac{d}{dt} \delta x(t) = -l \delta x(t) + \int dt' \Gamma_{\tilde{x}x, \text{fl.}}^{(2)}(t, t') \delta x(t') + \xi(t), \quad (37)$$

where $\langle \xi(t) \rangle = 0$ and $\langle \langle \xi(t) \xi(t') \rangle \rangle = D \delta(t - t') + \Gamma_{\tilde{x}\tilde{x}, \text{fl.}}^{(2)}(t, t')$.

By construction this stochastic integro-differential equation (37) reproduces the stationary variance $\Delta_{xx}(t, s) = W_{xx}^{(2)}(t, s) = \langle \delta x(t) \delta x(s) \rangle$ as well as the linear response $\Delta_{x\tilde{x}}(t, s) = W_{x\tilde{x}}^{(2)}(t, s) = \langle \delta x(t) \delta \tilde{x}(s) \rangle$ of the full system, because the solution of the Gaussian system (36) implicitly inverts the kernel $\Gamma^{(2)}$, which, by (20), yields the covariance matrix $W^{(2)}$. We could also take into account the effect of transient values of $x(t)$ on the variance to obtain a corresponding reduction that is valid in the non-stationary case. For this, however, we would need to know $\Gamma_{\tilde{x}x, \text{fl.}}^{(2)}$ evaluated at arbitrary $x(t)$. In this case, it is therefore more convenient to use the second Legendre transform that treats the variance as given, just like x^* in the case of the first Legendre transform, as shown by Bravi and co-workers [84].

The construction of a linear system leads to a new perspective of the effect of the nonlinearity: Up to the second cumulant, the nonlinear system is equivalent to a linear one with a specific causal memory kernel and a corresponding non-white Gaussian noise term, caused by the self-energy correction $\Gamma_{\tilde{x}\tilde{x}}^{(2)}$.

D. Functional Renormalization Group

The loopwise expansion, by virtue of approximating the effective action, yields self-consistent equations for the mean. But we saw above that also the second order statistics and the higher order vertex functions experience fluctuation corrections. One would therefore like to have a scheme that is self-consistent also with regard to these higher order vertex functions.

One possible approach that has lead to reasonable results, is to correct the mean, the propagator and the interaction vertex by the one-loop results and therein replace the bare quantities by the corrected ones to gain an even better approximation. This procedure is repeated until the result eventually converges. This approach corresponds to taking into account only specific diagrams with infinitely many loops and is called self-consistent one-loop approximation. It typically corrects the mean value and the self-energy while keeping the interaction vertices at their bare values; it is then known as the ‘‘Hartree-Fock approximation’’ [8, 59]. But of course this scheme can be extended to arbitrary order of the vertex functions. A formal way to derive such approximations systematically is by multiple Legendre transforms, an idea going back to the seminal work by De Dominicis and Martin [85]: One re-expresses interaction potentials in terms of connected correlation functions. Parquet equations are, for example, obtained by the fourth Legendre transform of an even theory [see e.g. 59, for a review, especially chap. 6.2.10].

We here want to follow a different scheme that is inherently self-consistent to arbitrary desired orders, the functional renormalization group (fRG). The fRG scheme naturally takes into account fluctuation corrections by renormalizing the mean value, the propagators, and all interaction vertices simultaneously.

Technically, the functional Renormalization Group (fRG) [34] is an alternative way to calculate Γ . It is one of the exact Renormalization Group (eRG) schemes [35, 86, 87], in essence going back to the seminal work by Wegner and Houghton [33]. It does not rely on an expansion in a small parameter, in contrast to the loopwise expansion, but it is nevertheless represented by diagrams with a one-loop structure. The technique induces an infinite hierarchy of coupled differential equations for $\Gamma^{(n)}$, so that in practice, we have to apply approximations, typically by truncating the hierarchy. Yet, this technique is, as all exact Renormalization Group-schemes, exact only on the level of the full functional $\Gamma[x, \tilde{x}]$ and not for a particular truncation in terms of a subset of $\Gamma^{(n)}$.

The essential technical trick of the fRG is to simplify the theory by adding an initially large quadratic term, the regulator R_λ , to the action. It is a differentiable function of a so called flow parameter λ and can be chosen arbitrarily up to the following properties:

$$\lim_{\lambda \rightarrow \Lambda} |R_\lambda| = \infty \text{ and } \lim_{\lambda \searrow 0} R_\lambda = 0. \quad (38)$$

The first property ensures that the theory for $\lambda = \Lambda$ has no fluctuations and its vertices correspond to the ones of the bare action, while for $\lambda = 0$, the original system is recovered. For more complicated systems it is necessary that the regulator is consistent with the symmetries of the effective action, so that they are conserved during the flow. To interpolate between the two limits of the non-interacting and the full system, a functional differential equation for the effective action is derived by differentiating with respect to λ . This is the Wetterich equation [34], whose derivation for our setting, in particular for the presence of the response field, we will sketch in the following adhering to the conventions of Berges et al. [35]. We will derive the Wetterich equation for the effective action evaluated at stationary X^* and \tilde{X}^* so that the resulting equation boils down to an ODE.

Since the regulator R_λ is intended to suppress fluctuations, it is sufficient for our case to add it to the off-diagonal terms of the free part of the action, defining

$$\begin{aligned} S_\lambda[X, \tilde{X}] &= S_0[X, \tilde{X}] + \Delta S_\lambda[X, \tilde{X}] + S_{\text{int}}[X, \tilde{X}], \quad \text{where} \\ \Delta S_\lambda[X, \tilde{X}] &= -\frac{1}{2} \int \frac{d\omega}{2\pi} \begin{pmatrix} X(-\omega) \\ \tilde{X}(-\omega) \end{pmatrix} \begin{pmatrix} 0 & \frac{1}{2}R_\lambda \\ \frac{1}{2}R_\lambda & 0 \end{pmatrix} \begin{pmatrix} X(\omega) \\ \tilde{X}(\omega) \end{pmatrix} \\ S_{\text{int}}[X, \tilde{X}] &= -\beta \int \frac{d\omega}{2\pi} \int \frac{d\omega'}{2\pi} \tilde{X}(\omega) X(\omega') X(-\omega - \omega'). \end{aligned} \quad (39)$$

By (29), the regulator modifies the leak term m , thus controlling the variance of the fluctuations. A general discussion on the choice of frequency-dependent regulators can be found in [88]: The XX -diagonal element must always be zero to maintain normalization (see also Section IV A). A regulator on the $\tilde{X}\tilde{X}$ element corresponds to a modification of the second cumulant of the driving noise. For systems in equilibrium, the fluctuation-dissipation theorem constrains the choice of the regulator further.

For the choice in (39), the bare propagator reads

$$\Delta_\lambda^0(\omega, \omega') = \begin{pmatrix} \frac{D}{\omega^2 + (m + \frac{1}{2}R_\lambda)^2} & \frac{1}{-i\omega + m + \frac{1}{2}R_\lambda} \\ \frac{1}{i\omega + m + \frac{1}{2}R_\lambda} & 0 \end{pmatrix} 2\pi\delta(\omega + \omega').$$

We notice that R_λ has to be negative to avoid a vanishing leak term (since $m < 0$) and thus a fluctuation singularity at $\omega = 0$ along the RG trajectory. We define $\tilde{\Gamma}_\lambda[X^*, \tilde{X}^*]$ as the Legendre transform of the cumulant generating functional, given by

$$W_\lambda[J, \tilde{J}] = \ln \int \mathcal{D}X \int \mathcal{D}\tilde{X} \exp(S_\lambda[X, \tilde{X}] + J^T X + \tilde{J}^T \tilde{X}),$$

where we used the abbreviation $J^T X = \int d\omega J(\omega)X(\omega)$. Defining Γ_λ , we remove the “direct” effect of the regulator

$$\Gamma_\lambda[X^*, \tilde{X}^*] := \tilde{\Gamma}_\lambda[X^*, \tilde{X}^*] + \Delta S_\lambda[X^*, \tilde{X}^*], \quad (40)$$

so that $\lim_{\lambda \rightarrow \Lambda} \Gamma_\lambda = -S$ and $\lim_{\lambda \rightarrow 0} \Gamma_\lambda = \Gamma$. To derive the flow equation for the effective action of the theory defined in (39), we take the partial derivative of W_λ with respect to the flow parameter and deduce from this the respective derivatives of $\tilde{\Gamma}_\lambda$ and Γ_λ (for details consult appendix Section IV K), which results in the Wetterich equation

$$\begin{aligned} \frac{\partial \Gamma_\lambda[X^*, \tilde{X}^*]}{\partial \lambda} &= \frac{1}{2} \text{Tr} \left\{ \Delta_{\tilde{X}X, \lambda} \frac{\partial R_\lambda}{\partial \lambda} \right\} \\ &= \frac{1}{2} \text{Tr} \left\{ \left[\Gamma_\lambda^{(2)}[X^*, \tilde{X}^*] + \begin{pmatrix} 0 & \frac{1}{2} R_\lambda \\ \frac{1}{2} R_\lambda & 0 \end{pmatrix} \right]_{\tilde{X}X}^{-1} \frac{\partial R_\lambda}{\partial \lambda} \right\} = \frac{1}{2} \text{ (diagram) }, \end{aligned} \quad (41)$$

where in this section, lines denote full propagators

$$\Delta_\lambda := \left(\tilde{\Gamma}_\lambda^{(2)} \right)^{-1} = \left(\Gamma_\lambda^{(2)} + \begin{pmatrix} 0 & \frac{1}{2} R_\lambda \\ \frac{1}{2} R_\lambda & 0 \end{pmatrix} \right)^{-1} \quad (42)$$

and open squares represent $\frac{\partial R_\lambda}{\partial \lambda}$. For the final result ($\lambda = 0$), the choice of the concrete form of R_λ is arbitrary as long as it fulfills (38) and does not lead to acausal terms in the action. The interpretation of Γ_λ along the trajectory of the flow equations, however, depends on the regulator.

The simplest choice is the uniform regulator, for example $R_\lambda = -\lambda$. In this case all frequencies get damped equally. Its equivalence to an additional leak term (compare (10) and (42)) bears a second interpretation: We may as well interpret each point along the solution of the flow equation as one system with a different value for the leak term. In this context, a vanishing value and hence a pole in the propagator at vanishing frequency becomes meaningful again: it corresponds to a critical point where fluctuations dominate the system behavior.

The simplest measure to extract from Γ_λ is the mean value \tilde{x}_λ defined by the equation of state $\tilde{\Gamma}_{\tilde{x}, \lambda}^{(1)}[x_\lambda^*, \tilde{x}_\lambda^*] = 0$ ⁵. Differentiating this equation with respect to λ leads to

$$\begin{aligned} 0 &= \frac{d}{d\lambda} \tilde{\Gamma}_\lambda^{(1)}(\omega) = \frac{\partial \tilde{\Gamma}_\lambda^{(1)}(\omega)}{\partial \lambda} + \int d\omega' \tilde{\Gamma}_\lambda^{(2)}(\omega, \omega') \frac{\partial}{\partial \lambda} \left(\tilde{X}_\lambda(\omega') \right) \\ \Leftrightarrow \frac{\partial}{\partial \lambda} \left(\tilde{X}_\lambda(\sigma) \right) &= -\Delta_\lambda(\sigma) \left[\frac{\partial \Gamma_\lambda^{(1)}(-\sigma)}{\partial \lambda} + \frac{1}{4\pi} \frac{\partial R_\lambda}{\partial \lambda} \left(\tilde{X}_\lambda(\sigma) \right) \right]. \end{aligned} \quad (43)$$

To obtain (43), we have multiplied the line above by the propagator Δ_λ and used $\Delta_\lambda \tilde{\Gamma}_\lambda^{(2)} = 1$. We observe that we

⁵ The condition $\tilde{\Gamma}_{\tilde{x}, \lambda}^{(1)}[x_\lambda^*, \tilde{x}_\lambda^*] = 0$ would of course lead to the same result because we are eventually interested in $\lambda = 0$, where both quantities agree, but using $\tilde{\Gamma}$ leads to the occurrence of the propagator including the regulator term in (43), which is more convenient.

by

$$\begin{aligned}
\frac{\partial \Gamma_{\tilde{X}X,\lambda}^{(2)}(\sigma_1, \sigma_2)}{\partial \lambda} &= \frac{1}{2} \text{diagram 1} + \frac{1}{2} \text{diagram 2} \\
&+ \frac{1}{2} \text{diagram 3} \\
\frac{\partial \Gamma_{\tilde{X}\tilde{X},\lambda}^{(2)}(\sigma_1, \sigma_2)}{\partial \lambda} &= \frac{1}{2} \text{diagram 4} + \sigma_1 \leftrightarrow \sigma_2.
\end{aligned}$$

The translation of these diagrams is shown in [Section IV L](#) where also the respective diagrams for the interaction vertex are shown. In general, the diagrams have the same form as those that appear in the fluctuation expansion, except for the presence of a single regulator in one of the propagator lines. The combination of two propagators “sandwiching” a regulator $\Delta_\lambda(\omega, -\omega) \frac{\partial R_\lambda}{\partial \lambda}(\omega, -\omega) \Delta_\lambda(\omega, -\omega)$ is called single scale propagator, because the regulator is often chosen in a way such that its derivative is peaked around frequencies with $|\omega| = \lambda$, thus contributing at a single scale. Due to the one-loop structure of the diagrams and the conservation of frequencies at the vertices, we have to perform one integral over an internal frequency for every possible combination of fixed external frequencies. Therefore the numerical evaluation of $\Gamma^{(n)}$ becomes increasingly computationally expensive for higher orders because at n -th order we have $n - 1$ independent external frequencies. For practical computations we thus have to truncate the hierarchy after $n = 3$ if we want to keep the full frequency dependence of $\Gamma^{(n)}$. Even at this order, the integration takes many hours on a usual desktop PC when we choose the external frequencies to range from -25 to 25 with a resolution of 0.1 . Therefore, it is legitimate to ask if one can reduce the number of required frequency-integrals by assuming a simplified frequency-dependence of higher order vertices.

1. The BMW scheme

A scheme that assumes a simplified momentum dependence of higher order vertices has been suggested by Blaizot, Méndez and Wschebor (BMW, [\[45, 90\]](#)). It has been successfully applied for example to the Kardar-Parisi-Zhang model [\[91\]](#). The principal idea is to neglect the frequency-dependence of the effective action as much as possible. The most radical choice in this respect would be to assume it to be constant, which is known as the local potential approximation (LPA). BMW refined this scheme by including the exact frequency-dependence of all vertices up to a certain order s , which are functions of $s - 1$ external frequencies, and to approximate vertices of the next two orders by evaluating the additional derivatives at their zero frequency-components obtaining a partial differential equation [\[92\]](#). We will pursue a different route by deriving approximate flow equations for $\Gamma^{(s+1)}$ and $\Gamma^{(s+2)}$ with the simplified frequency dependence.

More precisely, we consider a typical contribution of a vertex within the Wetterich flow equation for the vertex $\Gamma^{(s)}$ containing

$$\begin{aligned}
&\Gamma_\lambda^{(s+1)}(\sigma_1, \dots, \sigma_s + \omega, -\omega), \\
&\Gamma_\lambda^{(s+2)}(\sigma_1, \dots, \sigma_s, \omega, -\omega),
\end{aligned} \tag{47}$$

where ω is the loop frequency, that represents the frequency at the regulator. For simplicity we do not specify different components of the field. For the approximation we assume the vertices to depend only weakly on ω and therefore set $\omega = 0$ in [\(47\)](#), replacing the vertices by

$$\begin{aligned}
&\Gamma_\lambda^{(s+1)}(\sigma_1, \dots, \sigma_s, 0), \\
&\Gamma_\lambda^{(s+2)}(\sigma_1, \dots, \sigma_s, 0, 0).
\end{aligned} \tag{48}$$

The frequency dependence on ω in the propagators and the regulator is, however, kept.

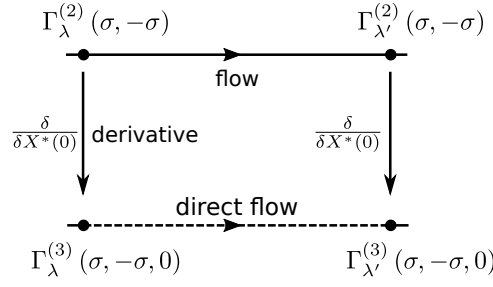


Figure 5. Implementation of the BMW scheme within the vertex expansion. In the original formulation (top) we have to evaluate the derivatives $\delta/\delta X^*(0)$ numerically at each λ . In the new interpretation (bottom) we derive an additional flow equation for $\Gamma^{(3)}(\sigma, -\sigma, 0)$ (dashed line).

The second step of the BMW scheme allows the closure of the system: Due to the vanishing momentum on one or two legs of the vertices (48), the vertex functions with $s+1$ and $s+2$ legs can be expressed as the derivative of $\Gamma_\lambda^{(s)}$ with respect to a uniform (background) field $X_0^* \coloneqq X^*(\sigma=0)$:

$$\Gamma_\lambda^{(s+1)}(\sigma_1, \dots, \sigma_s, 0) = \frac{\delta}{\delta X_0^*} \Gamma_\lambda^{(s)}(\sigma_1, \dots, \sigma_s) \quad (49)$$

$$\Gamma_\lambda^{(s+2)}(\sigma_1, \dots, \sigma_s, 0, 0) = \frac{\delta^2}{\delta X_0^{*2}} \Gamma_\lambda^{(s)}(\sigma_1, \dots, \sigma_s). \quad (50)$$

If we now use (49) and (50) to replace $\Gamma_\lambda^{(s+1)}$ and $\Gamma_\lambda^{(s+2)}$ by the ordinary derivatives of $\Gamma_\lambda^{(s)}$ with respect to the zero-modes of X , \tilde{X} , we close the set of flow equations and additionally we take into account the flow of order $s+1$ and $s+2$, at least approximately. Since we reduced the number of independent frequencies by one (or two, respectively), the computation time decreases significantly.

But the resulting equation is a partial differential equation in λ and X_0^* [92, eq. (19)]; we hence have to evaluate the derivatives with respect to X_0^* for every step at which we compute $\partial_\lambda \Gamma^{(s)}$. Below we develop an alternative scheme that circumvents this complication and entirely stays within the realm of a vertex expansion.

2. Removing the PDE

We aim to apply the BMW approximation at order $s=2$, thus keeping the full frequency dependence of the self-energy. However, within the vertex expansion scheme it remains unclear how to compute the derivatives of $\Gamma^{(2)}$ numerically. This is because at each given λ we know the value of $\Gamma^{(2)}$ only for the true mean value $\tilde{X}_\lambda(0)$, but not in a vicinity around it; we therefore cannot approximate the derivative by a quotient built from finite differences.

We can circumvent this problem by deriving an additional flow equation for $\Gamma_\lambda^{(3)}(\sigma_1, \sigma_2, 0)$ (illustrated in Figure 5; the more complex situation with x and \tilde{x} fields will be addressed below) and in principle also for $\Gamma_\lambda^{(4)}(\sigma_1, \sigma_2, 0, 0)$, which we neglect in our model because the largest contribution of $\Gamma^{(4)}$ is suppressed by a factor β due to an additional interaction vertex. We obtain this flow equation by differentiating the flow equation for $\Gamma_\lambda^{(2)}$ with respect to $X^*(0)$, i.e. $\frac{\delta}{\delta X^*(0)} \partial_\lambda \Gamma_\lambda^{(2)} = \partial_\lambda \Gamma_\lambda^{(3)}$ and then setting those frequencies of the original three-point vertices to zero that are connected to the single scale propagator, in line with the BMW scheme. But we need to keep the dependence on ω of the vertices that emerge when we differentiate a propagator by the background field, so that we treat the frequency dependence of this additional vertex like that of the regulator in the original diagram. Otherwise we would make an additional approximation on top of BMW. Thus, drawing only the first argument of the propagators, in diagrammatic

language we obtain

$$\begin{aligned}
 \frac{\delta}{\delta X(0)} \frac{\partial \Gamma_{\lambda}^{(2)}(\sigma_1, -\sigma_1)}{\partial \lambda} &= \frac{\delta}{\delta X(0)} \frac{1}{2} \text{diagram (1)} \\
 &\quad \text{diagram (1)}: \text{circle with vertices (1) and (2), wavy lines } \sigma_1, \sigma_2, \text{ and } \sigma_1 + \omega, \text{ and a square box on the top arc.} \\
 &\quad \text{diagram (2)}: \text{circle with vertices (3), (4), (5), and (6), wavy lines } \sigma_1, \sigma_2, \text{ and } \sigma_1 + q, \text{ and a square box on the right arc.} \\
 &\quad \text{diagram (3)}: \text{circle with vertices (6), (7), (8), and (9), wavy lines } \sigma_1, \sigma_2, \text{ and } \sigma_1 + q, \text{ and a square box on the top arc.} \\
 &\quad \text{diagram (4)}: \text{circle with vertices (9) and (10), wavy lines } \sigma_1, \sigma_2, \text{ and } \sigma_1 + \omega, \text{ and a square box on the top arc.} \\
 &\quad + \sigma_1 \leftrightarrow -\sigma_1
 \end{aligned}$$

where the vertex functions are given by

$$\begin{aligned}
 (1) : \Gamma_{\lambda}^{(3)}(\sigma_1, \omega, -\sigma_1 - \omega) & \quad (2) : \Gamma_{\lambda}^{(3)}(-\sigma_1, -\omega, \sigma_1 + \omega) \\
 (3) : \Gamma_{\lambda}^{(3)}(\sigma_1, 0, -\sigma_1) & \quad (4) : \Gamma_{\lambda}^{(3)}(-\sigma_1, 0, \sigma_1) & \quad (5) : \Gamma_{\lambda}^{(3)}(\omega, -\omega, 0) \\
 (6) : \Gamma_{\lambda}^{(3)}(\sigma_1, 0, -\sigma_1) & \quad (7) : \Gamma_{\lambda}^{(3)}(-\sigma_1, 0, \sigma_1) & \quad (8) : \Gamma_{\lambda}^{(3)}(\sigma_1 + \omega, -\sigma_1 - \omega, 0) \\
 (9) : \Gamma_{\lambda}^{(4)}(\sigma_1, 0, -\sigma_1, 0) & \quad (10) : \Gamma_{\lambda}^{(3)}(-\sigma_1, 0, \sigma_1)
 \end{aligned}$$

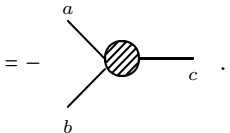
The crucial point to notice is that all vertices that appear in the diagrams have only two nonzero frequencies. The set of differential equations is therefore closed; the last diagram requires a four point vertex for which we can obtain a flow equation analogously. So we have found an explicit flow equation for $\Gamma_{\lambda}^{(3)}(\sigma_1, \sigma_2 = -\sigma_1, 0)$, indicated by the dashed line in [Figure 5](#). As a consequence we have to solve a coupled set of ODEs instead of a PDE.

If we do not want to neglect the flow of the four point vertex completely, we can differentiate the diagrams once again, which leads to a flow equation of $\Gamma_{\lambda}^{(4)}(\sigma_1, \sigma_2, 0, 0)$. This flow equation then depends on $\Gamma_{\lambda}^{(3)}(\sigma_1, \sigma_2, 0)$, $\Gamma_{\lambda}^{(4)}(\sigma_1, \sigma_2, 0, 0)$ and $\Gamma_{\lambda}^{(5)}(\sigma_1, \sigma_2, 0, 0, 0)$. Due to the emergence of the latter, the set of equations can be closed only if we truncate the series at some order (unlike the original BMW scheme).

The scheme described above also generalizes to the case where we have two fields components x, \tilde{x} and the corresponding propagators $\Delta_{\tilde{x}x}, \Delta_{xx}$. We then get two sets of twelve diagrams each (compare [Section IV L](#)) the first of which describing the flow of the two one-dimensional sections $\Gamma_{\tilde{x}xx, \text{fl.}}^{(3)}(0, \sigma_1, -\sigma_1)$ (type 1) and the second one that of $\Gamma_{\tilde{x}xx, \text{fl.}}^{(3)}(\sigma_1, -\sigma_1, 0)$ (type 2). Every diagram consists of three three-point interaction vertices that are either of type 1 or of type 2. Thus, the common flow of the two sections is computed consistently within this approximation.

[Figure 6](#) compares the three point vertices obtained from the truncated flow equation to the result from the BMW approximation. The latter of course only yields the three-point vertex $\Gamma_{\tilde{x}xx}^{(3)}(\sigma_1, \sigma_2, \sigma_3)$ along the one-dimensional sections $-\sigma_1 = \sigma_2 + \sigma_3 = 0$ (type 1, panel C) and $\sigma_3 = 0$ (type 2, panel B). The agreement between the two approximations is high. This result is to be expected, since the fluctuation corrections per se are small in the regime considered, so that the bare vertices still constitute the largest contributions to any fluctuation correction.

Even though we here consider the dynamics of a single neuron, the formalism transparently extends to compute higher order statistics of neuronal activity also across different neurons, a topic of considerable interest [\[93\]](#). Once the vertex functions $\Gamma^{(n)}$ are known, all higher order cumulants can be computed as tree graphs, with vertex functions as nodes and edges formed by the full propagators $(\Gamma^{(2)})^{-1}$ (see e.g. Zinn-Justin [\[4, Section 6.3\]](#) or Helias and Dahmen [\[61, Section XIII\]](#)). The third order cumulants, for example, follow as

$$\begin{aligned}
 W_{abc}^{(3)} &= - \sum_{a'b'c'} \Gamma_{a'b'c'}^{(3)} (\Gamma^{(2)})_{a'a}^{-1} (\Gamma^{(2)})_{b'b}^{-1} (\Gamma^{(2)})_{c'c}^{-1} \\
 &= - \text{diagram (a)}
 \end{aligned}$$


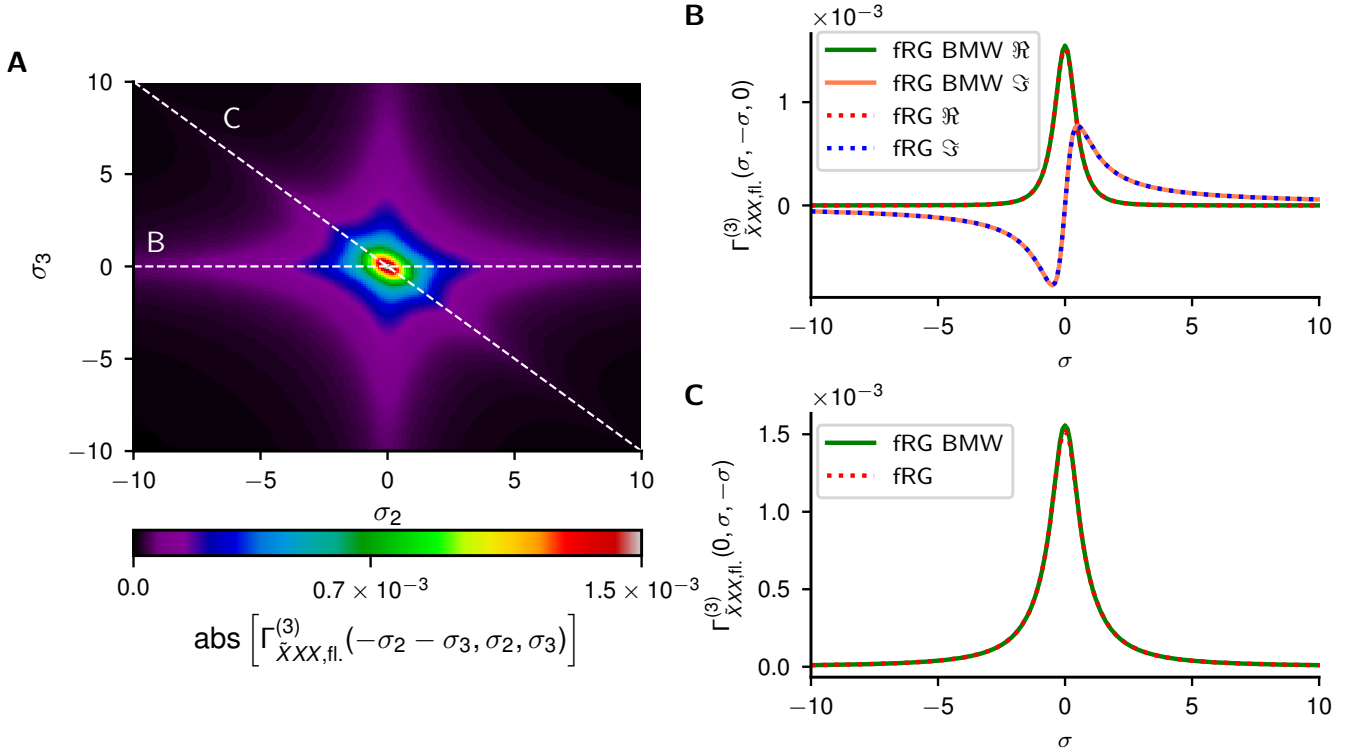


Figure 6. $\Gamma_{xxx,fl.}^{(3)}$ computed by fRG schemes. **A** Full frequency dependence as a result of the calculation that takes into account the flow of the mean value, $\Gamma_{fl.}^{(2)}$, and $\Gamma_{xxx,fl.}^{(3)}$. **B, C** $\Gamma_{xxx,fl.}^{(3)}(-\sigma_2 - \sigma_3, \sigma_2, \sigma_3)$ along the sections $\sigma_3 = 0$ (**B**) and $\sigma_2 = -\sigma_3$ (**C**), as indicated by the white dashed lines in (**A**); comparison to the respective types of vertices that appear in the BMW approximation. $\Gamma_{xxx,fl.}^{(3)}(-\sigma_2, \sigma_2, 0)$ in panel (B) quantifies the change of the linear response function due to an altered constant mean activity (indicated by the derivative with respect to the zero mode $\sigma_3 = 0$) — in more neuroscientific terms: it shows the dependence of the susceptibility (the neuron's linear response strength to an input) on the baseline activity to linear order. $\Gamma_{xxx,fl.}^{(3)}(0, \sigma_2, -\sigma_2)$ in panel (C) is somewhat complementary: It is the lowest order term describing the fluctuation-mediated effect of time-dependent deviations on the constant part of the mean activity. This term, for example, quantifies the change of the constant baseline activity due to a small sinusoidal stimulus with frequency σ_2 — the linear order of this response averages out over time, but the quadratic response does not. Note that $\Gamma_{xxx,fl.}^{(3)}(0, \sigma_2, -\sigma_2) \in \mathbb{R}$ because its Fourier transform $\Gamma_{xxx,fl.}^{(3)}(0, t_2, -t_2)$ is real by definition and symmetric because the last two arguments are those of two x 's at different time points, which are interchangeable.

Depending on the choice of the sources a, b, c , we either get the third order cumulant of the variable x (for $a = j(s)$, $b = j(t)$, $c = j(u)$) or the second order response kernel of the mean to a perturbation of the system (for $a = j(s)$, $b = j(t)$, $c = j(u)$), or the change of the variance due to a perturbation at linear order (for $a = j(s)$, $b = j(t)$, $c = j(u)$). The combination with a, b, c each equal to a \tilde{j} vanishes identically in stationary states, because the moments of \tilde{x} all vanish.

III. DISCUSSION

This article surveys methods to obtain self-consistent approximations by functional and diagrammatic techniques for stochastic differential equations as they appear in models of neuronal networks. Besides a systematic introduction, going from simple to more complex methods, we present three main new findings.

First, we expose the fundamental relation between the Onsager-Machlup (OM) effective action, which has a direct physical and probabilistic interpretation, and the Martin - Siggia - Rose - de Dominicis - Janssen (MSRDJ) effective action, which is computationally favorable. The general exposition of this fundamental link, to our knowledge, has been missing in the literature; it has earlier surfaced in specific problems in certain approximations [67]. In particular, the derivation of the OM effective action from the corresponding MSRDJ effective action naturally extends the definition of the former beyond Gaussian noise. The Onsager-Machlup effective action in addition allows the analysis

of bifurcations in stochastic systems. These can be studied conveniently by help of the corresponding effective potential, which exposes whether the stochastic system makes a first order phase transition or a continuous phase transition and which allows the assessment of fluctuations at the transition. We show for the neuroscientifically important example of the balanced state [10], that the loss of balance, which in the deterministic system causes a pitchfork bifurcation, in the stochastic system becomes a continuous phase transition dominated by fluctuations. We also expose the relation to the de Dominicis effective potential [57] in equilibrium systems.

Second we derive two effective equations that are equivalent to the stochastic non-linear system. The first is a deterministic integro-differential equation that captures the time evolution of the mean of the process. A related equation has previously been derived within the Doi-Peliti formalism of Markovian dynamics [68]. The second is a stochastic, but linear integro-differential equation that has identical second order statistics as the full system. These effective equations serve us here to provide an intuitive interpretation of the meaning of various vertex functions and to show how to relate stochastic nonlinear models to effective deterministic or stochastic linear systems.

Third, we develop a truncation scheme for the hierarchy of flow equations that arises in the functional renormalization group, which is based on the BMW scheme [45]. We here transfer this method from the derivative expansion to the vertex expansion, and demonstrate that this scheme yields a closed set of flow equations for the vertex functions which accurately captures the statistics of the system. The presented scheme is generic and may therefore be employed beyond the application to neuronal dynamics.

The link between the OM and the MSRDJ formalism also allows us to comment on a set of more subtle points. We carefully consider the convexity of the cumulant-generating functional W and discuss physically relevant cases in which W becomes non-differentiable as a result of degeneracy, for example by spontaneous symmetry breaking as it appears in attractor networks or in networks that show bi-stability: the existence of a convex set of solutions to the equation of state. The relation to the OM effective action enables us to address the question whether the effective action in the MSRDJ formalism is well-defined. To our knowledge, this is still an open question [see also 9]. The work by Andersen [94] presents a mathematically rigorous version of the MSR operator formalism [36] and concludes that there are cases where the Legendre transform cannot be applied. The problem in defining a Legendre transform for both sources j and \tilde{j} at once is their mutual dependence. This necessitates Andersen [94] to consider an ensemble of paths with an initial period of trivial dynamics (see i.p. their section V and their Appendix D). In the path-integral formulation that we follow here, albeit not mathematically rigorous in a strict sense, we are able to address the problem from another view point. We separate the Legendre transform into two steps. The first, which can rigorously be done thanks to the convexity of W in j , and a second, which is in fact only needed formally: we show that the solutions of the equation of state obtained from the MSRDJ formalism fulfill the requirement $\langle x \rangle = x^*$, as requested by the well-defined Onsager-Machlup effective action. What hence remains open is to show that all solutions of the OM equation of state also solve the MSRDJ equation of state.

The model systems studied in the current manuscript are intentionally left simple to illustrate the techniques in a minimal setting. In the following we therefore provide a slightly wider outlook for potential applications that are of relevance to the study of neuronal networks.

The initial part of this manuscript reformulates the problem of finding self-consistency equations by help of the effective action. We here apply the standard approach known from quantum field theory and statistical physics [59]. This technique yields self-consistent equations for the mean of the process that incorporate fluctuation corrections. Applications to neuronal networks include the study of bifurcations in the network dynamics, as we demonstrate here. Pitchfork bifurcations, for example, are responsible for the occurrence of multi-stability, the basis of classical attractor networks [13]. The effective action allows us to transfer the concept of a bifurcation in a deterministic differential equation [95] to a stochastic system: We need to investigate the bifurcations of the stationary points of the effective action, instead of studying the differential equation itself. A pitchfork bifurcation, the transition from a regime with a unique solution to a one with multiple fixed points, corresponds in the stochastic system to a critical point; the effective action changes from having a single minimum to exhibiting a flat segment that, beyond the bifurcation point, admits a continuum of stationary states. Traversing the bifurcation point, the curvature vanishes and hence fluctuations diverge. We here showed that the Onsager-Machlup effective action clearly exposes this fundamental property in the example of a network at the point where feedback changes from dominance of inhibition to dominance of excitation. Beyond the transition point, the system may be brought to jump from one end of the plateau to the other - showing a first order phase transition as an external parameter is varied; the network is bistable.

The study of transitions to oscillatory states, as they are ubiquitously observed in neuronal systems [96], would require the computation of the effective action as a functional of a field with Fourier components at non-zero frequencies. If the stationary point of the functional is assumed at a constant field configuration at one side of the bifurcation and by an oscillatory state on the other side, we have the stochastic analogue of a Hopf bifurcation. These bifurcations play a central role for the generation of oscillations [97] and for the appearance of spatio-temporal waves which are observed in cortical networks [98, 99]. The formalism exposed here makes the influence of noise on such bifurcations accessible. For example, the recently found second order phase transition at the onset of an oscillatory

state [100] could be analyzed within this framework. Bifurcations in neuronal networks in the presence of symmetries can be studied by means of the equivariant branching lemma [101]. So far these techniques neglect the influence of the noise altogether (i.e. employ the tree-level approximation) and therefore their applicability is limited to network states with weak noise. The formulation of bifurcations in terms of the effective action would allow an extension of this method to study how symmetries constrain bifurcations between fluctuation-dominated states.

A closely related point is the transition between multiple stable states, such as up- and down states [102, 103] or the different states of an attractor network [13]. The average noise-driven paths of transitions between such metastable states allows the assessment of the statistics of transitions between multiple states, for example to quantify the vulnerability to noise of information encoded in the activation of an attractor. Technically, one here seeks escape solutions to the equation of state which have non-vanishing values for the response field \tilde{x} [56, 104][see 55, i.p. Chapter 10 for a review]. In the setting of given initial value and free endpoint (relaxation), however, we can use that $\tilde{x} = 0$ and we can limit ourselves to small deviations δx of the physical variable. This enables the computation of the effective equation of motion for the mean value as a Taylor expansion of the equation of state. The theoretical prediction agrees with the simulation reasonably well. A related approach was here used to provide an approximation for the effective potential: If the approximation of the MSRDJ effective action is quadratic in the response field, taking the supremum over \tilde{x} is equivalent to integrating out the response field to obtain the OM effective action. This technique has an advantage over the computation of $\Gamma[x, \tilde{x}]$ for arbitrary values of $\tilde{x} \neq 0$, because in the latter case closed response loops do not vanish, neither do the propagators $\Delta_{\tilde{x}\tilde{x}}$, thus proliferating the number of diagrams to compute.

The loop expansion is shortly reviewed here, because it provides qualitative insights into the leading order of the fluctuation corrections. In the context of neuronal networks, the seminal work by Buice and Cowan [76] has introduced this technique to the study of neuronal networks. Since the structure of the one-loop diagrams is identical to those that appear in the functional renormalization group, one may use this method to check which additional vertices are produced along the RG flow, thus providing information for a good ansatz for the effective action. We here show that the loop expansion for the considered example is an expansion $\propto \beta^2 D$, where D is the amplitude of the noise and β the prefactor of the nonlinearity. In our example, fluctuations are small so that the one-loop result is already quite accurate. The sign of the fluctuation corrections together with the form of the effective equations for the mean and for the second order fluctuations, moreover expose qualitative mechanisms that arise from the fluctuation corrections: We show that a convex non-linearity always causes a positive shift of the mean of the process and that the additional linear memory kernel that arises from the self-energy has a sign that diminishes the leak term, thus causing a slower relaxation of the system - the interplay of noise and non-linearity thus prolongs the memory of a stimulus within the system. For small deflections from the steady state, this indirect contribution, moreover, typically dominates over the effect of the nonlinearity per se. Nevertheless, many studies of neuronal networks neglect this feedback, and keep the nonlinear terms at their mean field level. This approach has been shown to yield good results [105, eq. (6)], [106, eq. (3.8)] if fluctuations are not too strong. This is in line with our results provided that the noise level is low, because the linear memory kernel scales with $D\beta^2$, as can be seen in (35). Therefore for $D\beta^2 \ll 1$, while $\beta = \mathcal{O}(1)$, it might indeed be sufficient to consider the deterministic effect of the nonlinearity, but not the interaction with the noise. However, for $D\beta^2 = \mathcal{O}(1)$ while $\beta \ll 1$, the nonlinear effects by themselves are negligible, but their interaction with the noise induces a significant memory term. Setting β exactly to zero obviously makes both effects vanish, which for very noisy environments might lead to the erroneous conclusion that the nonlinearity without the noise is the reason for the deviation from the linear case. For large times especially, the linear noise-mediated component due to its “memory” wins over the deterministic nonlinear part. Correspondingly we show that the power spectrum at low frequencies is enhanced. Convex non-linearities of the gain functions of neurons, that are required for these qualitative features to hold, are typical in regimes in which neurons are driven by fluctuations [11].

The functional renormalization group (fRG) approach is presented here in the context of neuronal dynamics as a method that overcomes the limitations of the loop expansion with regard to self-consistency that is restricted to the mean. Instead, all vertex functions are potentially renormalized by fluctuation corrections, thus in principle allowing a fully self-consistent treatment also including corrections to the propagators and the interaction vertices. In the regime of weak fluctuations, we show that the results are slightly superior to the one-loop approximation, but here do not yield qualitatively new results. Computing higher order loop approximations is, moreover, inherently difficult, whereas all integrals in the fRG approach always have one-loop structure. The fRG approach, however, leads to improved results over the one-loop approximation even though the frequency-resolution of higher order vertices is limited by the adapted BMW approximation introduced here. Given in addition that similar ansätze have been successfully applied to spatially extended systems like the KPZ-model [91], we believe that the insights gained by this work will prove useful in studying neuronal networks embedded in space. Here, also more sophisticated approaches might become useful, for example the decomposition of vertices in so-called channels, characterized by the way they can be separated into two pieces by cutting two lines (particle-particle, particle-hole and crossed particle-hole in solid state physics terms). For a momentum-independent bare interaction, the contribution of each channel has a characteristic momentum structure, which can be used to drastically reduce the numerical effort both in fRG [107, 108] and parquet

calculations [109].

From a conceptual point of view, the functional renormalization group is interesting, because the flow generates new interaction vertices that are not contained in the original model. Thus, this method shows how the description of a neuronal network changes as fluctuations are integrated out: It exposes which effective interactions are generated. A specific feature of a flat regulator in frequency domain is its direct physical interpretation as a leak term of the neuronal dynamics. It controls the relaxation rate. Each point along the renormalization group flow therefore corresponds to a physical system with a different neuronal time scale. This insight may be used to study the approach towards a critical point at which the leak term vanishes and the time scale of fluctuations diverges. A more general discussion of frequency-dependent regulators can be found in Duclut and Delamotte [88].

This view is complementary to the typical application of an RG analysis, where mostly a momentum-dependent regulator is used so that the short-ranged degrees of freedom are subsequently integrated out. A rescaling of the momenta then yields identical momentum ranges before and after this marginalization, so that fixed points may occur [see e.g. 110, i. p. "The Scaling Form of the RG Equation of the Dimensionless Potential"]. In this view, each point on the RG trajectory represents the same system, just described at a different level of coarse graining.

Despite its simplicity, the here-considered model exposes two fundamental properties: First, the fluctuation corrections to the self-energy $\Gamma_{\bar{x},\text{fl.}}^{(2)}$ shift the point of transition with regard to mean-field theory. The latter predicts criticality at the point of vanishing leak term $m = 0$. The self-energy corrections reduce the leak term, thus promoting critical fluctuations. The critical point is therefore reached already at a non-zero negative value $m_c < 0$ of the leak term. Qualitatively, the behavior of the self-energy corrections is therefore opposite to the best known text book model of criticality, the φ^4 theory, where the transition is delayed to a negative mass term [e.g. 60, eq. 6.26]. In addition, a second mechanism causes a shift of the transition point, which is absent in an even theory as the φ^4 model: Fluctuation corrections to the mean value increase the mean value \bar{x} . Thus, the effective leak term $m(\bar{x})$ is weakened, further promoting the approach to the critical point.

These generic observations only depend on the assumption of an expansive non-linear neuronal gain function, so that we expect qualitatively similar results for example in a (fully or densely connected) network. The shift of the transition point obviously depends on the amplitude of the noise. It is known that fluctuations vary in neuronal networks in response to stimuli [111, 112]. Thus, neuronal systems may dynamically change their distance to the critical point within short periods of time.

A particularly interesting feature of the approach to the critical point are trajectories that depart from the stationary mean towards the location of the second, unstable, fixed point. Their dynamics slows down not only due to the reduced leak term by the two mechanisms described above, but also due to passing the vicinity of the second, unstable fixed point. In neuronal systems this mechanism may be useful to generate transient behavior on slow time scales, beyond the slow down of fluctuations close to the stable fixed point. One may speculate if such mechanisms play a role in long transient behavior observed in delayed response tasks [113].

Recently a Ginzburg-Landau type theory of neuronal activity has been formulated by DiSanto et al. [100]. A bit earlier, Henningson and Illes [114] have succeeded in fitting a simpler, linear model - a leaky heat equation with additional Gaussian noise - to the recordings of subthreshold fluctuations in acute hippocampal brain slices from a rat. Such models, expressed as partial stochastic differential equations, naturally fall into the realm of the statistical field theoretical methods discussed here. In particular the study of second order phase transitions has come into reach now - either by employing the established formalism of statistical field theory based on Wilson's renormalization group for non-equilibrium stochastic dynamics [see 5, for an authoritative review] or by the functional renormalization group methods presented here. Whether or not non-trivial fixed points in neuronal networks are accessible by former methods that rely on the closeness of the fixed point to a Gaussian one is so far unclear. The closely related Kardar-Parisi-Zhang model [115], for example, exhibits fixed points in the strong coupling regime, which is therefore only accessible by non-perturbative methods, for example the fRG approach presented here [116].

The currently employed theory of second order phase transitions in neuronal networks follows two main themes. The first employs dynamic models like branching processes. It is determined by the branching parameter, the average number of downstream descendants produced by the current activity [117, 118]. It relates second order phase transitions to the transition originally studied in the sandpile model [119]. In a similar spirit, Buice and Cowan [76] have introduced a network of neurons, which can be either active, quiescent or refractory and are described by a Master equation. This model also shows a dynamic phase transition - so this is part of the first theme. In the second theme, experimentally measured activity is compared to equilibrium ensembles, such as pairwise maximum entropy models [93, 120]; the discrepancy between the non-equilibrium dynamics of neuronal networks and this latter approach based on equilibrium thermodynamics has been identified as a pressing problem [121]. Following a field theoretical approach would in particular allow the study of critical exponents in models where neuronal activity unfolds in a spatially extended field, representing a coarse-grained view on the activity of mesoscopic numbers of neurons at each space point. Thus it would enable experimental predictions, for example with regard to the spatial structure of correlated activity. For the Manna sandpile model [122] such a continuous theory has been formulated and it has been found to

belong to the universality class of directed percolation with a conserved quantity (C-DP) [123–125]; the conservation of the number of sand grains here gives rise to the conserved quantity. Belonging to the C-DP universality class, the Manna sandpile model in particular features an absorbing state. Also the three-state neural dynamics by Buice and Cowan can be shown to belong to the C-DP universality class [76]. Therefore, this model has an absorbing state, too. In neuronal networks, though, we typically see ongoing activity; the absence of an absorbing state would therefore give rise to a different structure of the effective field theory, possibly also affecting the universality class. An alternative approach is therefore to start at the biophysics of neuronal networks on the microscopic level and to derive the structure of an effective long-range field theory. Investigating such models, the functional renormalization group has proven one of the few tools that make non-perturbative RG fixed points accessible [126].

So far field theoretical methods have been applied to neuronal networks with Markovian dynamics on discrete state spaces [76, 127], employing the Doi-Peliti [77] formalism or the alternative approach by Biroli et al. [128, 129], which is closer to the MSRDJ formulation used here. Also neuronal dynamics described by stochastic differential equations [7, 8, 44, 130–132] and stochastically spiking models (non-linear Hawkes processes [133, 134]) have recently been formulated by field theoretical methods [135]. For quadratic integrate-and-fire models in the mean driven regime, a mapping to a coupled set of phase oscillators, moreover, allows the application of the MSRDJ formalism [136, 137]. The renormalization group methods that we presented here can directly be applied to these systems.

Networks of leaky integrate-and-fire models [138] in the fluctuation driven, asynchronous irregular state [11, 12] are, however, inherently complicated to treat by field theoretical methods; the reason is that an action for such models is cumbersome to define due to the hard threshold and reset of the membrane potential. This model and its biophysically more realistic extensions [74], however, form a kind of gold standard. It would therefore be a major step to treat networks of such models by systematic approaches as they are offered by field theory. So far methods for this central model are constrained to ad-hoc mean-field approximations, typically resting on the annealed approximation of the connectivity [12, 139]; in particular this mean-field based approach prohibits a systematic study of critical phenomena.

In summary, the current work imports methods from established fields of physics into the field of theoretical neuroscience that we think have a high potential to solve some of the technical difficulties that arise in the study of neuronal networks in the presence of fluctuations, non-linearities, phase transitions, and critical phenomena.

ACKNOWLEDGMENTS

We thank PierGianLuca Porta Mana for fruitful discussions. This work was partly supported by the Exploratory Research Space seed funds MSCALE and G:(DE-82)ZUK2-SF-CLS002 (partly financed by Hans Herrmann Voss Stiftung) of the RWTH university; the JARA Center for Doctoral studies within the graduate School for Simulation and Data Science (SSD); the Helmholtz association: Young investigator’s grant VH-NG-1028; European Union’s Horizon 2020 Framework Programme for Research and Innovation under the Specific Grant Agreement No. 785907 (Human Brain Project SGA2); Juelich Aachen Research Alliance (JARA).

IV. APPENDIX

A. Normalization and escape

It is often stated that in stationary settings all moments of the response field vanish [65, p. 38][140]. This statement follows from the normalization of the probability functional $p[x|\tilde{j}]$ for all paths, $\int \mathcal{D}x p[x|\tilde{j}] = 1$. The latter is given by

$$p[x|\tilde{j}] = \int \mathcal{D}\tilde{x} \exp(S[x, \tilde{x}] + \tilde{j}^T \tilde{x}). \quad (51)$$

The normalization can therefore also be written as $Z[0, \tilde{j}] \equiv 1$, which, upon n -fold differentiation by \tilde{j} , yields

$$\langle \tilde{x}(t_1) \cdots \tilde{x}(t_n) \rangle \equiv 0 \quad \forall t_1, \dots, t_n, n. \quad (52)$$

Note, however, that this only holds for paths for which either the endpoint or the starting point is given. Fixing both, as it is done for escape problems [see e.g. 55, Chapter 10], effectively leads to an additional term in the action and therefore to nonzero moments of powers of the response field: Specifying the end point of the path, we implicitly restrict the ensemble of paths in the integral appearing in Z . In the path integral formulation, we include the initial point x_0 and the final point x_T as

$$Z[j, \tilde{j}] = \int \mathcal{D}x \int \mathcal{D}\tilde{x} \exp(S[x, \tilde{x}] - \tilde{x}^T \delta(\circ) x_0 + j^T x + \tilde{j}^T \tilde{x}) \delta(x(T) - x_T).$$

The presence of the initial condition x_0 obviously does not affect the normalization - it can as well be absorbed into a shift of $\tilde{j} \rightarrow \tilde{j} - \delta(\circ)x_0$. Fixing the final condition x_T , however, leads to the relation

$$\mathcal{Z}[0, \tilde{j}] = p(x(T) = x_T | x_0, \tilde{j}),$$

which is the conditional probability to reach the final point x_T from the initial point x_0 given the inhomogeneity \tilde{j} . This probability is not necessarily independent of \tilde{j} , so that in general non-zero moments (52) appear.

B. General properties of the effective action in the MSRDJ-formalism

Multiple derivatives of Γ with respect to x **only** are always zero, as we will demonstrate in this section. We have seen in Section IV A that if we do not specify an endpoint for x , the expectation value of all powers of \tilde{x} vanish. As a consequence, we see from (20) that $\Gamma_{xx}^{(2)}[x^*, 0] = 0$. Extending our analysis to higher order derivatives of Γ not involving \tilde{x} , we observe that

$$\begin{aligned} \Gamma_{xxx}^{(3)} &= \sum_{y \in \{x, \tilde{x}\}} \sum_{y_1, y_2, y_3} \Gamma_{x_1 y_1}^{(2)} \Gamma_{x_2 y_2}^{(2)} \Gamma_{x_3 y_3}^{(2)} W_{y_1, y_2, y_3} \\ \Gamma_{x\tilde{x}}^{(2)=0} &= \sum_{\tilde{x}_1, \tilde{x}_2, \tilde{x}_3} \Gamma_{x_1 \tilde{x}_1}^{(2)} \Gamma_{x_2 \tilde{x}_2}^{(2)} \Gamma_{x_3 \tilde{x}_3}^{(2)} \underbrace{W_{\tilde{x}_1, \tilde{x}_2, \tilde{x}_3}}_{=0} = 0. \end{aligned} \quad (53)$$

Similarly, we can argue for all higher order vertices: They can be decomposed into “tree diagrams” with derivatives of W as nodes and $\Gamma^{(2)}$ as connecting elements. A tree diagram is defined by having the property to not include loops and especially, that means that two nodes are connected by at most one element $\Gamma^{(2)}$. Because we have only x ’s at the external legs and $\Gamma_{xx}^{(2)} = 0$, we have all $W^{(n)}$ connected to external legs to be with respect to \tilde{j} . Therefore, the only possibility to “justify” j -derivatives are $\Gamma_{x\tilde{x}}^{(2)}$ -components acting as internal connecting elements providing one j -derivative each. Since the graphs are tree-like, we have exactly one $W^{(n)}$ -node more than connecting elements. However, we need at least one j -derivative at every node to prevent that it vanishes. We deduce that the contribution of at least one of the nodes is zero. This demonstrates that

$$\Gamma_{\underbrace{x, \dots, x}_{n \text{ times}}}^{(n)} = 0 \quad \forall n.$$

C. Convexity and spontaneous symmetry breaking

Cumulant generating functions are convex. This can be seen from the Hoelder inequality that holds for two non-negative sequences $g_k, h_k \geq 0$ with $\alpha + \beta = 1$ and $0 \leq \alpha, \beta \leq 1$

$$\sum_k (g_k)^\alpha (h_k)^\beta \leq \left(\sum_k g_k \right)^\alpha \left(\sum_k h_k \right)^\beta \quad (54)$$

and from the fact that probabilities are positive, so that one can always define an “action” as the log probability $p(x) =: e^{S(x)}$ (we here omit the normalization by the partition function for brevity that would read $p(x) = e^{S(x) - \ln \mathcal{Z}}$). We here follow a modified version of the argument in [141]; a similar proof can be found in [63]. Applied to the moment-generating function $Z(j) = \langle e^{j^T x} \rangle$ one gets with a generalization of Hoelder’s inequality for infinite-dimensional spaces

$$\begin{aligned} Z(\alpha j_1 + \beta j_2) &= \langle e^{(\alpha j_1 + \beta j_2)^T x} \rangle = \int_x e^{(\alpha j_1 + \beta j_2)^T x + S(x)} \\ &\stackrel{\alpha + \beta = 1}{=} \int_x e^{\alpha(S(x) + j_1^T x)} e^{\beta(S(x) + j_2^T x)} \\ &= \int_x \left(e^{S(x) + j_1^T x} \right)^\alpha \left(e^{S(x) + j_2^T x} \right)^\beta \\ &\stackrel{\text{Hoelder}}{\leq} \left(\int_x e^{S(x) + j_1^T x} \right)^\alpha \left(\int_y e^{S(y) + j_2^T y} \right)^\beta \\ &= Z(j_1)^\alpha Z(j_2)^\beta. \end{aligned} \quad (55)$$

So consequently the cumulant generating function $W = \ln Z$

$$W(\alpha j_1 + \beta j_2) \leq \alpha W(j_1) + \beta W(j_2) \quad (56)$$

has a graph that is always below its chord; it is convex down.

In the case that $W(j)$ is differentiable, this means that its Hessian is positive definite (a corresponding short proof can be found in [4, p. 166]). The definition of the effective action by the Legendre-Fenchel transform instead of the ordinary Legendre transform is only required if W is non-analytic; if it has a cusp at a certain value j^* . Such a cusp corresponds to the situation of spontaneous symmetry breaking: The mean value that is conjugate to j is different if j^* is approached from above or below:

$$\begin{aligned} \langle x^+ \rangle &:= \lim_{j \searrow j^*} W^{(1)}(j) \\ &\neq \lim_{j \nearrow j^*} W^{(1)}(j) \\ &=: \langle x^- \rangle. \end{aligned}$$

The authoritative book by Vasiliev contains a more detailed discussion of the role of Legendre transforms in the study of phase transitions [59, i.p. section 6].

The Legendre transform \mathcal{L} of any function $f(j)$ is convex down. This is because for

$$g(x) := \sup_j j^T x - f(j)$$

we find with $\alpha + \beta = 1$ that

$$\begin{aligned} g(\alpha x_a + \beta x_b) &= \sup_j j^T (\alpha x_a + \beta x_b) - (\alpha + \beta) f(j) \\ &\leq \sup_{j_a} \alpha (j_a^T x_a - f(j_a)) + \sup_{j_b} \beta (j_b^T x_b - f(j_b)) \\ &= \alpha g(x_a) + \beta g(x_b), \end{aligned} \quad (57)$$

which shows that g is convex down. Convexity of f is not required here. This general result holds in particular for the effective action defined as

$$\Gamma(x^*) := \sup_j j^T x^* - W(j), \quad (58)$$

which therefore is convex down, too.

Furthermore, the Legendre transform is an involution on convex functions; applied twice we come back to the original function. However, in the case that the original function was not convex, the result would be the convex envelope of the original function [see e.g. 142, i.p. Fig 9 and surrounding text]). So far, this issue cannot arise if we were able to compute Γ or W exactly; both functions are convex and therefore are the Legendre transforms of one another. Moreover, $\Gamma(x^*)$ for a typical physical system is in addition differentiable everywhere. For if it had a cusp, this would mean that $W(j)$ has a flat segment; the value of the source j would not affect the mean $\langle x \rangle$ for values within this segment, an untypical behavior (thinking of j being the external magnetic field and $\langle x \rangle$ the magnetization).

An issue arises when approximations are made. We will illustrate the point with help of the simplest tree level approximation, the loopwise approximation to lowest order. The approximation of the effective action then is

$$\Gamma_0(x^*) = -S(x^*),$$

which is not necessarily convex; let us think of the action $S(x) = -\frac{1}{2}x^2 + \frac{1}{4}x^4$, for example, which has two minima at $x_{\pm}^* = \pm 1$ and an intermediate local maximum at $x = 0$; clearly a non-convex function, that is meant to approximate the convex function Γ . Legendre-transforming this approximation to $W_0(j) = \mathcal{L}\{\Gamma_0\}(j) = \mathcal{L}\{-S\}(j)$ yields a function in j with a cusp at $j^* = 0$, because the supremum operation in $W(j) = \sup_x jx + S(x)$ for $j < 0$ finds the supremum at $x \leq -1$, and for $j > 0$ finds the supremum at $x \geq 1$. As j moves through zero from below, the point of the supremum thus jumps from $x = -1$ to $x = +1$. Since the position of the supremum is the left-sided (for $j < 0$) or the right-sided (for $j > 0$) slope of $W(j)$, the latter function has a cusp at zero

$$\langle x^{\pm} \rangle \equiv W^{(1)}(0_{\pm}) = \pm 1. \quad (59)$$

We may perform the Legendre transform explicitly by finding the supremum as the solution to $\partial_x(S(x) + jx) = 0$ for $x \in (-\infty, -1]$ for $j < 0$ and within $x \in [1, \infty)$ for $j > 0$. Transforming back to $\Gamma_0^* := \mathcal{L}\{W_0\}$, we obtain the convex envelope of the original Γ_0 : The two minima at $x_\pm = \pm 1$ are joined by a straight line. This follows directly from the cusp of W in (59), because computing $\Gamma_0^*(x^*) = \sup_j jx - W(j)$ for $x^* \in (-1, 1)$ always assumes the supremum for j at $j = 0$; so the resulting function Γ^* is flat on this segment, the value of which is $W(0)$. These relations are easiest appreciated graphically. A detailed explanation including graphical illustrations can for example be found in [142, i.p. Fig 9].

The fRG, in particular in its implementation with the derivative expansion, has the interesting property that the resulting partial differential equation for the effective action (or effective potential, the effective action at vanishing Fourier mode k) becomes convex as the flow parameter evolves [see e.g. 110, i.p. Fig 2.15 and discussing text]. This is in contrast to simpler approximation schemes, such as the loop expansion, as we have illustrated above on its lowest order approximation. Still, as more loop corrections are incorporated, the plateau becomes successively flatter.

D. Convexity of the MSRDJ cumulant-generating functional

In the form (8), $W[j]$ is a cumulant generating functional of the field x and thus, by (56), a convex functional in j . We can therefore perform the Legendre transform with regard to j to obtain the effective action

$$\Gamma_1[x^*, \tilde{j}] := \sup_j j^T x^* - W_{\text{MSRDJ}}[j, \tilde{j}] \quad (60)$$

as in (58) only that we left \tilde{j} as a parameter indicating some additional input; the Legendre transform with regard to j is hence involutive. By the convexity of W in j it is assured that the mapping between x^* and j is one-to-one.

Necessity of the Legendre-Fenchel transform

Let us first show that the cumulant-generating functional $W[j, \tilde{j}]$ indeed may have non-analytical behavior that requires the use of the Legendre-Fenchel transform rather than the ordinary Legendre transform – this happens for example in a bistable system. For concreteness, let us assume the stochastic differential equation of the form

$$dx(t) = -V'(x) dt + dW(t) \quad (61)$$

with $V(x) = -\frac{1}{2}x^2 + \frac{1}{4}x^4$ and initial condition $x(0) = 0$ on the local maximum of V . For $\tilde{j} = 0$ depending on the realization of the noise dW , the system will move close to either of the two minima $x_\pm = \pm 1$ of the potential V ; for sufficiently small noise, the system will stay close to the spontaneously chosen minimum for prolonged times.

We first consider the analytical properties of W in j at $\tilde{j} = 0$. The presence of the source term $\int_0^T j(t)x(t) dt$ for $j = \epsilon$ assigns a different probability to the paths $x(t) = x_\pm$, namely

$$p[x(t) = x_+ = 1]/p[x(t) = x_- = -1] = e^{2\epsilon T}. \quad (62)$$

So in the $T \rightarrow \infty$ limit, a non-zero source j suppresses either of these symmetric solutions in the integration measure. Here time T plays a similar role as system size for spontaneous symmetry breaking in static thermodynamics [see e.g. 141, i.p. section 2.9]. Therefore,

$$\begin{aligned} \lim_{T \rightarrow \infty} \frac{1}{T} \int_0^T \langle x(t) \rangle_\pm dt &= \frac{1}{T} \lim_{\epsilon \searrow 0} \frac{1}{\pm \epsilon} (W[j(t) = \pm \epsilon, 0] - W[0, 0]) \\ &\simeq \pm 1 \end{aligned}$$

yields a different left and right-sided derivative and hence mean value. So indeed one needs a Legendre-Fenchel transform to define Γ_1 as in (60).

We now consider the dependence of Γ_1 on the source $\tilde{j} \neq 0$. Such a non-zero source term corresponds to an inhomogeneity on the right hand side of (61)

$$\begin{aligned} dx(t) &= -V'(x) dt + dW(t) - \tilde{j} \\ &= -(V(x) + \tilde{j}x)' dt + dW(t). \end{aligned} \quad (63)$$

In a system in thermodynamic equilibrium, we may write the stationary probability distribution of (61) as

$$p(x(t)) \propto \exp\left(-\frac{2}{D} V(x(t)) - \frac{2}{D} \tilde{j} x(t)\right). \quad (64)$$

The additional inhomogeneity $-\tilde{j}$ in (63) can therefore be regarded as a modified source term $(j(t) - \frac{2}{D} \tilde{j})x(t)$. We therefore have

$$W[j, \tilde{j}] = \ln \int \mathcal{D}x \exp\left(\dots + \int (j(t) - \frac{2}{D} \tilde{j}) x(t) dt\right).$$

The Legendre transform with regard to j eliminates the non-differentiability in \tilde{j} . This is because the left and right-sided derivatives are identical, as both limits

$$\begin{aligned} \frac{\partial \Gamma_1[x^*; \pm\epsilon]}{\delta\epsilon} &= \lim_{\epsilon \searrow 0} \frac{1}{\pm\epsilon} \left(\sup_j j^T x^* - W[j, \pm\epsilon] - \left(\sup_k k^T x^* - W[k, 0] \right) \right) \\ &= \lim_{\epsilon \searrow 0} \frac{1}{\pm\epsilon} \left(\sup_j j^T x^* - W[j \mp \underbrace{\frac{2}{D}\epsilon}_{\tilde{j}}, 0] - \left(\sup_k k^T x^* - W[k, 0] \right) \right) \\ &= \lim_{\epsilon \searrow 0} \frac{1}{\pm\epsilon} \left(\sup_{\hat{j}} (\hat{j} \pm \frac{2}{D}\epsilon)^T x^* - W[\hat{j}, 0] - \left(\sup_k k^T x^* - W[k, 0] \right) \right) \\ &= \lim_{\epsilon \searrow 0} \frac{1}{\pm\epsilon} \left(\pm \epsilon^T \frac{2}{D} x^* \right) = \frac{2}{D} x^* \end{aligned}$$

exist for non-zero D and are identical. We here used that a one-dimensional dynamics can always be considered as following an equilibrium distribution of the form (64). For systems for which the right hand side is not given by the gradient of a potential (in contrast to (63)), it is less clear that the Legendre transform with respect to j is differentiable with respect to \tilde{j} . However, it is plausible that the effective action depends smoothly on the input $-\tilde{j}$.

Consistency of Legendre transform in \tilde{j}

It is left to be checked that the additional transform from \tilde{j} to \tilde{x}^*

$$\Gamma[x^*, \tilde{x}^*] = \Gamma_1[x^*; \tilde{j}] - \tilde{j}^T \tilde{x}^*$$

is also such that a one-to-one relationship exists. Here a proof of the convexity of $\Gamma_1[x^*; \tilde{j}]$ seems not to be straight forward; it can, however, easily be checked in the case of an Ornstein-Uhlenbeck process that Γ_1 is convex down in \tilde{j} . For the non-Gaussian case, we were, however, unable to find such a proof. To the contrary, it can be shown rigorously that for certain systems the Legendre transform with regard to j and \tilde{j} is not well-defined [94]. We therefore follow a different route here and demonstrate a weaker condition: We derive the non-trivial equation of state of the MSRDJ formalism directly from the well-defined effective action Γ_1 .

We start by rewriting the definition of the Legendre-Fenchel transform as

$$\Gamma_1[x^*; \tilde{j}] = -\sup_j \ln \int_x \exp(S_{\text{OM}}[x; \tilde{j}] + j(x - x^*)).$$

The supremum assumed at the physical value $j = 0$ implies that $x^* = \langle x \rangle$ equals the mean of the process. This condition, with $\delta x = x - x^*$, is equivalently given by

$$0 \stackrel{!}{=} \langle \delta x \rangle \equiv \int_{\delta x} \delta x \exp(S_{\text{OM}}[x^* + \delta x; \tilde{j}]), \quad (65)$$

where we assumed the Onsager-Machlup form of the action, but kept the dependence on the source \tilde{j} :

$$S_{\text{OM}}[x^*; \tilde{j}] = -\frac{1}{2D} (\partial_t x - f(x) + \tilde{j})^T (\partial_t x - f(x) + \tilde{j}).$$

We have seen in (9) that we may express it as the Legendre transform with respect to the auxiliary field \tilde{x} ; this is so because S_{OM} is convex and every convex function can be written as a Legendre transform of a suitably chosen function (namely its Legendre transform)

$$S_{\text{OM}}[x^*; \tilde{j}] = \sup_{\tilde{x}} \tilde{x}^{\text{T}} (\partial_t x - f(x) + \tilde{j}) + \frac{D}{2} \tilde{x}^{\text{T}} \tilde{x}. \quad (66)$$

The supremum is hence attained at $\tilde{x} = -D^{-1}(\partial_t x - f(x) + \tilde{j})$. This allows us to rewrite the Onsager-Machlup action, expanded in $\delta x = x - x^*$, as

$$\begin{aligned} S_{\text{OM}}[x^* + \delta x] &= \frac{1}{2} \underbrace{\frac{-1}{D} (\partial_t x - f(x) + \tilde{j})^{\text{T}}}_{\tilde{x}^{\text{T}}} (\partial_t x^* - f(x^*) + \tilde{j} + \partial_t \delta x - f^{(1)}(x^*) \delta x + \sum_{n=2}^{\infty} \frac{f^{(n)}(x^*)}{n!} \delta x^n) \\ &= \sup_{\tilde{x}} \tilde{x}^{\text{T}} (\partial_t \delta x - f^{(1)}(x^*) \delta x) + \frac{D}{2} \tilde{x}^{\text{T}} \tilde{x} \\ &\quad + \tilde{x}^{\text{T}} (\partial_t x^* - f(x^*) + \tilde{j}) \\ &\quad + \tilde{x}^{\text{T}} \sum_{n=2}^{\infty} \frac{f^{(n)}(x^*)}{n!} \delta x^n. \end{aligned}$$

The second line here contains all terms bi-linear in δx and \tilde{x} ; so it defines the propagator. The third line can be regarded as a shift of the mean of the noise; a term that is linear in \tilde{x} . The last line contains the non-Gaussian terms that produce corrections. If we neglected these corrections, the remaining terms would correspond to an Ornstein-Uhlenbeck process δx that is driven by a noise ξ with mean $\langle \xi \rangle = \partial_t x^* - f(x^*) + \tilde{j}$ and variance D . Because the noise is chosen to be Gaussian, we can rewrite the supremum condition (66) as an integral over \tilde{x} :

$$\begin{aligned} 0 \stackrel{!}{=} \langle \delta x \rangle &\equiv \int_{\delta x, \tilde{x}} \delta x \exp \left(\tilde{x}^{\text{T}} (\partial_t - f^{(1)}(x^*)) \delta x + \frac{D}{2} \tilde{x}^{\text{T}} \tilde{x} \right. \\ &\quad \left. + \tilde{x}^{\text{T}} (\partial_t x^* - f(x^*) + \tilde{j}) + \tilde{x}^{\text{T}} \sum_{n=2}^{\infty} \frac{f^{(n)}(x^*)}{n!} \delta x^n \right). \end{aligned} \quad (67)$$

In the following we will show that this equation is fulfilled if the term $\partial_t x^* - f(x^*) + \tilde{j}$ is represented by the negative of all one-line irreducible diagrams with one uncontracted \tilde{x} -leg; we denote the sum of these diagrams by Ξ . If we assume (as we normally do) that the representation by diagrams is convergent, this can be seen as the defining property of $\Gamma_{\text{MSRDJ}, \tilde{x}, \text{fl.}}^{(1)}$ that we formally obtain from a Legendre transform with respect to both, j and \tilde{j} . We can then conclude that $\partial_t x^* - f(x^*) + \tilde{j} = -\Xi = \Gamma_{\text{MSRDJ}, \tilde{x}, \text{fl.}}^{(1)}$. We will first demonstrate how to obtain this result from a formal Legendre transform also with regard to \tilde{j} . Afterwards, we will demonstrate that indeed the identification of $\partial_t x^* - f(x^*) + \tilde{j} = -\Xi$ solves (67).

The equations of state derived from the formally performed Legendre transform of $W[j, \tilde{j}]$ with regard to j and \tilde{j} to $\Gamma_{\text{MSRDJ}}[x^*, \tilde{x}^*]$ are

$$\begin{aligned} \tilde{j}(t) &= \frac{\delta \Gamma_{\text{MSRDJ}}}{\delta \tilde{x}^*(t)} \rightarrow \partial_t x^* - f(x^*) + D \tilde{x}^* + \tilde{j} = \Gamma_{\text{MSRDJ}, \tilde{x}, \text{fl.}}^{(1)}[x^*, \tilde{x}^*], \\ j(t) &= \frac{\delta \Gamma_{\text{MSRDJ}}}{\delta x^*(t)} \rightarrow -\partial_t \tilde{x}^* - f'(x^*) \tilde{x}^* + j = \Gamma_{\text{MSRDJ}, x, \text{fl.}}^{(1)}[x^*, \tilde{x}^*]. \end{aligned} \quad (68)$$

The second equation for the physically relevant value $j \equiv 0$ can be shown to admit the solution $\tilde{x}^* \equiv 0$. This is so because the left hand side is linear in \tilde{x}^* and the right hand side vanishes for $\tilde{x}^* = 0$, because one cannot produce any non-vanishing diagrams with one amputated x -leg. One can therefore insert $\tilde{x}^* \equiv 0$ into the first equation of state to obtain a single non-trivial equation

$$\partial_t x^* - f(x^*) + \tilde{j} = \Gamma_{\text{MSRDJ}, \tilde{x}, \text{fl.}}^{(1)}[x^*, 0], \quad (69)$$

which shows the first part of our assertion by the usual proof that $\Gamma_{\text{fl.}}$ is composed of one-line irreducible diagrams alone (see e.g. Kleinert [48] sec 3.23.6 or Helias and Dahmen [61] section XIV).

We hence are left to show the diagrammatic statement, namely that

$$0 = \int_{\delta x, \tilde{x}} \delta x \exp \left(\tilde{x}^T (\partial_t - f^{(1)}(x^*)) \delta x + \frac{D}{2} \tilde{x}^T \tilde{x} - \tilde{x}^T \Xi(x^*) + \tilde{x}^T \sum_{n=2}^{\infty} \frac{f^{(n)}}{n!} \delta x^n \right). \quad (70)$$

The Gaussian part in the first line defines the usual propagators $\Delta_{xx} = \langle xx \rangle$ and $\Delta_{\tilde{x}x} = \langle \tilde{x}x \rangle$, whereas $\Delta_{\tilde{x}\tilde{x}} \equiv 0$. A non-vanishing contribution requires the explicitly present term δx in the integrand to be contracted. It cannot be contracted by the propagator Δ_{xx} , because the other leg of the propagator would need to connect to a δx from an interaction vertex of the form $\tilde{x} \delta x^n$; contracting the remaining \tilde{x} would hence require at least one closed response loop formed by $\Delta_{\tilde{x}x}$, so the contribution vanishes. For the same reason there cannot appear any tadpole subdiagrams that are attached by a δx . The only possibility is hence to contract the explicitly present δx with an \tilde{x} of an interaction vertex by the propagator $\Delta_{\tilde{x}x}$. Thus the produced diagrammatic corrections to the mean are of the form of tadpole diagrams

$$\Delta_{x\tilde{x}} \text{graph with single uncontracted } \tilde{x}.$$

We defined $-\Xi$ to contain all one-line irreducible diagrams with one amputated \tilde{x} -leg and negative sign. The presence of the term $-\tilde{x} \Xi(x^*)$ hence cancels all irreducible tadpole diagrams with a single amputated \tilde{x} -leg. Likewise, reducible contributions cannot appear, because any reducible diagram would contain at least one tadpole sub-diagram; but these subdiagrams are canceled by the presence of $-\tilde{x} \Xi(x^*)$ as well. As a result, we conclude that no diagrams remain and hence (70) holds. This proves that the solution to the equations of state (69), obtained from the formal joint Legendre transform with regard to both, j and \tilde{j} , solves condition (67) (even if it is not clear that is the only solution).

In summary, the specific feature of the MSRDJ formalism that the expectation value of \tilde{x} vanishes cures the fact that the Legendre transform with respect to \tilde{j} is not necessarily well-defined, because it allows the reduction from the pair of equations of state (68) to a single one (69). The latter can be derived in the well-defined OM-formalism. The second Legendre transform from $\Gamma_1[x^*, \tilde{j}]$ to $\Gamma[x^*, \tilde{x}^*]$ can therefore be considered a formal step, merely used to simplify the diagrammatic derivation of the equation of state.

E. The effective action in the MSRDJ and the Onsager-Machlup-formalism

Considering Γ as a potential whose extremal points are the solutions of a differential equation and that $\tilde{x} = 0$ is the extremizing solution, we might conclude from $\Gamma_{x\dots x}^{(n)} = 0$ (shown in (53)) that Γ is constant (or at least nonanalytic in $(\tilde{x}, 0)$). However, Γ is clearly non-constant. It turns out that setting $\tilde{x} = 0$ is correct for the stationary point \tilde{x} , but does not give us the true shape of the “energy landscape” for a different x in a neighborhood of \tilde{x} . This is so because it is forbidden to set \tilde{x} to a constant value prior to the calculation of the statistics of x ; instead we must integrate it out, since it is just a Hubbard-Stratonovich auxiliary field used to formulate a constraint. Only for Gaussian noise, this leads to the Onsager-Machlup-action (5). For arbitrary noise distributions, we can define the cumulant-generating function without the need to first define the OM-action by writing

$$W_{\text{OM}}[j] = \ln \int \mathcal{D}x \int \mathcal{D}\tilde{x} \exp(S[x, \tilde{x}] + j^T x) \quad (71)$$

This makes sense because we introduced \tilde{x} as an auxiliary variable to represent the delta-distribution and \tilde{j} to measure the response function. If we are not interested in the latter, but just in the statistics of x , we can drop \tilde{j} in (16) to obtain (71). The Onsager-Machlup-type effective action then takes the form

$$\begin{aligned} \Gamma_{\text{OM}}[x^*] &= \sup_j j^T x^* - W_{\text{OM}}[j] \\ &= [j^T x^* - W_{\text{OM}}[j]]_{j \text{ such that } x^* = \frac{\partial}{\partial j} W_{\text{OM}}[j]}. \end{aligned} \quad (72)$$

Let us expose the connection to the MSRDJ-formalism more clearly by performing the Legendre transform with respect to j and \tilde{j} gradually instead of simultaneously:

$$\begin{aligned} \Gamma_1[x^*, \tilde{j}] &:= \sup_j j^T x^* - W[j, \tilde{j}] \\ \Gamma_2[x^*, \tilde{x}^*] &:= \tilde{j} \tilde{x}^* + \Gamma_1[x^*, \tilde{j}] \Big|_{\tilde{j} \text{ such that } \tilde{x}^* = \partial_{\tilde{j}} \Gamma_1[x^*, \tilde{j}]}. \end{aligned}$$

In order to define Γ_2 , we had to assume that the relation $\tilde{j} \rightarrow \partial_{\tilde{j}}\Gamma_1[x^*, \tilde{j}]$ is invertible. This is given if Γ_1 is convex in \tilde{j} . So this is a sufficient condition, but not a necessary one⁶. We easily see that $\Gamma_{\text{OM}}[x^*] = \Gamma_1[x^*, 0]$. For the identification of Γ_2 , observe that for the elimination of j obtaining Γ_1 , we choose $j[x^*, \tilde{j}]$ such that

$$x^* = \frac{\partial W}{\partial j}[j[x^*, \tilde{j}], \tilde{j}].$$

Note that by this notation, we have also lifted possible ambiguities due to a multi-valued derivative of W with respect to j , because we have fixed $W^{(1)}$ to x^* (see also [Section IV C](#)). In the second step, yielding Γ_2 , we determine \tilde{j} in the following way:

$$\begin{aligned} \tilde{x}^* &= -\frac{d}{d\tilde{j}}\Gamma_1[x^*, \tilde{j}] = -\frac{d}{d\tilde{j}}\{j[x^*, \tilde{j}]x^* - W[j[x^*, \tilde{j}], \tilde{j}]\} \\ &= -\frac{\partial j}{\partial \tilde{j}}x^* + \underbrace{\frac{\partial W}{\partial j}[j[x^*, \tilde{j}], \tilde{j}]}_{=x^*} \frac{\partial j}{\partial \tilde{j}} + \frac{\partial W}{\partial \tilde{j}}[j[x^*, \tilde{j}], \tilde{j}] = \frac{\partial W}{\partial \tilde{j}}[j[x^*, \tilde{j}], \tilde{j}], \end{aligned}$$

which leads to the identification $\Gamma_{\text{MSRDJ}}[x^*, \tilde{x}^*] = \Gamma_2[x^*, \tilde{x}^*]$. Therefore, we obtain Γ_{OM} by performing the Legendre transform of Γ_{MSRDJ} with respect to \tilde{x}^* and setting $\tilde{j} = 0$ afterwards, which is equivalent to finding the \tilde{x}^* extremizing $\Gamma_{\text{MSRDJ}}[x^*, \tilde{x}^*]$ for given x^* , or, in other words,

$$\Gamma_{\text{OM}}[x^*] = \underset{\tilde{x}}{\text{extremize}} \Gamma_{\text{MSRDJ}}[x^*, \tilde{x}] = \underset{\tilde{x}}{\text{extremize}} \Gamma[x^*, \tilde{x}].$$

The Legendre transform (72) implies

$$\frac{\delta^2}{\delta x(t) \delta x(t')} \Gamma_{\text{OM}}[x] = \left[\frac{\delta^2}{\delta j(t) \delta j(t')} W[j, \tilde{j}] \right]^{-1}. \quad (73)$$

So, expressed in words, the second derivative of Γ_{OM} at x^* equals the inverse of $\langle \delta x \delta x \rangle$. Note that all $[\cdot]^{-1}$ are meant as the inverse of operators acting on functions. For our model, in frequency domain these inversions are simple (matrix) inversions, whereas in time domain this amounts to finding the Green's function of the operator or, in other words, solving a differential equation. Therefore, we can relate the integrated covariances, given by the zero mode of the covariances in Fourier space by Fourier-transforming (73) and inverting it:

$$\frac{\delta^2}{\delta J(\omega) \delta J(\omega')} W[J, \tilde{J}] = \left[\frac{\delta^2}{\delta X(\omega) \delta X(\omega')} \Gamma_{\text{OM}}[X] \right]^{-1}.$$

F. Relation between S_{OM} and S_{MSRDJ} in case of non-Gaussian noise

In this section, we demonstrate that approximations of Γ_{OM} and Γ_{MSRDJ} are not as simply related as their exact counterparts. For non-Gaussian noise, even the comparison of the tree-level-approximations of the effective actions in both formalisms yields counterintuitive results, for example

$$-S_{\text{OM}}[x] \neq \sup_{\tilde{x}} -S_{\text{MSRDJ}}[x, \tilde{x}] \text{ in general,} \quad (74)$$

so even in tree level the equality, which holds for the respective full effective actions, is violated. To see this, consider the SDE:

$$\frac{d}{dt}x = f(x) + \xi,$$

with the cumulant generating function of the noise ξ given by

$$W_{\xi}(y) = \frac{D}{2}y^2 + \frac{\alpha}{3!}y^3 + \mathcal{O}(y^4),$$

⁶ Consider for example the function $f: \mathbb{R}^2 \rightarrow \mathbb{R}^2: (x, y)^T \rightarrow \frac{1}{2}(x^2 - y^2)$, which is not convex, but Legendre-transformable (namely on itself).

where we assume that $\frac{\alpha}{D^2} \ll 1$ and that we can neglect all higher order terms $\mathcal{O}(y^4)$. The MSRDJ-action is given by

$$S_{\text{MSRDJ}}[x, \tilde{x}] = \tilde{x}(\dot{x} - f(x)) + W_\xi(\tilde{x}).$$

We want to calculate

$$S_{\text{OM}} := \ln \left(\int d\tilde{x} \exp(S_{\text{MSRDJ}}[x, \tilde{x}]) \right)$$

to linear order in α . We expand S_{MSRDJ} around the saddle point $\tilde{x}_0[x]$, defined by

$$\frac{\partial S_{\text{MSRDJ}}}{\partial \tilde{x}}[x, \tilde{x}_0[x]] = 0,$$

which leads to

$$\tilde{x}_0[x] = \frac{f(x) - \dot{x}}{D} - \frac{\alpha}{2} \frac{(f(x) - \dot{x})^2}{D^2} + \mathcal{O}(\alpha^2).$$

By expanding $\tilde{x}_0[x]$ in α and inserting it into S and $\frac{\partial^2 S}{\partial \tilde{x}^2}$, we observe that

$$\begin{aligned} S_{\text{MSRDJ}}[x, \tilde{x}_0[x]] &= -\frac{(\dot{x} - f(x))^2}{2D} + \frac{\alpha}{3!} \frac{(f(x) - \dot{x})^3}{D^3} + \mathcal{O}(\alpha^2) \\ \frac{\partial^2 S_{\text{MSRDJ}}}{\partial \tilde{x}^2}[x, \tilde{x}_0[x]] &= D \left(1 - \frac{\alpha}{D^2} (\dot{x} - f(x)) \right) + \mathcal{O}(\alpha^2). \end{aligned} \quad (75)$$

Computing the contribution from the fluctuations around the stationary point with respect to \tilde{x} yields

$$\begin{aligned} & \int d\tilde{x} \exp(S_{\text{MSRDJ}}[x, \tilde{x}]) \\ &= \int d\tilde{x} \exp \left(S_{\text{MSRDJ}}[x, \tilde{x}_0] + \frac{\partial^2 S_{\text{MSRDJ}}}{\partial \tilde{x}^2}[x, \tilde{x}_0] \frac{(\tilde{x} - \tilde{x}_0[x])^2}{2} + \underbrace{\frac{\partial^3 S_{\text{MSRDJ}}}{\partial \tilde{x}^3}[x, \tilde{x}_0]}_{=\alpha} \frac{(\tilde{x} - \tilde{x}_0[x])^3}{3!} \right) \\ & \stackrel{y := (\tilde{x} - \tilde{x}_0[x])}{=} \exp(S_{\text{MSRDJ}}[x, \tilde{x}_0[x]]) \int dy \exp \left(\frac{1}{2} \frac{\partial^2 S_{\text{MSRDJ}}}{\partial \tilde{x}^2}[x, \tilde{x}_0] y^2 \right) \left(1 + \frac{1}{3!} \alpha y^3 \right) + \mathcal{O}(\alpha^2) \\ &= \exp(S_{\text{MSRDJ}}[x, \tilde{x}_0[x]]) \sqrt{\frac{2\pi}{\frac{\partial^2 S_{\text{MSRDJ}}}{\partial \tilde{x}^2}[x, \tilde{x}_0]}} + \mathcal{O}(\alpha^2) \\ &= \exp(S_{\text{MSRDJ}}[x, \tilde{x}_0[x]]) \sqrt{\frac{2\pi}{D \left(1 - \frac{\alpha}{D^2} (\dot{x} - f(x)) \right)}} + \mathcal{O}(\alpha^2) \\ &= \exp \left(-\frac{(\dot{x} - f(x))^2}{2D} + \frac{\alpha}{3!} \frac{(f(x) - \dot{x})^3}{D^3} \right) \sqrt{\frac{2\pi}{D} \left(1 + \frac{\alpha}{2D^2} (\dot{x} - f(x)) \right)} + \mathcal{O}(\alpha^2). \end{aligned}$$

So, in total, we have

$$S_{\text{OM}}[x] = \frac{1}{2} \ln \left(\frac{2\pi}{D} \right) - \underbrace{\frac{(\dot{x} - f(x))^2}{2D} - \frac{\alpha}{3!} \frac{(\dot{x} - f(x))^3}{D^3}}_{= \sup_{\tilde{x}} S_{\text{MSRDJ}}[x, \tilde{x}]} + \frac{\alpha}{2D^2} (\dot{x} - f(x)) + \mathcal{O}(\alpha^2).$$

So the fluctuations around the saddle-point value of the action lead to additional terms contributing to S_{OM} , not only constant, but also x -dependent ones. We can reformulate this to (74), so the relation we obtained for the respective effective actions does not hold for the actions, i.e. the tree-level approximations of the effective actions.

G. Effective potential from MSRDJ formalism: equilibrium systems

For systems in thermodynamic equilibrium, where the statistical weight for each configuration $x(t)$ is of Boltzmann form (setting the inverse temperature $\beta = \frac{2}{D}$)

$$p(x) \propto \exp \left(-\frac{2}{D} V(x) \right), \quad (76)$$

a construction of such an effective action has been given in the seminal work of de Dominicis [57, Appendix]. In this particular case, the Langevin equation

$$dx(t) = -V'(x) dt + dW(t) \quad (77)$$

has an equilibrium distribution of the form (76), given that the variance D of the noise is $\langle dW(s)dW(t) \rangle = D\delta_{ts}dt$; a condition that follows from demanding vanishing probability flux in the associated Fokker-Planck equation [see e.g. 141]; it is one expression of the fluctuation-dissipation theorem that holds in equilibrium systems.

Moreover, a linear term $\frac{D}{2} h x(t)$ in addition to the potential V leads to a source term $h^T \tilde{x}$ in the MSRDJ action $S[x, \tilde{x}] = \tilde{x}^T (\partial_t x + V'(x)) + \frac{D}{2} \tilde{x}^T \tilde{x} + h^T \tilde{x}$ which corresponds to (77). The equation of state (18) for \tilde{x} admits a solution $\tilde{x} \equiv 0$, for which the equation of state for x takes the form

$$\begin{aligned} h[x^*] &= \frac{\delta \Gamma}{\delta \tilde{x}^*(t)} = -\frac{\delta S}{\delta \tilde{x}^*(t)} + \dots \\ &= \partial_t x^* + V'(x^*) + \dots, \end{aligned} \quad (78)$$

where \dots denotes all fluctuation corrections. The construction of the effective action by de Dominicis proceeds by functionally integrating the equation of state [57, eq. A4]

$$\begin{aligned} \Gamma_{\text{DD}}[x^*] &:= \int_0^{x^*} \delta x h[x] \\ &= \Gamma_{\text{DD}}[0] + \frac{1}{2} x^{*T} \partial_t x^* + V(x^*) + \dots \end{aligned} \quad (79)$$

The last step requires that the equation of state (78) be the derivative of a functional; otherwise the functional integration would not yield a unique result, independent of the integration path. This is where the equilibrium properties, the existence of a Boltzmann weight (76), enter. The latter implies further that the problem can be treated with statics alone. For a constant solution $x^*(t) = \bar{x}^*$, the effective potential is thus

$$U_{\text{DD}}[\bar{x}^*] := \Gamma[\bar{x}^*] = V(\bar{x}^*) + \dots \quad (80)$$

H. Effective potential in a bistable network model

We here compute the one-loop corrections to the Onsager-Machlup effective potential for the bistable system (24). The MSRDJ action is

$$S[x, \tilde{x}] = \tilde{x}^T \left[(\partial_t + r) x + \frac{u}{3} x^3 \right] + \frac{D}{2} \tilde{x}^T \tilde{x}.$$

To lowest order in the fluctuations we have $\Gamma_0[x^*, \tilde{x}^*] = -S[x^*, \tilde{x}^*]$ for the MSRDJ effective action and the Onsager-Machlup effective action (23) is $S_{\text{OM}}[x^*] = \frac{1}{2D} [(\partial_t + r) x + \frac{u}{3} x^3]^2$. Next, we assume a stationary solution \bar{x}^* and compute all corrections around vanishing response fields $\tilde{x} = 0$.

Corrections to the mean The only one-loop contribution to $\Gamma_{\tilde{x}, \text{fl.}}^{(1)}$ is given by the tadpole diagram

$$\begin{aligned} \Gamma_{\tilde{x}, \text{fl.}}^{(1)} &= (-1) \text{ (tadpole diagram) } \\ &= -\frac{u D x^*}{2|m|}, \end{aligned}$$

where m is a function of the mean value and given by $m(x) = -r - ux^2$. Including this into the equation of state, its physically relevant solutions read

$$\begin{aligned} x_0 &= 0 \\ x_{\pm} &= \pm \sqrt{-2\frac{r}{u} + \sqrt{\left(\frac{r}{u}\right)^2 - \frac{3}{2}\frac{D}{u}}}. \end{aligned}$$

Self-energy The one-loop corrections to $\Gamma^{(2)}$ are given by the following diagrams

$$\Gamma_{\tilde{X}\tilde{X},\text{fl.}}^{(2)}(\sigma_1, \sigma_2) = (-1) \text{ (diagram 1) } + (-1) \text{ (diagram 2) }$$

$$\Gamma_{\tilde{X}\tilde{X},\text{fl.}}^{(2)}(\sigma_1, \sigma_2) = -\frac{1}{2} \text{ (diagram 3) } .$$

The zero frequency components of the self-energy read

$$\int d\sigma_2 \Gamma_{\tilde{x}x,\text{fl.}}^{(2)}(0, \sigma_2) = \frac{1}{2\pi} \left[\frac{(ux^*)^2 D}{m^2} + \frac{uD}{2m} \right]$$

$$\int d\sigma_2 \Gamma_{\tilde{x}\tilde{x},\text{fl.}}^{(2)}(0, \sigma_2) = \frac{1}{4\pi} \frac{(ux^*)^2 D^2}{m^3}.$$

Construction of correction to effective potential We have now expanded the effective action around the reference point $\tilde{x}^* = 0$ and \bar{x}^* , which takes the form

$$\Gamma[x^*, \tilde{x}^*] = \tilde{x}^* \left[\overbrace{-rx^* - \frac{u}{3}x^{*3} + \Gamma_{\tilde{x},\text{fl.}}^{(1)}}^{\text{eq. of state}_0} + \left(-\partial_t - r - ux^{*2} + \Gamma_{\tilde{x}x,\text{fl.}}^{(2)} \right) (\bar{x}^* - x^*) \right]$$

$$+ \frac{1}{2} \tilde{x}^* \left(-D + \Gamma_{\tilde{x}\tilde{x},\text{fl.}}^{(2)} \right) \tilde{x}^* + \mathcal{O}\left((\bar{x}^* - x^*)^2\right).$$

We compute only terms up to linear order in $\bar{x}^* - x^*$ because this generates all terms up to quadratic order in the effective potential. This is enough to calculate its curvature which equals the integrated covariance at the stationary points. The response field still appears quadratically in $\Gamma[x^*, \tilde{x}^*]$, so that we can take the supremum over \tilde{x}^* by writing the Onsager-Machlup effective action with corrected vertices as

$$\Gamma_{\text{OM}}[x^*] = \sup_{\tilde{x}^*} \Gamma[x^*, \tilde{x}^*]$$

$$= \left[\left(-\partial_t - r - ux^{*2} + \Gamma_{\tilde{x}x,\text{fl.}}^{(2)} \right) \delta x^* \right]$$

$$\times \frac{1}{2} \left[D - \Gamma_{\tilde{x}\tilde{x},\text{fl.}}^{(2)} \right]^{-1} \times$$

$$\times \left[\left(-\partial_t - r - ux^{*2} + \Gamma_{\tilde{x}x,\text{fl.}}^{(2)} \right) \delta x^* \right],$$

where $\delta x^* = \bar{x}^* - x^*$. Computing the effective potential we get

$$U(\bar{x}^*) = \Gamma_{\text{OM}}[\bar{x}^*]/T \tag{81}$$

$$= \frac{1}{2} \frac{\left[\left(r + ux^{*2} - D \left(\frac{ux^*}{m} \right)^2 - \frac{uD}{2m} \right) \delta x^* \right]^2}{D - \frac{(ux^*D)^2}{2m^3}},$$

where $m = m(x^*) = -r - ux^{*2}$.

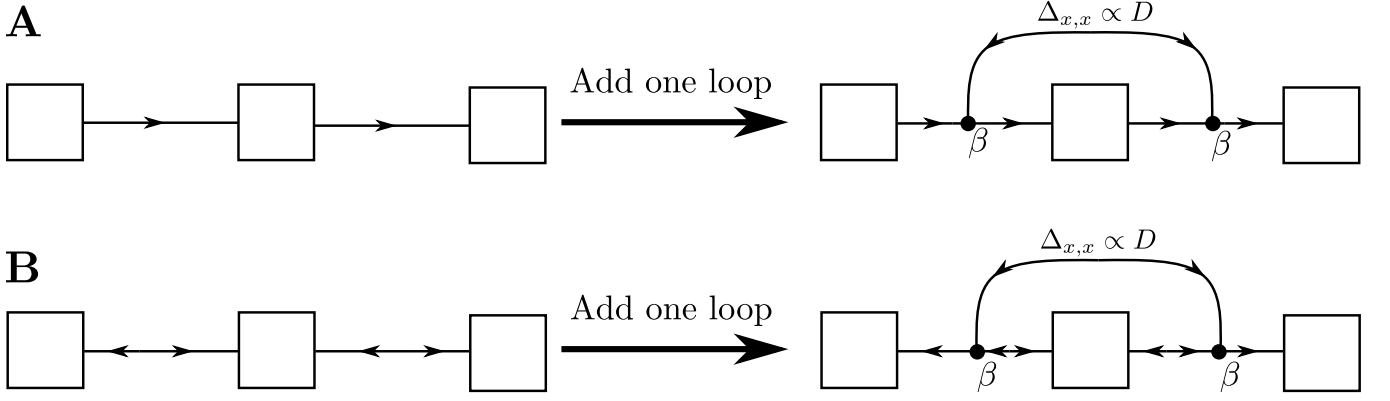


Figure 7. Adding an additional loop to an arbitrary diagram: In (A), we attach the concerning line to two $\Delta_{x\bar{x}}$ -lines, in (B) to two Δ_{xx} -lines. The mixed case is analogous and therefore omitted.

I. The loop expansion for vertices up to order three, the propagator and its small parameter

In this chapter, we explain in more detail which diagrams contribute to the first order of the loop expansion. This is of course textbook knowledge [4, 48] and has been shown for our stochastic differential equation by Chow and Buice [7], at least up to the second-order vertex. However, we find it useful to recapitulate the calculation in our notation preparing the introduction of the functional Renormalization Group and furthermore, it gives us the opportunity to show what is the small parameter in our model. This is unclear a priori because its action is not multiplied by a small constant, as usually assumed in the context of a loop expansion.

First, let us argue that the diagram shown in eq. (30) is indeed the only one to consider for the one-point vertex. This is indeed so because in the Ito convention, all loops containing only directed propagators pointing in the same direction (response loops) vanish [8]. Therefore, every additional loop requires exactly one Δ_{xx} -propagator. We see this as follows: Adding a loop means attaching a propagator-line to two points in the original diagram. This requires points at which exactly three lines meet; if we had interactions higher than three, there could also be more. The interaction bears the strength β which leads to the part β^2 in the loop expansion-parameter. It is not clear a priori, however, that the line connecting these two interactions cannot be a $\Delta_{\bar{x}x}$ -line. But Figure 7 demonstrates that the form of the interaction with two ingoing lines and one outgoing line always forces us to plug in an undirected line or, in another words, a Δ_{xx} -propagator, which introduces the factor D . So, the loop expansion in our case is an expansion in the parameter $\beta^2 D$. This consideration only compares different loop orders and not the first loop order to the tree level and therefore, this is not in contradiction to (31).

The first fluctuation corrections to the propagators consist of those diagrams that have two interaction vertices and two amputated legs, also called self-energy corrections,

$$\Gamma_{\tilde{X}X,\text{fl.}}^{(2)}(\sigma_1, \sigma_2) = (-1) \text{ (diagram with two vertices and two external legs) } = \left[\Gamma_{X\tilde{X},\text{fl.}}^{(2)}(\sigma_1, \sigma_2) \right]^*$$

$$\Gamma_{\tilde{X}\tilde{X},\text{fl.}}^{(2)}(\sigma_1, \sigma_2) = -\frac{1}{2} \text{ (diagram with two vertices and two external legs) },$$

which evaluate to

$$\Gamma_{\text{fl.}}^{(2)}(\sigma_1, \sigma_2) = \begin{pmatrix} 0 & \frac{1}{-i\sigma_1+2m} \\ \frac{1}{i\sigma_1+2m} & \frac{D}{\sigma_1^2+(2m)^2} \end{pmatrix} \frac{2\beta^2 D}{2\pi m} \delta(\sigma_1 + \sigma_2).$$

Making use of the property of the Legendre transform (20), we obtain the one-loop approximation of the propagator and hence, the variance and the response functions by solving $\Gamma^{(2)} \Delta = \left(-S^{(2)} + \Gamma_{\text{fl.}}^{(2)} \right) \Delta = 1$ for Δ .

1. The propagator in one-loop approximation

In frequency domain this yields

$$1 = \begin{pmatrix} \Gamma_{X\bar{X}}^{(2)}(\omega) \Delta_{\bar{X}X}(-\omega) & \Gamma_{X\bar{X}}^{(2)}(\omega) \Delta_{\bar{X}\bar{X}}(-\omega) \\ \Gamma_{\bar{X}X}^{(2)}(\omega) \Delta_{XX}(-\omega) - \Gamma_{\bar{X}\bar{X}}^{(2)}(\omega) \Delta_{\bar{X}X}(-\omega) & \Gamma_{\bar{X}X}^{(2)}(\omega) \Delta_{X\bar{X}}(-\omega) - \Gamma_{\bar{X}\bar{X}}^{(2)}(\omega) \Delta_{\bar{X}\bar{X}}(-\omega) \end{pmatrix}, \quad (82)$$

where

$$\Gamma^{(2)}(\omega) = \begin{pmatrix} 0 & (-i\omega + m + \frac{A}{-i\omega + 2m}) \\ (i\omega + m + \frac{A}{i\omega + 2m}) & D \left(1 - \frac{A}{\omega^2 + (2m)^2} \right) \end{pmatrix}.$$

The variables m and A are expressed in terms of the model parameters as $m = -l + 2\beta x^*$ and $A = 2\beta^2 D/m$. Equation (82) is solved by

$$\begin{aligned} \Delta_{\bar{X}\bar{X}}(\omega) &= 0 \\ \Delta_{\bar{X}X}(\omega) &= [\Delta_{X\bar{X}}(\omega)]^* = \frac{i\omega + 2m}{(i\omega + m)(i\omega + 2m) + A} \\ \Delta_{XX}(\omega) &= \Delta_{x\bar{x}}(\omega) D \Delta_{\bar{x}x}(\omega) - \Delta_{x\bar{x}}(\omega) \Gamma_{\bar{X}X, \text{fl.}}^{(2)}(\omega) D A \Gamma_{X\bar{X}, \text{fl.}}^{(2)}(\omega) \Delta_{\bar{x}x}(\omega), \end{aligned}$$

where, we introduced the notation $\Delta(\omega, \omega') = \Delta(\omega) 2\pi \delta(\omega + \omega')$. In time domain these equations read

$$\Delta_{\bar{x}x}(t, t') = \Delta_{x\bar{x}}(t', t) = -H(t' - t) \left[\frac{m_1 - 2m}{m_1 - m_2} e^{m_1|t-t'|} + \frac{2m - m_2}{m_1 - m_2} e^{m_2|t-t'|} \right] \quad (83)$$

$$\Delta_{xx}(t', t) = - \left[\frac{D(m_1^2 - (2m)^2 + A)}{2(m_1^2 - m_2^2)m_1} e^{m_1|t-t'|} + \frac{D((2m)^2 - m_2^2 - A)}{2(m_1^2 - m_2^2)m_2} e^{m_2|t-t'|} \right], \quad (84)$$

where $m_{1/2} = 3m/2 \pm \sqrt{m^2/4 - A}$ for which the relation $m_2 < 2m < m < m_1 < 0$ holds in case of a choice of parameters for which the classical fixed point x_0 is stable.

2. The three-point vertex in one-loop approximation

The corrections to the three-point interaction vertex read as

$$\begin{aligned} \Gamma_{\bar{X}XX, \text{fl.}}^{(3)}(\sigma_1, \sigma_2, \sigma_3) &= -8 \left[\text{Diagram 1} + \sigma_2 \leftrightarrow \sigma_3 + \text{Diagram 2} \right] \\ &= -\frac{8\beta^3 D}{(2\pi)^2 m} \frac{(4m + i\sigma_1)}{(2m + i\sigma_1)(2m - i\sigma_2)(2m - i\sigma_3)} \delta(\sigma_1 + \sigma_2 + \sigma_3). \end{aligned}$$

Often, it is useful to go into the time domain, which yields

$$\Gamma_{\bar{x}xx, \text{fl.}}^{(3)}(t_1, t_2, t_3) = \begin{cases} -8\beta^3 \frac{D}{m} e^{2m(t_1 - t_3)} & , t_1 > t_2 > t_3 \\ -8\beta^3 \frac{D}{m} e^{2m(t_1 - t_2)} & , t_1 > t_3 > t_2 \\ 0 & , \text{else} \end{cases} \quad (85)$$

For the BMW approximation we will need the two quantities $\Gamma_{\tilde{X}XX,\text{fl.}}^{(3)}(\sigma_1, -\sigma_1, 0)$ and $\Gamma_{\tilde{X}XX,\text{fl.}}^{(3)}(0, \sigma_2, -\sigma_2)$ which in one-loop approximation read

$$\begin{aligned}\Gamma_{\tilde{X}XX,\text{fl.}}^{(3)}(\sigma_1, -\sigma_1, 0) &= -\frac{4\beta^3 D}{(2\pi)^2} \frac{4m + i\sigma_1}{m^2 (2m + i\sigma_1)^2} \\ \Gamma_{\tilde{X}XX,\text{fl.}}^{(3)}(0, \sigma_2, -\sigma_2) &= -\frac{16\beta^3 D}{(2\pi)^2} \frac{1}{m \sigma_2^2 + 4m^2},\end{aligned}$$

which in time domain yields

$$\begin{aligned}\Gamma_{\tilde{x}xx,\text{fl.},1}^{(3)}(t_1, t_2) &= -\frac{8\beta^3 D}{2\pi m} H(t_1 - t_2) \left(t_1 - t_2 - \frac{1}{2m}\right) e^{2m(t_1 - t_2)} \\ \Gamma_{\tilde{x}xx,\text{fl.},2}^{(3)}(t_1, t_2) &= \frac{8\beta^3 D}{2\pi m} \frac{1}{2m} e^{2m|t_1 - t_2|}.\end{aligned}$$

A comparison between the fluctuation corrections $\Gamma_{\text{fl.}}$ and the corresponding terms in the action S reveals that $\Gamma_{x\tilde{x},\text{fl.}}^{(2)}$ counteracts the tree-level contribution m , whereas the $\tilde{x}\tilde{x}$ - and the $\tilde{x}xx$ -contributions are enhanced. Therefore, the linear term m of the differential equation gets weakened such that for large noise it could even effectively vanish. This would correspond to a second order phase transition signaled by the divergence of fluctuations [given by the Ginzburg criterion, see e.g. 60, i.p. section 6.4]. However, we are unable to explore this regime because the destabilization of the trivial fix point is always accompanied by a breakdown of the loop expansion, as we will demonstrate in the following.

3. Reduction from three to one parameter

Obviously, we increase the escape probability by decreasing the leak term, which amounts to approaching the critical point. These two effects cannot be decoupled by appropriately redefining the noise level D . We see this by rescaling the time as $s = lt$ and accordingly the fields $\tilde{y}(s) = \sqrt{D/l} \tilde{x}(t)$ and $y(s) = \sqrt{l/D} x(t)$ which leads to

$$S[\tilde{y}, y] = \int ds \left[\tilde{y}^T (\partial_s + 1) y - \beta' \tilde{y}^T y^2 + \tilde{y}^T \frac{1}{2} \tilde{y} \right], \quad \text{where } \beta' = \sqrt{\frac{D}{l^3}}.$$

The unstable fixed point is then given by $x_0 = 1/\beta'$ in the noise-less case. Therefore, β' is the only free parameter of the model and the strength of the nonlinearity determines also the distance between the stable and the unstable fixed point. So it is impossible to find a set of parameters for which on the one hand the system operates far from the unstable fixed point so that the expansion around the stable fixed point is accurate and for which on the other hand and concurrently the effect of the nonlinearity is stronger than the linear part.

J. Equation of motion for δx from Fokker-Plank equation

We start by multiplying the Fokker-Plank equation [58] for a time-dependent density

$$\tau \partial_t \rho(x, t) = -\partial_x \left(f(x) - \frac{D}{2} \partial_x \right) \rho(x, t)$$

by x and integrating over x :

$$\begin{aligned}\partial_t \langle x \rangle(t) &= - \int dx x \left(\partial_x (f(x) \rho(x, t)) - \frac{D}{2} \partial_x^2 \rho(x, t) \right) \\ &= \int dx f(x) \rho(x, t) = -l \langle x(t) \rangle + \beta \langle x(t)^2 \rangle,\end{aligned}$$

where from the first to the second line we used partial integration. From the second term only a derivative under an integral remains, which vanishes because we assume that ρ vanishes at the borders of the integral - a property that we will use repeatedly in the following. In the last equality, furthermore, we inserted $f(x) = -lx + \beta x^2$. Now, we need

an ODE for the second moment, which we obtain analogously:

$$\begin{aligned}
\partial_t \langle x^2 \rangle (t) &= - \int dx x^2 \left(\partial_x (f(x) \rho(x, t)) - \frac{D}{2} \partial_x^2 \rho(x, t) \right) \\
&= \int dx (2xf(x) \rho(x, t) - Dx \partial_x \rho(x, t)) \\
&= \int dx (2xf(x) \rho(x, t) + D \rho(x, t)) \\
&= -2l \langle x^2 \rangle (t) + 2\beta \langle x^3 \rangle (t) + D.
\end{aligned}$$

Truncating the hierarchy of moments by a Gaussian closure, that is

$$\begin{aligned}
\langle x^3 \rangle &= \langle\langle x^3 \rangle\rangle + 3\langle\langle x^2 \rangle\rangle \langle x \rangle + \langle x \rangle^3 \\
&= \langle\langle x^3 \rangle\rangle + 3\langle x^2 \rangle \langle x \rangle - 2\langle x \rangle^3 \approx 3\langle x^2 \rangle \langle x \rangle - 2\langle x \rangle^3
\end{aligned}$$

leads to

$$\partial \langle x^2 \rangle (t) \approx -2l \langle x^2 \rangle (t) + 6\beta \langle x^2 \rangle (t) \langle x \rangle (t) - 4\beta (\langle x \rangle (t))^3 + D.$$

Using $\langle\langle x^2 \rangle\rangle = \langle x^2 \rangle - \langle x \rangle^2$, the equations for the first two cumulants read:

$$\partial_t \langle x \rangle (t) = -l \langle x \rangle (t) + \beta (\langle\langle x^2 \rangle\rangle (t) + (\langle x \rangle (t))^2) \quad (86)$$

$$\partial_t \langle\langle x^2 \rangle\rangle (t) = -2l \langle\langle x^2 \rangle\rangle (t) + 4\beta \langle\langle x^2 \rangle\rangle (t) \langle x \rangle (t) + D \quad (87)$$

We can interpret the one-loop equation of motion as an approximation of the solution of the Fokker-Planck equations of motion (86) and (87). To see this, we formally solve (87) and insert the result into (86). It is convenient to express the time dependence of x and Δ as a deviation from the stationary solution, defining

$$\langle x \rangle (t) = \bar{x} + \delta x (t) \quad (88)$$

$$\langle\langle x^2 \rangle\rangle (t) = \bar{\Delta} + \delta \Delta (t) \quad (89)$$

$$\bar{m} = -l + 2\beta \bar{x}$$

$$m(t) = -l + 2\beta \langle x \rangle (t) = \bar{m} + 2\beta \delta x (t).$$

Using these definitions, we obtain for the stationary case

$$0 = -l\bar{x} + \beta \bar{x}^2 + \beta \bar{\Delta} \quad \text{and} \quad \bar{\Delta} = -\frac{D}{2\bar{m}},$$

which follows from (86) and (87), respectively. Expressing these equations in the new variables (88) and (89) yields

$$\begin{aligned}
\partial_t \delta x (t) = \partial_t \langle x \rangle (t) &= -(l - 2\beta \bar{x}) \delta x (t) + \beta \delta x (t) \underbrace{-l\bar{x} + \beta \bar{x}^2 + \beta \bar{\Delta}}_{=0} + \beta \delta \Delta (t) \\
&= \bar{m} \delta x (t) + \beta \delta x (t)^2 + \beta \delta \Delta (t)
\end{aligned} \quad (90)$$

and

$$\begin{aligned}
\partial_t \delta \Delta (t) &= \underbrace{2\bar{m}\bar{\Delta} + D}_{=0} + 2(\bar{m} + 2\beta \delta x (t)) \delta \Delta (t) + 4\beta \bar{\Delta} \delta x (t) \\
&= 2m(t) \delta \Delta (t) + 4\beta \bar{\Delta} \delta x (t).
\end{aligned}$$

The latter equation turns out to be more convenient for our purpose compared to (87). Solving it by variation of constants, we obtain

$$\begin{aligned}
\delta \Delta (t) &= 4\beta \bar{\Delta} \int_{t_0}^t dt'' \delta x (t'') e^{\int_{t_0}^t dt' 2m(t')} \\
&= 4\beta \bar{\Delta} \int_{t_0}^t dt'' \delta x (t'') e^{2\bar{m}(t-t'')} e^{4\beta \int_{t_0}^t dt' \delta x (t')},
\end{aligned} \quad (91)$$

where we introduced the initial time t_0 . We notice that $\langle x^2 \rangle(t = t_0) = \Delta^*$, since $\delta\Delta(t = t_0) = 0$. This corresponds to x being distributed according to the stationary distribution with mean value shifted by the initial deflection $\delta x(t_0)$. If we assume that $\delta x(t)$ is small for all t , we can expand the second exponential function in (91) and neglect terms of $\mathcal{O}(\delta x^3)$. Thus

$$\begin{aligned}\delta\Delta(t) &= 4\beta\bar{\Delta} \int_{t_0}^t dt'' \delta x(t'') e^{2\bar{m}(t-t'')} + 16\bar{\Delta}\beta^2 \int_{t_0}^t dt'' \delta x(t'') e^{2\bar{m}(t-t'')} \int_{t''}^t dt' \delta x(t') + \mathcal{O}(\delta x^3) \\ &= 4\beta\bar{\Delta} \int_{t_0}^t dt' \delta x(t') e^{2\bar{m}(t-t')} + 16\bar{\Delta}\beta^2 \int_{t_0}^t dt' \delta x(t') \int_{t_0}^{t'} dt'' \delta x(t'') e^{2\bar{m}(t-t'')} + \mathcal{O}(\delta x^3).\end{aligned}$$

If we insert this result into (90) we obtain up to second order

$$\begin{aligned}\partial_t \delta x(t) &= \bar{m} \delta x(t) + \beta \delta x(t)^2 \\ &\quad + 4\beta^2 \bar{\Delta} \int_{t_0}^t dt' \delta x(t') e^{2\bar{m}(t-t')} \\ &\quad + 16\bar{\Delta}\beta^3 \int_{t_0}^t dt' \delta x(t') \int_{t_0}^{t'} dt'' \delta x(t'') e^{2\bar{m}(t-t'')},\end{aligned}$$

which equals exactly the one-loop result (35).

K. Derivation of fRG-flow equations

For completeness, the derivation of the Wetterich equation [34] as presented in [35] is repeated in the following. The difference of the current presentation is the additional presence of the response field. We will use the property $\partial_\lambda \Gamma_\lambda = -\partial_\lambda W_\lambda$, which holds generally for Legendre transforms of quantities depending on a parameter, here λ [4, eq. (1.93)]. This yields, using the regulator of the form introduced in (39),

$$\begin{aligned}\frac{\partial \tilde{\Gamma}_\lambda[X^*, \tilde{X}^*]}{\partial \lambda} &= -\frac{\partial W_\lambda[J, \tilde{J}]}{\partial \lambda} \\ &= -\frac{1}{\mathcal{Z}[J, \tilde{J}]} \int \mathcal{D}X \int \mathcal{D}\tilde{X} \frac{\partial}{\partial \lambda} \Delta S_\lambda[X, \tilde{X}] \exp(S_\lambda[X, \tilde{X}]) \\ &\quad \times \exp(J^T X + \tilde{J}^T \tilde{X}) \\ &= \frac{1}{2} \int d\omega \int d\omega' \langle X(\omega) \frac{\partial R_\lambda(\omega, \omega')}{\partial \lambda} \tilde{X}(\omega') \rangle \\ &= \frac{1}{2} \int d\omega \int d\omega' \left\{ \Delta_{\tilde{X}X, \lambda}(\omega', \omega) \frac{\partial R_\lambda(\omega, \omega')}{\partial \lambda} + X^*(\omega) \frac{\partial R_\lambda(\omega, \omega')}{\partial \lambda} \tilde{X}^*(\omega') \right\} \\ &= \frac{1}{2} \text{Tr} \left\{ \Delta_{\tilde{X}X, \lambda} \frac{\partial R_\lambda}{\partial \lambda} \right\} + \frac{\partial}{\partial \lambda} \Delta S_\lambda[X^*, \tilde{X}^*].\end{aligned}\tag{92}$$

In the third line we used $\langle \tilde{X}(\omega') X(\omega) \rangle = \langle \tilde{X}(\omega) X(\omega') \rangle + \langle \tilde{X}(\omega') \rangle \langle X(\omega) \rangle = \Delta_{\tilde{X}X, \lambda}(\omega', \omega) + X^*(\omega) \tilde{X}^*(\omega')$. From the relation (40) between $\tilde{\Gamma}_\lambda$ and Γ_λ we arrive directly at the final form of the Wetterich equation as presented in eq. (41).

L. Flow equations for the self-energy and the interaction vertex

The non-vanishing diagrams for the self-energy translate to

$$\begin{aligned}
\frac{\partial \Gamma_{\tilde{X}X,\lambda}^{(2)}(\sigma_1, -\sigma_1)}{\partial \lambda} &= \frac{1}{2} \int \frac{d\omega}{(2\pi)} \Gamma_{\tilde{X}XX,\lambda}^{(3)}(\sigma_1, -\sigma_1 - \omega, \omega) \Delta_{XX,\lambda}(\omega) \frac{\partial R_\lambda}{\partial \lambda} \Delta_{\tilde{X}X,\lambda}(\omega) \\
&\quad \times \Gamma_{XX\tilde{X},\lambda}^{(3)}(-\sigma_1, -\omega, \sigma_1 + \omega) \Delta_{\tilde{X}X,\lambda}(\sigma_1 + \omega) \\
&+ \frac{1}{2} \int \frac{d\omega}{(2\pi)} \Gamma_{\tilde{X}XX,\lambda}^{(3)}(\sigma_1, -\sigma_1 - \omega, \omega) \Delta_{XX,\lambda}(\omega) \Gamma_{XX\tilde{X},\lambda}^{(3)}(-\sigma_1, -\omega, \sigma_1 + \omega) \\
&\quad \times \Delta_{\tilde{X}X,\lambda}(\sigma_1 + \omega) \frac{\partial R_\lambda}{\partial \lambda} \Delta_{\tilde{X}X,\lambda}(\sigma_1 + \omega) \\
&+ \frac{1}{2} \int \frac{d\omega}{(2\pi)} \Gamma_{\tilde{X}XX,\lambda}^{(3)}(\sigma_1, -\sigma_1 - \omega, \omega) \Delta_{X\tilde{X},\lambda}(\omega) \Gamma_{X\tilde{X},\lambda}^{(3)}(-\sigma_1, -\omega, \sigma_1 + \omega) \\
&\quad \times \Delta_{XX,\lambda}(\sigma_1 + \omega) \frac{\partial R_\lambda}{\partial \lambda} \Delta_{\tilde{X}X,\lambda}(\sigma_1 + \omega) \\
\frac{\partial \Gamma_{\tilde{X}\tilde{X},\lambda}^{(2)}(\sigma_1, -\sigma_1)}{\partial \lambda} &= \frac{1}{2} \int \frac{d\omega}{(2\pi)} \Gamma_{\tilde{X}XX,\lambda}^{(3)}(\sigma_1, -\sigma_1 - \omega, \omega) \Delta_{XX,\lambda}(\omega) \frac{\partial R_\lambda}{\partial \lambda} \Delta_{\tilde{X}X,\lambda}(\omega) \\
&\quad \times \Gamma_{\tilde{X}XX,\lambda}^{(3)}(-\sigma_1, -\omega, \sigma_1 + \omega) \Delta_{XX,\lambda}(\sigma_1 + \omega) \\
&+ \sigma_1 \rightarrow -\sigma_1.
\end{aligned}$$

The diagrams for the flow of the interaction vertex are given by

$$\begin{aligned}
&\frac{\partial \Gamma_{\tilde{X}XX,\lambda}^{(3)}(\sigma_1, \sigma_2, \sigma_3)}{\partial \lambda} \\
&= -\frac{1}{2} \left[\begin{array}{c} \text{Diagram 1: Circle with vertices } \sigma_1, \sigma_2, \sigma_3. \text{ A square box is on the arc between } \sigma_2 \text{ and } \sigma_3. \\ \text{Diagram 2: Circle with vertices } \sigma_1, \sigma_2, \sigma_3. \text{ A square box is on the arc between } \sigma_1 \text{ and } \sigma_2. \\ \text{Diagram 3: Circle with vertices } \sigma_1, \sigma_2, \sigma_3. \text{ A square box is on the arc between } \sigma_1 \text{ and } \sigma_3. \\ \text{Diagram 4: Circle with vertices } \sigma_1, \sigma_2, \sigma_3. \text{ A square box is on the arc between } \sigma_2 \text{ and } \sigma_3. \\ \text{Diagram 5: Circle with vertices } \sigma_1, \sigma_2, \sigma_3. \text{ A square box is on the arc between } \sigma_1 \text{ and } \sigma_2. \\ \text{Diagram 6: Circle with vertices } \sigma_1, \sigma_2, \sigma_3. \text{ A square box is on the arc between } \sigma_1 \text{ and } \sigma_3. \end{array} \right] \\
&+ \sigma_2 \leftrightarrow \sigma_3.
\end{aligned}$$

M. Definition of the Fourier transform

By choosing the Fourier transform of the fields and the sources as the inverse of each other, we arrive at a representation of our formulas that look similar in time and frequency domain. Therefore we define

$$\begin{aligned} x(t) &= \int \frac{d\omega}{2\pi} e^{i\omega t} X(\omega) & j(t) &= \int d\omega e^{-i\omega t} J(\omega) \\ X(\omega) &= \int dt e^{-i\omega t} x(t) & J(\omega) &= \int \frac{dt}{2\pi} e^{i\omega t} j(t). \end{aligned}$$

Thus, we obtain $x^T j = \int dt x(t) j(t) = \int d\omega X(\omega) J(\omega)$. Moreover, we get with $y := (x, \tilde{x})^T$ for the matrix A of the quadratic part of the action $S_0[x, \tilde{x}] = \int dt \int dt' y(t) A(t, t') y(t')$

$$\begin{aligned} A(t, t') &= \int d\omega \int d\omega' e^{-i(\omega t + \omega' t')} A(\omega, \omega') & A^{-1}(t, t') &= \int \frac{d\omega}{2\pi} \int \frac{d\omega'}{2\pi} e^{i(\omega t + \omega' t')} A^{-1}(\omega, \omega') \\ A(\omega, \omega') &= \int \frac{dt}{2\pi} \int \frac{dt'}{2\pi} e^{i(\omega t + \omega' t')} A(t, t') & A^{-1}(\omega, \omega') &= \int dt \int dt' e^{-i(\omega t + \omega' t')} A^{-1}(t, t') \end{aligned}$$

due to the chain rule for functional derivatives. From this we can derive the following useful identities

$$\begin{aligned} \int dt \int dt' y(t) A(t, t') y(t') &= \int d\omega \int d\omega' Y(\omega) A(\omega, \omega') Y(\omega') \\ \int dt \int dt' \bar{j}(t) A^{-1}(t, t') \bar{j}(t') &= \int d\omega \int d\omega' \bar{J}(\omega) A^{-1}(\omega, \omega') \bar{J}(\omega') \\ \int ds A(t, s) A^{-1}(s, t') &= \delta(t - t') & \Leftrightarrow & \int d\sigma A(\omega, \sigma) A^{-1}(\sigma, \omega') = \delta(\omega - \omega'). \end{aligned}$$

For the interaction part of the action we obtain

$$\int dt \tilde{x}(t) x^2(t) = \int \frac{d\omega}{2\pi} \int \frac{d\omega'}{2\pi} \tilde{X}(\omega) X(\omega') X(-\omega - \omega').$$

-
- [1] D. Dahmen, H. Bos, and M. Helias, *Phys Rev X* **6**, 031024 (2016).
 - [2] H. Sompolsky, *Physics Today* **41**, 70 (1988).
 - [3] V. Braitenberg and A. Schüz, *Anatomy of the Cortex: Statistics and Geometry* (Springer-Verlag, Berlin, Heidelberg, New York, 1991), ISBN 3-540-53233-1.
 - [4] J. Zinn-Justin, *Quantum field theory and critical phenomena* (Clarendon Press, Oxford, 1996).
 - [5] P. C. Hohenberg and B. I. Halperin, *Rev. Mod. Phys.* **49**, 435 (1977).
 - [6] U. C. Täuber, *Critical dynamics: a field theory approach to equilibrium and non-equilibrium scaling behavior* (Cambridge University Press, 2014), ISBN 9780521842235.
 - [7] C. Chow and M. Buice, *J Math. Neurosci* **5** (2015).
 - [8] J. A. Hertz, Y. Roudi, and P. Sollich, *Journal of Physics A: Mathematical and Theoretical* **50**, 033001 (2017).
 - [9] C. Duclut, *Theses, Université Pierre et Marie Curie - Paris VI* (2017), URL <https://tel.archives-ouvertes.fr/tel-01690438>.
 - [10] C. van Vreeswijk and H. Sompolsky, *Science* **274**, 1724 (1996).
 - [11] D. J. Amit and N. Brunel, *Network: Comput. Neural Systems* **8**, 373 (1997).
 - [12] N. Brunel, *J. Comput. Neurosci.* **8**, 183 (2000).
 - [13] J. J. Hopfield, *PNAS* **79**, 2554 (1982).
 - [14] I. Ginzburg and H. Sompolsky, *Phys. Rev. E* **50**, 3171 (1994).
 - [15] A. Renart, J. De La Rocha, P. Bartho, L. Hollender, N. Parga, A. Reyes, and K. D. Harris, *Science* **327**, 587 (2010).
 - [16] M. Helias, T. Tetzlaff, and M. Diesmann, *PLOS Comput. Biol.* **10**, e1003428 (2014).
 - [17] E. Shea-Brown, K. Josic, J. de la Rocha, and B. Doiron, *Phys. Rev. Lett.* **100**, 108102 (2008).
 - [18] V. Pernice, B. Staude, S. Cardanobile, and S. Rotter, *PLOS Comput. Biol.* **7**, e1002059 (2011).
 - [19] V. Pernice, B. Staude, S. Cardanobile, and S. Rotter, *Phys. Rev. E* **85**, 031916 (2012).
 - [20] T. Tetzlaff, M. Helias, G. T. Einevoll, and M. Diesmann, *PLOS Comput. Biol.* **8**, e1002596 (2012).
 - [21] J. Trousdale, Y. Hu, E. Shea-Brown, and K. Josic, *PLOS Comput. Biol.* **8**, e1002408 (2012).
 - [22] Y. Hu, J. Trousdale, K. Josić, and E. Shea-Brown, *Journal of Statistical Mechanics: Theory and Experiment* **2013**, P03012 (2013).

- [23] N. Brunel and V. Hakim, *Neural Comput.* **11**, 1621 (1999).
- [24] N. Brunel, *J. Comput. Neurosci.* **8**, 183 (2000).
- [25] M. Helias, T. Tetzlaff, and M. Diesmann, *New J. Phys.* **15**, 023002 (2013).
- [26] H. Bos, M. Diesmann, and M. Helias, *PLOS Comput. Biol.* **12**, e1005132 (2016).
- [27] J. M. Beggs and D. Plenz, *J. Neurosci.* **24**, 5216 (2004).
- [28] G. Tkačik, O. Marre, D. Amodei, E. Schneidman, W. Bialek, and M. J. Berry II, *PLoS Comp Biol* **10**, e1003408 (2014).
- [29] H. Jaeger, Tech. Rep. GMD Report 148, German National Research Center for Information Technology, St. Augustin, Germany (2001).
- [30] W. Maass, T. Natschläger, and H. Markram, *Neural Comput.* **14**, 2531 (2002).
- [31] R. Legenstein and W. Maass, *Neural Networks* **20**, 323 (2007).
- [32] K. G. Wilson, *Rev. Mod. Phys.* **47**, 773 (1975).
- [33] F. J. Wegner and A. Houghton, *Phys. Rev. A* **8**, 401 (1973).
- [34] C. Wetterich, *Physics Letters B* **30**, 90 (1993), ISSN 0370-2693.
- [35] J. Berges, N. Tetradis, and C. Wetterich, *Physics Reports* **363**, 223 (2002), ISSN 0370-1573, renormalization group theory in the new millennium.
- [36] P. Martin, E. Siggia, and H. Rose, *Phys. Rev. A* **8**, 423 (1973).
- [37] H.-K. Janssen, *Zeitschrift für Physik B Condensed Matter* **23**, 377 (1976).
- [38] C. De Dominicis, *J. Phys. Colloques* **37**, C1 (1976).
- [39] H. Sompolinsky and A. Zippelius, *Phys. Rev. Lett.* **47**, 359 (1981).
- [40] K. Fischer and J. Hertz, *Spin glasses* (Cambridge University Press, 1991).
- [41] A. Crisanti and H. Sompolinsky, *Phys Rev E* **98**, 062120 (2018).
- [42] J. Schuecker, S. Goedeke, and M. Helias, *Phys Rev X* **8**, 041029 (2018).
- [43] S. Song, P. Sjöström, M. Reigl, S. Nelson, and D. Chklovskii, *PLoS Biol.* **3**, e68 (2005).
- [44] D. Martí, N. Brunel, and S. Ostojic, *Phys. Rev. E* **97**, 062314 (2018).
- [45] J.-P. Blaizot, R. Méndez-Galain, and N. Wschebor, *Physics Letters B* **632**, 571 (2006), ISSN 0370-2693.
- [46] C. Gardiner, *Stochastic Methods: A Handbook for the Natural and Social Sciences* (Springer, Berlin, Heidelberg, 2009), 4th ed.
- [47] N. G. Van Kampen, *Stochastic Processes in Physics and Chemistry, Third Edition (North-Holland Personal Library)* (North Holland, 2007), 3rd ed.
- [48] H. Kleinert, *Path Integrals in Quantum Mechanics, Statistics, Polymer Physics, and Financial Markets* (World Scientific, 2009), 5th ed.
- [49] L. Onsager and S. Machlup, **91**, 1505 (1953).
- [50] R. L. Stratonovich, in *Proc. Sixth All-Union Conf. Theory Prob. and Math. Statist, Vilnius* (1960), pp. 471–482, translation to english by A. N. Rossolimo published in "Selected Transl. in Math. Statist. and Probability, Vol. 10, 1971".
- [51] C. W. Gardiner, *Handbook of Stochastic Methods for Physics, Chemistry and the Natural Sciences* (Springer-Verlag, Berlin, 1985), 2nd ed., ISBN 3-540-61634-9, 3-540-15607-0.
- [52] R. Graham, *Zeitschrift für Physik B Condensed Matter* **26**, 281 (1977), ISSN 1431-584X.
- [53] K. L. C. Hunt and J. Ross, *The Journal of Chemical Physics* **75**, 976 (1981), <https://doi.org/10.1063/1.442098>.
- [54] M. F. Weber and E. Frey, *Reports on Progress in Physics* **80**, 046601 (2017).
- [55] A. Altland and B. Simons, *Concepts of Theoretical Solid State Physics* (Cambridge University Press, 2010).
- [56] P. C. Bressloff, *SIAM J. appl. math.* **70**, 1488 (2009).
- [57] C. De Dominicis, *Phys. Rev. B* **18**, 4913 (1978).
- [58] H. Risken, *The Fokker-Planck Equation* (Springer Verlag Berlin Heidelberg, 1996), URL https://doi.org/10.1007/978-3-642-61544-3_4.
- [59] A. Vasiliev, *Functional Methods in Quantum Field Theory and Statistical Physics* (Gordon and Breach Science Publishers, 1998).
- [60] D. J. Amit, *Field theory, the renormalization group, and critical phenomena* (World Scientific, 1984).
- [61] M. Helias and D. Dahmen, arXiv pp. 1901.10416 [cond-mat.dis-nn] (2019).
- [62] P. Kopietz, L. Bartosch, and F. Schütz, *Introduction to the Functional Renormalization Group* (Springer, 2010).
- [63] G. L. Eyink, *Phys. Rev. E* **54**, 3419 (1996).
- [64] J. W. Negele and H. Orland, *Quantum Many-Particle Systems* (New York: Perseus Books, 1998).
- [65] A. C. C. Coolen, arXiv:cond-mat/0006011 (2000).
- [66] H. Sompolinsky, A. Crisanti, and H. J. Sommers, *Phys. Rev. Lett.* **61**, 259 (1988).
- [67] F. Cooper and J. F. Dawson, arxiv preprint arXiv:1406.2737 (2015).
- [68] M. A. Buice and C. C. Chow, *Phys. Rev. E* **76**, 031118 (2007).
- [69] J. E. Mayer and M. Goeppert-Mayer, *Statistical mechanics* (John Wiley & Sons, Inc., 1977), 2nd ed.
- [70] A. Roxin, N. Brunel, D. Hansel, G. Mongillo, and C. van Vreeswijk, *J. Neurosci.* **31**, 16217 (2011).
- [71] L. Ornigotti, A. Ryabov, V. Holubec, and R. Filip, *Phys. Rev. E* **97**, 032127 (2018).
- [72] R. Filip and P. Zemánek, *Journal of Optics* **18**, 065401 (2016).
- [73] P. E. Latham, B. J. Richmond, P. G. Nelson, and S. Nirenberg, *J. Neurophysiol.* **83**, 808 (2000).
- [74] R. Brette and W. Gerstner, *J. Neurophysiol.* **94**, 3637 (2005).
- [75] V. Elgart and A. Kamenev, *Phys. Rev. E* **70**, 041106 (2004).
- [76] M. A. Buice and J. D. Cowan, *Phys. Rev. E* **75**, 051919 (2007).
- [77] M. Doi, *Journal of Physics A: Mathematical and General* **9**, 1465 (1976).

- [78] L. Peliti, J. Phys. France pp. 1469–1483 (1985).
- [79] R. Zwanzig, *Nonequilibrium Statistical Mechanics* (Oxford University Press, 2001), ISBN 0-19-514018-4.
- [80] H. Sommers, A. Crisanti, H. Sompolinsky, and Y. Stein, Phys. Rev. Lett. **60**, 1895 (1988).
- [81] G. La Camera, A. Rauch, D. Thurbon, H.-R. Lüscher, W. Senn, and S. Fusi, Journal of Neurophysiology **96**, 3448 (2006), pMID: 16807345, <https://doi.org/10.1152/jn.00453.2006>.
- [82] R. Chaudhuri, K. Knoblauch, M.-A. Gariel, H. Kennedy, and X.-J. Wang, Neuron **88**, 419 (2015), ISSN 0896-6273.
- [83] B. A. W. Brinkman, F. Rieke, E. Shea-Brown, and M. A. Buice, PLOS Comput. Biol. **14**, e1006490 (2018).
- [84] B. Bravi, P. Sollich, and M. Oppen, Journal of Physics A: Mathematical and Theoretical **49**, 194003 (2016).
- [85] C. De Dominicis and P. C. Martin, Journal of Mathematical Physics **5**, 14 (1964).
- [86] T. R. MORRIS, International Journal of Modern Physics A **09**, 2411 (1994), <https://doi.org/10.1142/S0217751X94000972>.
- [87] C. Bagnuls and C. Bervillier, Physics Reports **348**, 91 (2001), ISSN 0370-1573, renormalization group theory in the new millennium. II.
- [88] C. Duclut and B. Delamotte, Phys. Rev. E **95**, 012107 (2017).
- [89] F. Schütz and P. Kopietz, Journal of Physics A: Mathematical and General **39**, 8205 (2006).
- [90] J.-P. Blaizot, R. Méndez-Galain, and N. Wschebor, Phys. Rev. E **74**, 051116 (2006).
- [91] L. Canet, H. Chaté, B. Delamotte, and N. Wschebor, Phys. Rev. Lett. **104**, 150601 (2010).
- [92] F. Benitez, J.-P. Blaizot, H. Chaté, B. Delamotte, R. Méndez-Galain, and N. Wschebor, Phys. Rev. E **85**, 026707 (2012).
- [93] E. Schneidman, M. J. Berry, R. Segev, and W. Bialek, Nature **440**, 1007 (2006).
- [94] H. C. Andersen, Journal of Mathematical Physics **41**, 1979 (2000).
- [95] S. H. Strogatz, *Nonlinear Dynamics and Chaos: with Applications to Physics, Biology, Chemistry, and Engineering* (Perseus Books, Reading, Massachusetts, 1994), ISBN 0-201-54344-3.
- [96] G. Buzsáki and A. Draguhn, Science **304**, 1926 (2004).
- [97] N. Brunel and X.-J. Wang, J. Neurophysiol. **90**, 415 (2003).
- [98] K. Takahashi, S. Kim, T. P. Coleman, K. A. Brown, A. J. Suminski, M. D. Best, and N. G. Hatsopoulos, Nature Communications **6** (2015).
- [99] M. Denker, L. Zehl, B. E. Kilavik, M. Diesmann, T. Brochier, A. Riehle, and S. Grün, Scientific Reports **8**, 1 (2018).
- [100] S. DiSanto, P. Villegas, R. Burioni, and M. A. Munoz, Proceedings of the National Academy of Sciences **115**, E1356 (2018), ISSN 0027-8424, <http://www.pnas.org/content/early/2018/01/26/1712989115.full.pdf>.
- [101] A. K. Barreiro, J. N. Kutz, and E. Shlizerman, The Journal of Mathematical Neuroscience **7**, 10 (2017), ISSN 2190-8567.
- [102] M. Steriade, A. Nuñez, and F. Amzica, J. Neurosci. **13**, 3252 (1993).
- [103] A. Destexhe, S. W. Hughes, M. Rudolph, and V. Crunelli, TINS **30**, 334 (2007), ISSN 0166-2236, july INMED/TINS special issue—Physiogenic and pathogenic oscillations: the beauty and the beast.
- [104] P. C. Bressloff and O. Faugeras, Journal of Statistical Mechanics: Theory and Experiment **2017**, 033206 (2017).
- [105] B. A. W. Brinkman, F. Rieke, E. Shea-Brown, and M. A. Buice, arXiv preprint arXiv:1702.00865 (2017).
- [106] B. Bravi and P. Sollich, Physical Biology **14**, 045010 (2017).
- [107] C. Husemann and M. Salmhofer, Phys. Rev. B **79**, 195125 (2009).
- [108] N. Wentzell, G. Li, A. Tagliavini, C. Taranto, G. Rohringer, K. Held, A. Toschi, and S. Andergassen, arxiv preprint, arXiv:1610.06520 (2016).
- [109] C. J. Eckhardt, G. A. H. Schober, J. Ehrlich, and C. Honerkamp, Phys. Rev. B **98**, 075143 (2018).
- [110] B. Delamotte, in *Renormalization groups and effective field theory approaches to many-body systems*, edited by J. S. Janos Polonyi (Springer, 2012), pp. 49–130.
- [111] M. M. e. a. Churchland, Nat. Neurosci. **13**, 369 (2010).
- [112] A. Litwin-Kumar, M. J. Chacron, and B. Doiron, PLOS Comput. Biol. **8**, e1002667 (2012).
- [113] M. Ohbayashi, K. Ohki, and Y. Miyashita, Science **301**, 233 (2003), ISSN 0036-8075, <http://science.sciencemag.org/content/301/5630/233.full.pdf>.
- [114] M. Henningson and S. Illes, Front Comput Neurosci **11** (2017).
- [115] M. Kardar, G. Parisi, and Y.-C. Zhang, Phys. Rev. Lett. **56**, 889 (1986).
- [116] K. J. Wiese, Journal of Statistical Physics **93**, 143 (1998), ISSN 1572-9613.
- [117] V. Priesemann, M. Wibral, M. Valderrama, R. Pröpper, M. Le Van Quyen, T. Geisel, J. Triesch, D. Nikolic, and M. H. J. Munk, **8**, 80 (2014), ISSN 1662-5137.
- [118] J. Wilting and V. Priesemann, Nature communications **9**, 2325 (2018).
- [119] P. Bak, C. Tang, and K. Wiesenfeld, Phys. Rev. Lett. **59**, 381 (1987).
- [120] L. Martignon, H. von Hasseln, S. Grün, A. Aertsen, and G. Palm, Biol. Cybern. **73**, 69 (1995).
- [121] T. Mora and W. Bialek, Journal of Statistical Physics **144**, 268 (2011), ISSN 1572-9613.
- [122] S. S. Manna, Journal of Physics A: Mathematical and General **24**, L363 (1991).
- [123] A. Vespignani, R. Dickman, M. A. Muñoz, and S. Zapperi, Phys. Rev. Lett. **81**, 5676 (1998).
- [124] R. Dickman, A. Vespignani, and S. Zapperi, Phys. Rev. E **57**, 5095 (1998).
- [125] P. Le Doussal and K. J. Wiese, Phys. Rev. Lett. **114**, 110601 (2015).
- [126] L. Canet, H. Chaté, and B. Delamotte, J Phys. A **44**, 495001 (2011).
- [127] M. A. Buice, J. D. Cowan, and C. C. Chow, Neural Comput. **22**, 377 (2010).
- [128] A. Andreanov, G. Biroli, J.-P. Bouchaud, and A. Lefevre, Phys. Rev. E **74**, 030101 (2006).
- [129] A. Lefevre and G. Biroli, Journal of Statistical Mechanics: Theory and Experiment **2007**, P07024 (2007).
- [130] O. Harish and D. Hansel, PLoS Comput Biol **11**, e1004266 (2015).
- [131] J. Schuecker, S. Goedeke, and M. Helias, arXiv (2017), 1603.01880v3 [q-bio.NC].

- [132] A. Crisanti and H. Sompolinsky, arxiv preprint, arXiv:1603.08270 (2018).
- [133] A. Hawkes, J. R. Statist. Soc. Ser. B **33**, 438 (1971).
- [134] A. Hawkes, Biometrika **58**, 83 (1971).
- [135] G. K. Ocker, K. Josić, E. Shea-Brown, and M. A. Buice, PLOS Computational Biology **13**, 1 (2017).
- [136] M. A. Buice and C. C. Chow, PLoS Comput Biol **9**, 1 (2013).
- [137] S. Qiu and C. Chow, arXiv preprint arXiv:1805.03601 (2018).
- [138] R. B. Stein, Biophys. J. **7**, 37 (1967).
- [139] D. J. Amit and N. Brunel, Cereb. Cortex **7**, 237 (1997).
- [140] H. Sompolinsky and A. Zippelius, Phys. Rev. B **25**, 6860 (1982).
- [141] N. Goldenfeld, *Lectures on phase transitions and the renormalization group* (Perseus books, Reading, Massachusetts, 1992).
- [142] H. Touchette, Physics Reports **478**, 1 (2009).